PNL--7170

DE90 016665

RESULTS FROM NNWSI SERIES 3 SPENT FUEL DISSOLUTION TESTS

C. N. Wilson

June 1990

Prepared for
the U.S. Department of Energy
Office of Civilian Radioactive Waste Management,
Yucca Mountain Project
under Contract DE-AC06-76RLO 1830

Pacific Northwest Laboratory
Richland, Washington 99352

1.0 BACKGROUND

The Yucca Mountain Project, formerly the Nevada Nuclear Waste Storage Investigations (NNWSI) Project, is investigating the suitability of the Topopah Spring Tuff at Yucca Mountain, Nevada, for potential use as a disposal site for spent nuclear fuel and other high-level waste forms. The repository horizon under study lies ~200 to 400 m above the water table in the unsaturated zone. Contact of the spent fuel by liquid water will not occur until the repository has cooled to below the 95°C boiling temperature at the repository elevation. At that time, which is predicted to be hundreds of years after disposal, a limited quantity of water infiltrating the rock could potentially enter a failed waste container and contact the spent fuel where cladding failures have also occurred. Migration of a limited quantity of such water from a failed waste container is considered to be the most probable mechanism for radionuclide release. In addition, there is the potential that ^{14}C (as CO_2) and possibly ^{129}I (as I_2) may migrate in the vapor phase.

Lawrence Livermore National Laboratory (LLNL) is the lead contractor for the Waste Package Task of the NNWSI Project. Westinghouse Hanford Company (Westinghouse Hanford) has been a subcontractor to LLNL, assisting them in determining the requirements for successful disposal of spent fuel at the Yucca Mountain Site.[a] The work at Westinghouse Hanford focused primarily on hot cell testing of spent fuel materials. Areas of investigation included leaching/dissolution behavior, cladding corrosion, and spent fuel low-temperature oxidation behavior. In the Spent Fuel Leaching/Dissolution Task at Westinghouse Hanford, three laboratory test series were conducted with pressurized water reactor (PWR) spent fuel specimens to characterize radionuclide release under NNWSI-relevant conditions.

In the Series 1 tests,[1] specimens prepared from Turkey Point (TP) Reactor Unit 3 fuel were tested in deionized distilled water in unsealed fused silica vessels under ambient hot cell air and temperature (25°C) conditions. Four specimen configurations were tested: 1) undefected fuel rod segments

(a) This work was transferred from the Westinghouse Hanford Company to the Pacific Northwest Laboratory on July 1, 1987, as part of the U.S. Department of Energy's Hanford Site Consolidation.

with water-tight end fittings, 2) fuel rod segments containing small laser-drilled holes through the cladding and with water-tight end fittings, 3) fuel rod segments with a machined slit through the cladding and water-tight end fittings, and 4) bare-fuel particles removed from the cladding plus the cladding hulls. A "semistatic" test procedure was developed in which periodic solution samples were taken with the sample volume replenished with fresh deionized distilled water. A constant water volume (250 mL) was maintained during all test cycles. Cycle 1 of the Series 1 tests was started during July 1983 and was 240 d in duration. At the end of the first cycle, the tests were sampled, the vessels stripped in 8 M HNO_3, and the specimens restarted in fresh deionized distilled water for a second cycle. Cycle 2 of the Series 1 tests was terminated at 128 d in July 1984.

The Series 2 tests were similar to the Series 1 tests except that: 1) the Series 2 tests were run in NNWSI reference J-13 well water, 2) each of the four specimen configurations was duplicated using both the TP and H. B. Robinson (HBR) Reactor PWR spent fuels, and 3) a vessel and specimen rinse procedure was added to the cycle termination procedures. Filtration of the collected rinse solution provided solids residues that were later examined for secondary-phase formation. Cycle 1 of the Series 2 tests was started in June 1984. All eight Series 2 specimens were run for a second cycle. Results from Cycles 1 and 2 of the Series 2 tests are reported in Reference 2. The two bare-fuel specimens were continued for Cycles 3, 4, and 5 for a total five-cycle testing time of 34 mo. Summary results for all five cycles of the Series 2 bare-fuel tests are given in References 3 and 4. A detailed report of the Series 2 bare-fuel test results is in preparation.

The Series 3 tests that are the subject of the current report used sealed stainless steel vessels and J-13 well water and were run at 85°C (one specimen at 25°C). The four specimen configurations tested in the Series 1 and Series 2 tests were also used in the Series 3 tests. The vessels used in Cycle 1 were fabricated from 304 stainless steel. New 304L stainless steel vessels were substituted in Cycles 2 and 3. During the time period of the Series 3 tests, 304L stainless steel was the NNWSI reference spent fuel container material. The Series 3 tests were started during February 1986 and

were run for three cycles for a total testing time of 15 mo. The purpose of this report is to provide detailed documentation of the NNWSI Series 3 Spent Fuel Dissolution Tests.

This work has been conducted under NNWSI work breakdown structure (WBS) element number 1.2.2.3.1.1.L and activity D-20-42 of the Scientific Investigation Plan for NNWSI Waste Form Testing.[5] Except where noted, this work has been conducted at Quality Level Assignment I.

2.0 TEST DESCRIPTION

A detailed description of the Series 3 tests is provided by the test plan[6] and in technical procedures that are identified in Appendix D. The intent of this section is to provide the reader with sufficient information about the test methods and fuel specimens to follow the discussion of results and calculation of the radionuclide fractional release values.

2.1 TEST SPECIMENS

The test matrix included six specimens that are identified in Table 2.1. All specimens were prepared from 5-in.-long fuel rod sections. The four specimen configurations tested are identical to those tested in the Series 1 and Series 2 tests and represent a range of potential degrees of cladding failure as follows.

- Undefected specimen with intact cladding and water-tight end fittings was run as a control specimen to indicate the amount of radionuclide release originating from residual cladding surface contamination and cladding crud deposits.

- Hole-defects specimen contained two small (~200-μm diameter) laser-drilled holes through the cladding near the center of the specimen. The ends of the hole-defects specimen were sealed with water-tight end fittings. The hole-defects specimen was intended to be representative of fuel rods containing small breaches, such as may result from pellet-cladding interaction (PCI) or stress corrosion cracking (SCC) cladding failures.

- Slit-defect specimen contained a 0.006-in. wide by 1-in. long machined slit through the cladding near the specimen center and was sealed at the ends with water-tight end fittings. The slit-defect specimen was intended to represent a more severe cladding failure, such as may occur if an SCC defect progressed to a relatively large crack or cladding cracks that may result from postirradiation handling.

- Bare-fuel specimens were prepared by machining axial slits through the cladding from end-to-end on opposite sides of the specimens, opening the split cladding, and removing the bare-fuel particles from the cladding. The cladding hulls are included with the fuel particles in these tests as part of the test specimen. The bare-fuel specimens are intended to represent the worst-case cladding failure, where the cladding has split open and the fuel has fallen out.

TABLE 2.1. Test Specimens

Test ID	Rod Section ID	Fuel Configuration[a]	Temp. (°C)	Fuel Weight[b] (g)
HBR/BF-25	C5C-I	HBR Bare Fuel	25	86.17 84.85 83.66
TP/BF-85	F6-2B	TP Bare Fuel	85	85.55 84.33 83.64
HBR/BF-85	C5C-K	HBR Bare Fuel	85	80.70 79.39 78.67
HBR/SD-85	C5B-D	HBR Slit Defect	85	85.77
HBR/HD-85	C5B-B	HBR Hole Defects	85	80.16
HBR/UD-85	C5B-A	HBR Undefected	85	85.07
HBR/BF-2-25	C5C-H	HBR Bare Fuel[c]	25	83.10 82.92 81.45
TP/BF-2-25	I9-24	TP Bare Fuel[c]	25	27.21 26.66 26.14

(a) HBR = H. B. Robinson.
TP = Turkey Point.

(b) Three weights given for bare-fuel tests are for Cycles 1, 2, and 3, respectively. Cladding weight was assumed to be 16.4 g for all specimens.

(c) Series 2 tests,[2] which are discussed in this report for comparison.

The Series 3 tests were conducted in sealed stainless steel vessels as shown in Figure 2.1, with different vessel internal configurations for bare-fuel specimens versus the clad fuel specimens with water-tight end fittings. One HBR fuel specimen in each of the four configurations was tested at 85°C. A bare-fuel specimen prepared from TP fuel was also tested at 85°C for comparison with the HBR fuel. The temperature was controlled at 85 ± 2°C using a constant-temperature oil bath. The 85°C temperature may be near the temperature at which liquid water could first form in a failed waste package under an air-steam atmosphere as the repository cools after several hundred years postclosure.[7] An additional HBR bare-fuel specimen was tested at 25°C to correlate dissolution behavior with temperature. The 25°C test also provides for correlation of results from Series 3 tests in sealed stainless steel vessels with those from unsealed silica vessels used in the Series 2 tests. Both vessel materials were relevant to the repository system; 304L stainless steel was the reference container material when the Series 3 tests were started and silica is chemically more similar to the tuff rock outside the container.

An important part of the specimen preparation procedures was the removal from the cladding exterior surface of fine particulate contamination that results from sectioning and handling in contaminated hot cells. Such contamination would seriously bias the test results if not removed. One purpose of the undefected test specimens in the test matrix was to provide an indication of the released radioactivity originating from residual contamination on the cladding exterior surface. Another purpose for the undefected specimen was to verify integrity of the O-ring seal in the end fittings used on the clad specimens. Before installing end fitting hardware on the undefected, hole-defects (laser-drilled), and slit-defect specimens, the cladding surface was decontaminated to less than 50 cpm smearable alpha and less than detectable beta/gamma above the Hanford 327 Building background (~150 cpm in a lead-shielded cave). The cladding exterior of the bare-fuel specimens was also decontaminated to less than 50 cpm smearable alpha before the cladding was axially split to remove the bare fuel.

The ends of the undefected, laser-drilled, and slit-defect specimens were sealed using water-tight end fittings fabricated from modified Cajon

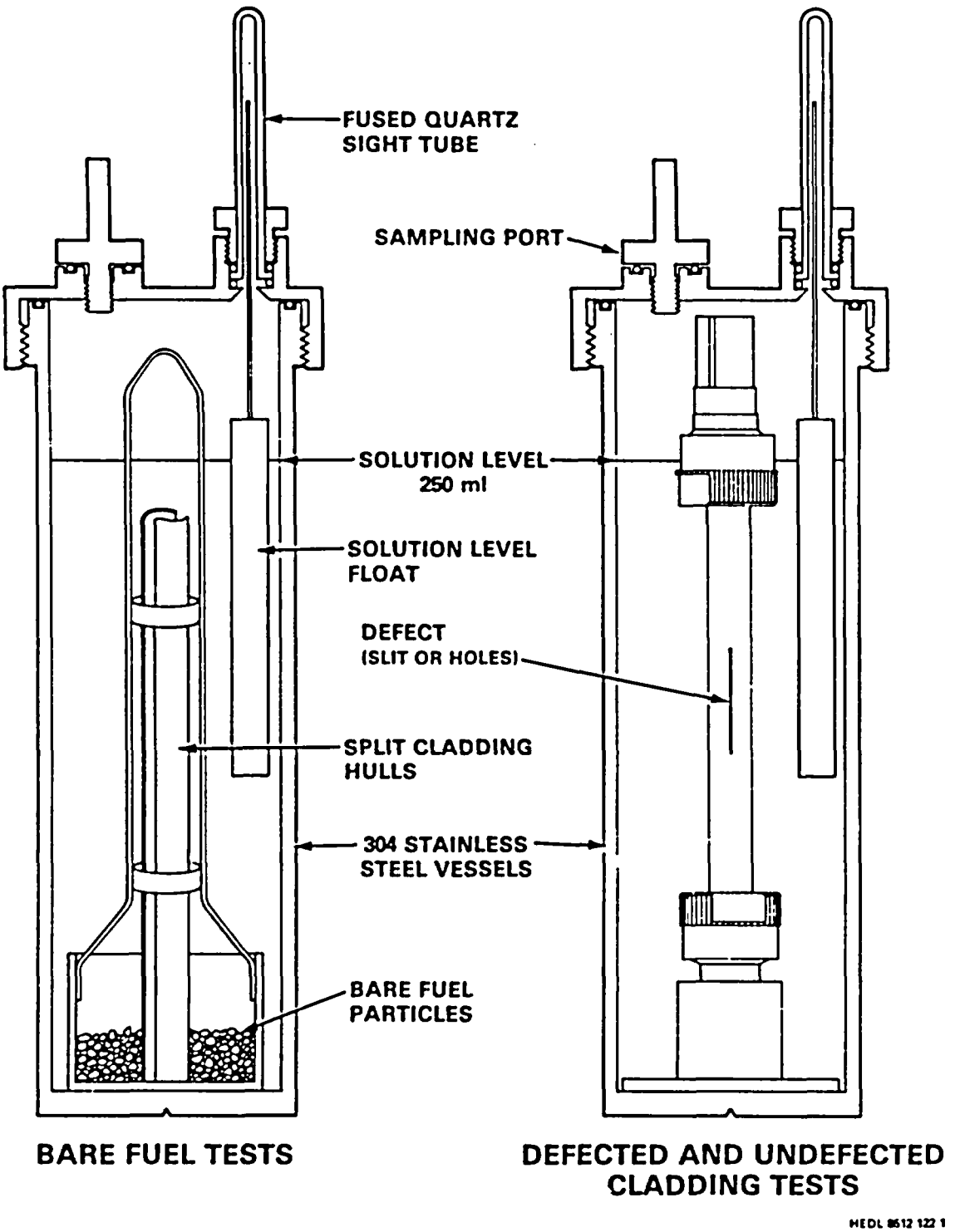

FIGURE 2.1. Series 3 Test Configurations (Neg. 8600029-1)

Model SS-8-UT-A-10 Ultra Torr[a] vacuum adaptors. The end-fitting seal was made using ethylene propylene O-rings chosen for their radiation resistance and water compatibility. The top fittings of both the hole-defects and slit-defect specimens contained a small vent hole above the test solution level to allow the defected cladding specimens to fill with solution to the external test solution level.

A ceramographic section showing a laser-drilled hole defect through the cladding of a TP fuel specimen (Series 1) is shown in Figure 2.2. A mosaic photograph showing the entire section in the as-polished condition is shown in Figure 2.3. The postirradiation thermal cracking pattern shown in Figure 2.3 is typical of that for the HBR and TP fuels used in the Series 3 tests and is indicative of the size of the resulting particles used in the bare-fuel tests.

2.2 FUEL CHARACTERISTICS AND HISTORY

The two fuel types used in the test matrix were similar PWR fuels, as indicated by the relevant fuel characteristics listed in Table 2.2. Both fuels were low-gas-release PWR fuels from the same vendor and approximately the same vintage.

The HBR fuel was obtained through the Pacific Northwest Laboratory (PNL) Materials Characterization Center (MCC) as an "approved testing material" (ATM) for geological repository testing and was identified by PNL-MCC as ATM-101.[8] The ATM-101 Rod C5 was cut into three sections during Spring 1983. The two HBR bare-fuel specimens were sectioned from the C5C center section of Rod C5. The slit-defect, hole-defects, and undefected specimens were sectioned from the top end of the C5B bottom section of Rod C5. The Series 2 HBR specimens were taken from the top portion of rod segment C5C. Other sections taken from the C5C and C5B segments were used for ^{14}C, burnup, and ceramographic analyses and examinations.

The TP specimen was sectioned from the center of a previously sectioned 24-in.-long rod segment identified as Section 2 from Rod F6. Axial location of the specimen is from 34 to 39 in. from the bottom of Rod F6. The original

(a) Ultra Torr is a trademark of Cajon Company, Macedonia, Ohio.

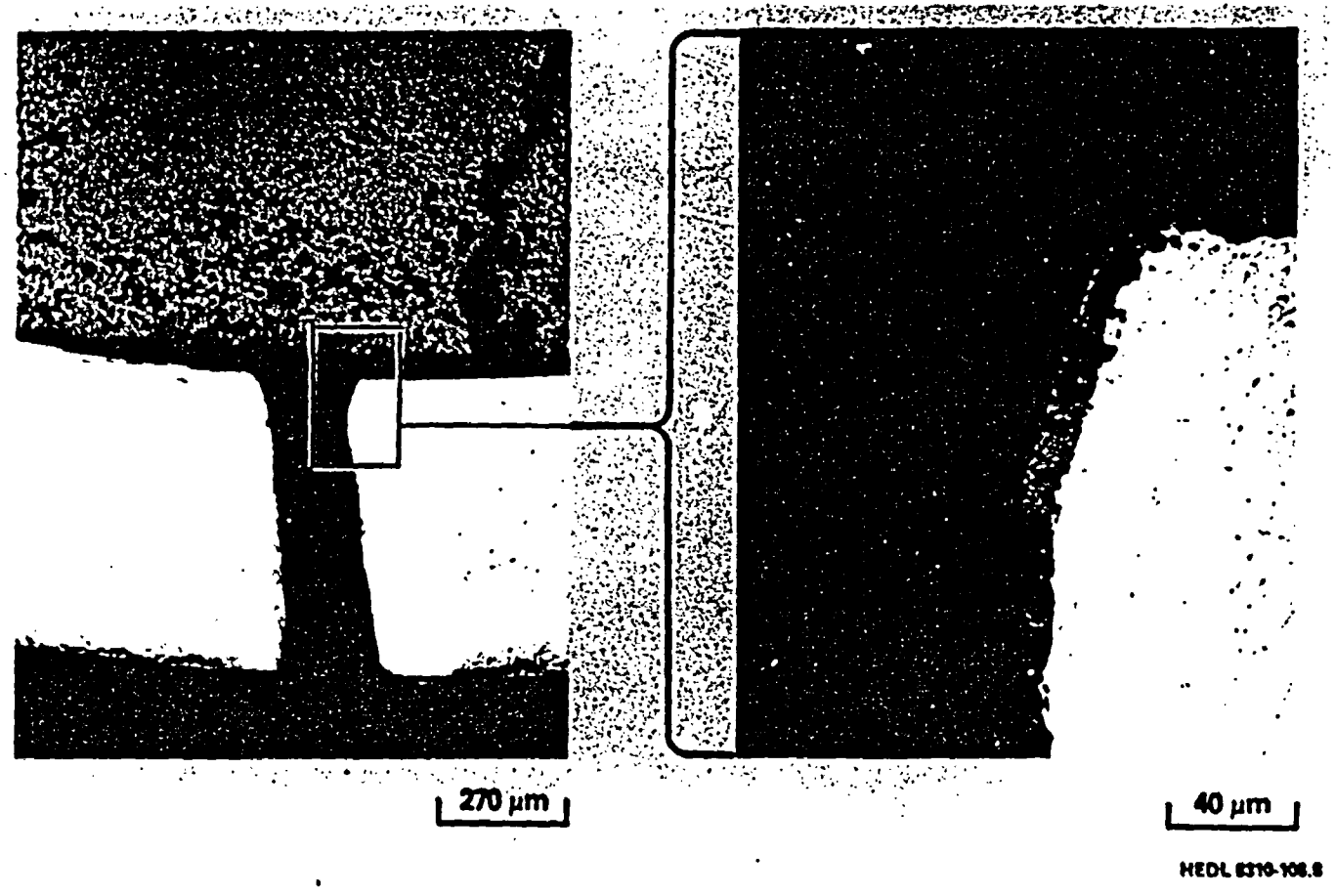

FIGURE 2.2. Ceramographic Section at Laser-Drilled Hole Defect Through the Cladding (Neg. 8307376-8)

TURKEY POINT ROD SPECIMEN J-8-19,
B-17 ASSEMBLY
LASER-DRILLED, LEACHED 60 DAYS

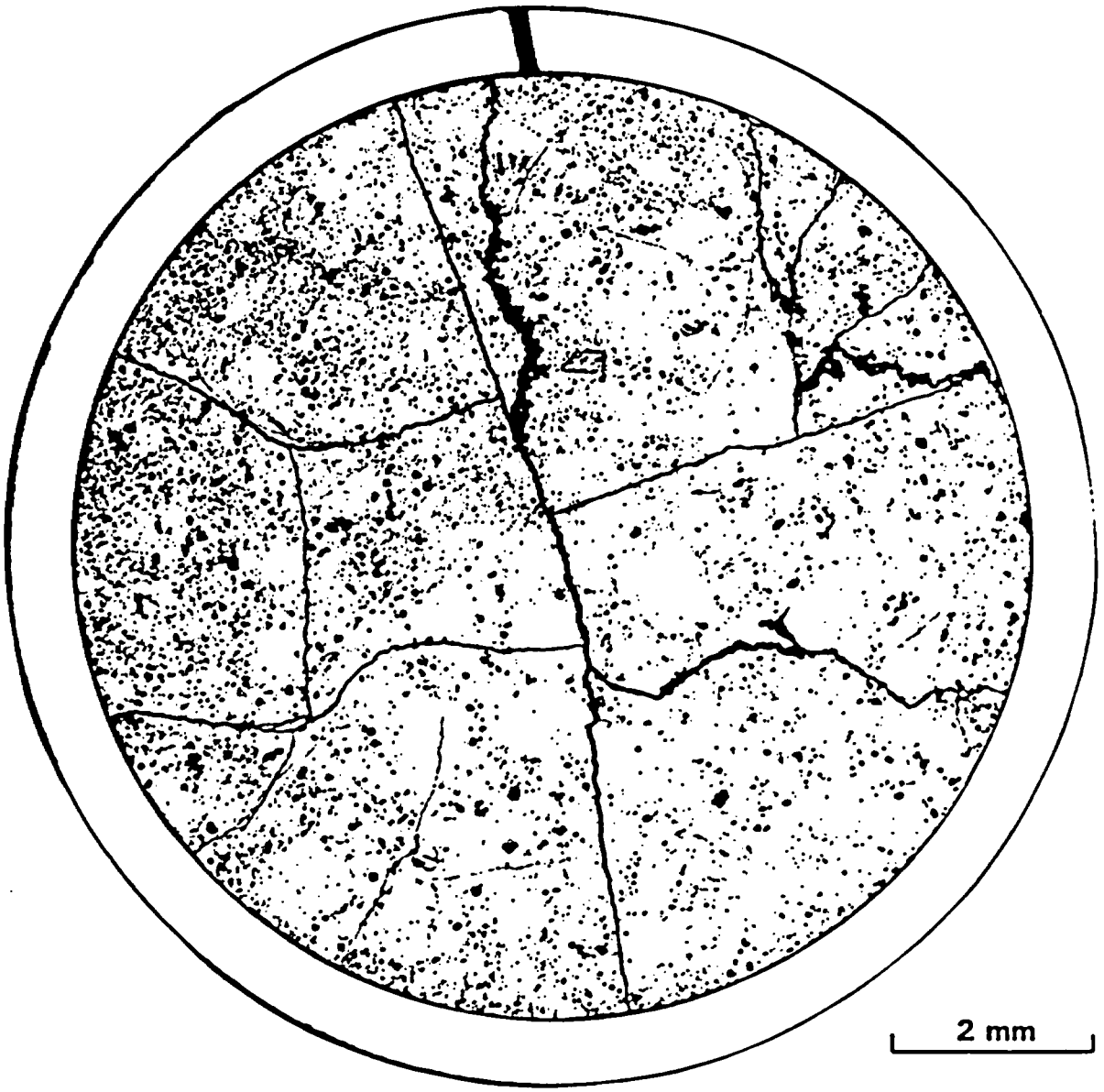

FIGURE 2.3. Ceramographic Mosaic of As-Polished Specimen Section at Laser-Drilled Hole Defect Showing Postirradiation Fuel Cracking. (Particle size in the bare-fuel tests were approximately that indicated by the postirradiation cracking.) (Neg. 8307465-1)

TABLE 2.2. Characteristics of H. B. Robinson Unit 2 and Turkey Point Unit 3 Fuels

Characteristic	H. B. Robinson	Turkey Point
Fuel Type	PWR 15 x 15	PWR 15 x 15
Assembly Identification	BO-5	B-17
Rod Identification	C5	F6
Discharge Date	May 6, 1974	November 25, 1975
Nominal Burnup	30 MWd/kgU	27 MWd/kgU
Fission Gas Release	0.2%	0.3%
Initial Enrichment	2.55 wt% ^{235}U	2.559 wt% ^{235}U
Initial Pellet Density	92% TD (UO_2)	92% TD (UO_2)
Initial Fuel Grain Size	~6 μm	~25 μm
Initial Rod Diameter	10.7 mm OD	10.7 mm OD
Cladding Material	Zircaloy-4	Zircaloy-4
Cladding Thickness	0.62 mm	0.62 mm
PNL-MCC Identification	ATM-101	--

rod sectioning was performed at Battelle Columbus Laboratories (BCL) in 1979 and is documented along with characterization data on Rods G7, G8, J8, I9, and H6 of Assembly B-17 in Reference 9.

Fuel rod sectioning diagrams for the C5B, C5C, and F6-2 rod segments used for the Series 3 specimens are contained in the test plan.[6] Axial locations for all specimens were chosen to avoid regions of nonuniform burnup that occur near spacer grid locations and towards the top and bottom ends of the fuel rod.

Inventories for the radionuclides analyzed were calculated from ORIGEN-2 data tabulated in Appendix E of Reference 8. The calculated inventory values along with radiochemically measured values on an HBR fuel sample are given in Table 2.3. The average times from discharge assumed (12 yr for HBR and 10.5 yr for TP) correspond to midway through Cycle 1. Linear interpolation was used to adjust the tabulated ORIGEN-2 data for burnup and time from discharge. Fractional release calculations for this report use a single ORIGEN-2 based inventory value for each radionuclide and are not corrected for changes in inventory during the 15-mo testing time. Of the principal radionuclides

TABLE 2.3. Specimen Radionuclide Inventories (μCi/g of fuel except as indicated)

Nuclide	H. B. Robinson ORIGEN-2[a]	H. B. Robinson Measured[b]	Turkey Point ORIGEN-2[a]
Burnup (MWd/kgM)	30.2[b]	30.2	27.5[c]
Uranium (μg/g of fuel)	8.45×10^5	--	8.48×10^5
^{244}Cm	1.28×10^3	1.43×10^3[d]	9.90×10^2
^{241}Am	1.77×10^3	1.63×10^3	1.51×10^3
$^{239+240}Pu$	7.44×10^2	7.16×10^2	7.04×10^2
^{237}Np	2.43×10^{-1}	2.35×10^{-1}	2.18×10^{-1}
^{137}Cs	6.37×10^4	6.57×10^4	6.04×10^4
^{129}I	2.65×10^{-2}	--	2.42×10^{-2}
^{126}Sn	6.74×10^{-1}	--	6.11×10^{-1}
^{99}Tc	1.05×10^1	8.34×10^0	9.74×10^0
^{90}Sr	4.17×10^4	--	4.03×10^4
^{14}C	--	(e)	

(a) Calculated from ORIGEN-2 data in PNL-5109,[8] assuming 12 yr from discharge for H. B. Robinson and 10.5 yr from discharge for Turkey Point.
(b) Radiochemically determined (September 1985) from Sample C5C-D.
(c) Reported burnup for Sample G7-15.[9]
(d) Actually $^{243+244}Cm$ since both isotopes have similar alpha energies; ORIGEN-2 data indicate that ^{243}Cm is ~1% of $^{243+244}Cm$.
(e) ^{14}C average of values measured on Samples C5C-J and C5B-C: Fuel = 0.49 μCi/g; Cladding = 0.53 μCi/g.

discussed, ^{244}Cm (with 5% decay in the 15 mo) showed the greatest inventory change. The specimen inventories used in fractional release calculations were obtained by multiplying the per gram inventories in Table 2.3 times the specimen weights given in Table 2.1. Progressive decreases in weights of the bare-fuel samples in successive cycles is due to removal of particles for characterization, losses because of dissolution, and losses of spalled grains from the particle surfaces during terminal specimen rinsing.

2.3 TEST SAMPLES AND ANALYSES

Each test cycle was started, sampled, terminated, and the samples were analyzed following approved procedures identified in Appendix D. The sampling schedule and specified analyses for Cycle 1 are given in the test plan.[6] Similar sampling schedules and analyses were specified for Cycles 2 and 3 with the more significant changes noted below.

2.3.1 Starting J-13 Water

At the beginning of each test cycle, the J-13 water used to start the cycle was analyzed (Appendix B). The following analyses were performed: pH, inductive coupled plasma (ICP) emission spectrometry for cations, ion chromatography (IC) for anions, and inorganic carbon for bicarbonate ion concentration calculation.

2.3.2 Periodic Solution Samples

Periodic solution samples were taken through the sampling port (see Figure 2.1) using preleached 20-mL plastic syringes with 6-in.-long stainless steel needles. The sampling depth was slightly higher than the upper lip of the internal bare-fuel sample basket, which is shown to scale in Figure 2.1. The 85°C test vessels remained in the oil bath during sampling so the samples were taken at temperature. Before drawing the sample, ~50 mL of air were bubbled through the vessel from the syringe at the sampling depth. The original purpose of the bubbling in the Series 1 and 2 tests was to provide for a small amount of convection or mixing effect just prior to sampling. Although this procedure is probably of questionable value for mixing, it was retained so that the sampling procedure would be consistent in all test series. Periodic solution sample volumes ranged from 10 to 30 mL, depending on the analyses that were to be performed. After the samples were removed, the sample volumes were replenished with fresh J-13 well water so that a constant water volume of 250 mL was maintained in the test vessels.

Solution samples were placed in preleached glass vials and capped in the hot cell. The samples were removed from the hot cell to a glovebox and aliquots prepared for analysis, usually within an hour of sampling. The first step when the sample vial was opened was to measure pH on an aliquot from the vial. Aliquots were also taken and placed in sealed vials for ^{14}C and ^{129}I

analyses if specified. The remaining sample was then usually separated into aliquots for the unfiltered, 0.4-μm filtered, and 18-Å filtered[(a)] fractions. Analysis of 18-Å filtered solution samples was deleted starting with the fifth sample (Day 62) of Cycle 2. Uranium, alpha (for $^{239+240}Pu$), gamma (for ^{137}Cs), ^{241}Am, ^{237}Np, ^{126}Sn, and ^{99}Tc analyses were routinely performed on all three filtered fractions; and ^{129}I, ^{90}Sr, and ^{14}C analyses were routinely performed on the unfiltered fractions. Solution chemistry (ICP, IC, and inorganic carbon) analyses were performed on the 0.4-μm filtered fraction, when specified. For sampling schedules, volumes and analyses performed refer to the radiochemistry and solution chemistry data tables in Appendices A and B.

2.3.3 Final Solution Samples

A final solution sample was taken immediately before termination of a test cycle on the termination day. The procedure for the final solution sampling is identical to that for the periodic solution samples, except that the sample volume was not replenished with fresh J-13 well water. For the purposes of data evaluation, the volume of the final solution sample is assumed to be the entire 250 mL of solution in the test.

2.3.4 Rinse Samples

After the final solution sample was taken, the vessels were removed from the constant temperature bath for cycle termination. The bare-fuel particles were removed to a 250-mL beaker, and the remaining final solution was decanted off. The fuel particles were rinsed in the 250-mL beaker with J-13 water (~50 mL), rocking the breaker from side to side ten times and allowing the particles to tumble in the bottom of the beaker. The bare-fuel rinse water was then decanted into a 1,000-mL beaker, and the bare-fuel rinse was repeated four more times. The bare-fuel rinse solution routinely became dark and turbid in appearance during the first few rinse cycles as surface grains (loosened by grain boundary dissolution) and sediment from the test became

---

(a) The 18-Å filtered fraction referred to in this report is a sample fraction centrifuge filtered through an Amicon Corporation type CF25 Centriflo membrane filter cone. Centriflo is a trademark of the Amicon Corporation, Lexington, Massachusetts.

temporarily suspended. Clad specimens with end fittings, cladding hulls from bare-fuel tests, specimen baskets or pedestals, floats, and the interior vessel surfaces were thoroughly rinsed with J-13 water from a squirt bottle with the rinse water draining into the 1,000-mL beaker. The rinse water volumes in the 1,000-mL beakers were made up to 600 mL after specimen and component rinsing by addition of fresh J-13 well water and then were left covered overnight to settle. A sample was removed from the top of the settled rinse solutions the next morning using a syringe and preleached sample vials. Routine requested analyses for the rinse solution samples included uranium, alpha spectrometry, gamma spectrometry, ^{241}Am, ^{237}Np, ^{99}Tc, ^{90}Sr, and ^{14}C. Rinse samples from bare-fuel tests were 0.4-μm filtered prior to analyses.

2.3.5 Acid Strip Samples

After rinsing, the internal components less the actual specimens were placed back in their respective vessels, and 300 mL of 8 M HNO_3 were added. The caps were replaced and the vessels rolled on their sides so that the interiors would be completely washed with the acid. The next day the acid was poured into a bottle, back into the vessel, and then back into the bottle again. The acid strip solution in the bottles was then sampled for analyses. Requested analyses routinely included uranium, alpha spectrometry, gamma spectrometry, ^{241}Am, ^{237}Np, ^{99}Tc, and ^{90}Sr.

2.3.6 Ceramographic Samples

Two random fuel particles were removed from the 250-mL beaker after cycle termination for later ceramographic examination. The particles were mounted in resin, ground to expose an internal section, polished, and examined in the as-polished condition. The intersection of the section plane with the particle surface was of primary interest and was examined for evidence of grain boundary dissolution or any other type of observable preferential dissolution.

2.3.7 Rinse Filters

After the rinse solution samples were taken, the remaining solutions in the 1,000-mL beakers were stirred to get the finer sediments back into suspension. The rinse solutions were then filtered through 0.4-μm filters, and the filtrate solutions were discarded. The filters were weighed to determine

the net amount of residue filtered from each rinse solution. The filters were later examined by scanning electron microscopy (SEM) and X-ray diffraction (XRD) to identify and characterize any secondary solid phases present.

2.3.8 Coarse Rinse Sediments

Coarser particles that would not remain in suspension long enough to be decanted off during filtration of the rinse solution were allowed to settle to the bottom of the 1,000-mL beakers. These sediments were allowed to dry and, if present in sufficient quantity (a few mg or more), removed and weighed. Samples of these coarse sediments were then examined in the SEM. The coarse rinse sediments consisted primarily of small particles of fuel.

2.4 CHEMISTRY

Chemical analyses of solution samples were divided into two types for the purposes of evaluation: the analyses of uranium and radionuclides originating from the fuel specimens (radiochemistry) and the analyses of species contained in the starting J-13 well water (solution chemistry).

2.4.1 Radiochemistry

A summary of the radiochemistry methods is given in Table 2.4. Principal radionuclides present in 1,000-year-old spent fuel were of primary interest and are summarized in Table 2.5. The 1,000-yr inventories are significant relative to the U.S. Nuclear Regulatory Commission (NRC) stated requirement that "release rate of any radionuclide from the engineered barrier system ... shall not exceed one part in 100,000 per year of the inventory of that radionuclide calculated to be present at 1,000 years."[11] Approximately 99% of the 1,000-yr activity is from plutonium and americium isotopes plus ^{99}Tc. Other long-lived nuclides analyzed were ^{237}Np, ^{14}C, ^{126}Sn, and ^{129}I. Shorter half-life radionuclides including fission products ^{137}Cs (30.2 yr), ^{134}Cs (2.2 yr), ^{90}Sr (28.6 yr), and ^{244}Cm (18.1 yr) and activation product ^{60}Co (5.3 yr) were also analyzed, since they represent a major fraction of the activity in spent fuel during the first few hundred years. Selenium-79 was dropped from the Series 3 analytical schedule, since attempts to measure it by liquid scintillation following separation in the Series 2 tests failed.[2] Possibly the most significant radionuclide listed in Table 2.5 that was not

TABLE 2.4. Summary of Radiochemistry Methods

Radionuclide	Method	Detection Limits (pCi/mL)	Detection Limits (ppb)	10^{-5} Inventory (pCi/mL)[a]
^{244}Cm	α-spectrometry	0.2	3×10^{-6}	4100
^{241}Am	α-spectrometry following separation	0.1	3×10^{-5}	5700
$^{239+240}Pu$	α-spectrometry	0.2	0.003	2380
^{237}Np	α-spectrometry following separation	0.1	0.14	0.8
^{137}Cs	γ-spectrometry	200	0.002	2.0×10^{5}
^{129}I	Neutron activation analysis	10^{-5}	0.0001	0.08
^{126}Sn	GeLi well γ-spectrometry following separation	0.2	0.02	2.2
^{99}Tc	β-proportional counting following separation	10	0.6	34
^{90}Sr	β-proportional counting following separation	20	0.0001	1.3×10^{5}
^{60}Co	γ-spectrometry	200	0.0002	(b)
^{14}C	Liquid scintillation counting following separation	20	0.004	2
U	Fluorescence	--	1	(3 ppm)

(a) Assumes 10^{-5} of H. B. Robinson test specimen inventory dissolved in 250 mL.
(b) ^{60}Co inventory is unknown.

TABLE 2.5. Pressurized Water Reactor Spent Fuel Radionuclide Inventories at 1,000 Years[a]

Radionuclide[b]	Half-Life (yr)	Ci/1,000 MTHM	1,000-Year Activity (% of Total)	Cumulative Activity (%)
^{241}Am	432	894,500	51.33	51.33
^{243}Am	7,380	31,080[c]	1.78[c]	53.11
^{240}Pu	6,569	476,900	27.37	80.48
^{239}Pu	24,130	304,700	17.45	97.96
^{242}Pu	375,800	1,755	0.10	98.07
^{238}Pu	88	967	0.06	98.12
^{99}Tc	213,000	13,030	0.75	98.87
^{59}Ni	80,000	5,150	0.295	
^{63}Ni	100	354	0.020	
^{93}Zr	1.53E+06	1,933	0.111	
^{93m}Nb	15	1,836	0.105	
^{94}Nb	20,300	1,240	0.071	
^{14}C	5,730	1,372	0.079[d]	
^{234}U	244,500	1,984	0.114	
^{238}U	2.47E+09	317	0.016	
^{236}U	2.34E+07	271	0.018	
^{237}Np	2.14E+06	1,000	0.057	
^{126}Sn	100,000	772	0.044	
^{79}Se	65,000	405	0.023	
^{135}Cs	3.00E+06	345	0.020	
^{151}Sm	90	163	0.009	
^{107}Pd	6.50E+6	112	0.006	
^{129}I	1.57E+07	32	0.0018	

(a) Based on ORIGEN-2 data in ORNL/TM-7431[10] for 33,000 MWd/MTM burnup PWR spent fuel, actinides plus fission products plus activation products.
(b) Radionuclides with 1,000-yr activity less than ^{129}I or half-life less than 1 yr omitted.
(c) Includes activity of ^{239}Np daughter product.
(d) ^{14}C activity may vary considerably depending on as-fabricated nitrogen impurities.

analyzed was activation product ^{59}Ni, which is primarily associated with fuel assembly structural components, which were not included in these tests.

The approximate detection limits for each radionuclide are compared in Table 2.4 to the activity that would result if 10^{-5} of the specimen inventory were to be dissolved in the 250 mL of test solution. In the Series 1 and 2 tests, actinide concentrations in solution tended to stabilize at values near or below concentrations corresponding to 10^{-5} of inventory in solution. The Table 2.4 radionuclides for which the detection limits were just adequate or borderline for the bare-fuel tests and not adequate for the lower release defected cladding tests were ^{237}Np, ^{126}Sn, and ^{99}Tc.

A discussion of detection limits and relative errors precedes the tabulated results of the radiochemistry analyses in Appendix A. Summaries of the principal radiochemistry procedures are contained in Appendix D.

2.4.2 Solution Chemistry

Solution chemistry measurements included pH, ICP for cations, IC for anions, and inorganic carbon. Bicarbonate (HCO_3^-) concentration in $\mu g/mL$ was calculated by multiplying the inorganic carbon results (also in $\mu g/mL$) by 5.0833 to correct for molecular weight. For certain analyses, organic carbon and total carbon were also reported. The detection limits of the solution chemistry analyses were generally on the order of 0.1 $\mu g/mL$, which was adequate for following the concentrations of ionic species in J-13 well water in order to determine if these species were being precipitated during the tests. Other purposes for the solution chemistry data were to indicate if significant corrosion of the vessels occurred or if test or sample contamination with nonradioactive species occurred.

2.5 TEST CYCLE RESTART

Experience in the Series 2 tests indicated that the fuel should be restarted for subsequent cycles as soon as possible and not allowed to dry between cycles, or an oxidized surface film could form on the fuel leading to enhanced dissolution and supersaturation of uranium early in the following cycle. New vessels and internal components were fabricated for Cycle 2, and the tests were restarted in the new vessels on the same day (within a few

hours) of Cycle 1 termination. When Cycle 2 was terminated, the vessels were reused for Cycle 3, requiring an extra day between cycles while the vessels were being stripped, neutralized, rinsed, and reassembled with new sight tubes and O-rings. The time between Cycle 2 termination and Cycle 3 start is estimated to be ~30 hours, during which time the bare-fuel specimens remained wet covered in the 250-mL beakers, and the cladding hulls and clad specimens were stored wet in plastic bags.

As in the Series 2 tests, only the bare-fuel specimens were originally to have been run for Cycle 3 of the Series 3 tests. However, for the purpose of not changing test geometry (and possibly the bath-to-vessel internal temperature gradient), it was decided to restart all the specimens for Cycle 3 but only sample the bare-fuel specimens. Since the duration of Cycle 3 was then shortened and the number of solution samples reduced, the budget at termination allowed a final solution sample from all the vessels. (The purpose for shortening Cycle 3 was to complete Quality Assurance Level I laboratory testing activities prior to their transfer from Westinghouse Hanford to PNL.)

3.0 RESULTS AND DISCUSSION BY ELEMENT

3.1 GENERAL COMMENTS ON DATA PRESENTATION

A complete tabulation of radiochemical results reported in pCi activity units (μg units for uranium) is contained in Appendix A. A complete tabulation of the nonradioactive water chemistry data for each test is contained in Appendix B. A detailed discussion of the results organized by element and radionuclide is contained in this chapter. Results for the actinides, whose concentrations and activities in solution were limited by their relatively low solubility, are presented before those of the more soluble fission and activation produce elements. A discussion of results from the characterization of secondary phases found in filtered solids residues follows the uranium results. Results from the bare-fuel tests are emphasized in most of the discussions.

A more general discussion of the bare-fuel test results is contained in the following chapter. The actinide results are compared to solubilities predicted by the EQ3/6 geochemical modeling code, and results for both the actinides and the more soluble fission and activation products are discussed relative to NRC release limits in that chapter.

3.1.1 Plotted Solution Sample Activity Data

Solution sample data for the various nuclides are plotted in composite plots showing data for the three sequential test cycles in adjacent boxes along the X-axis. Data reported as "less than" values are plotted with downward arrows with the plotted point representing the estimated detection limit for the particular measurement. A reference level is shown in the Cycle 3 box of many of the plots indicating the level that would result if the indicated fraction of the specimen inventory dissolved in the 250 mL of test solution. The same symbol is used for data from the same test in different plots, except for plots comparing filter fractions where the same symbols are used for the same filter fractions. Open symbols are used for Series 3 data, and closed (filled-in) symbols are used for Series 2 data that are included in some plots for comparison. Data are plotted as concentration (μg/mL for uranium) or activity (pCi/mL) measured in solution samples in this chapter.

Specimen inventory fractions of ^{137}Cs, ^{90}Sr, ^{99}Tc, ^{129}I, and ^{14}C measured in solution are plotted together for each of the three bare-fuel tests in the following chapter. Each data point in these plots represents the inventory fraction in the 250 mL of test solution on the sample date plus the inventory fractions estimated to have been removed in previous samples taken during the test cycle.

3.1.2 "Quantities Measured" Tables

Tables of the quantities of nuclides measured in the various types of liquid samples were compiled for each nuclide. The "periodic samples" values given in these tables are the sum of sample activities times sample volume for each periodic solution sample (excluding the final solution sample) in which detectable activities were measured. Since not all nuclides were measured in every sample, the periodic sample values may be in some cases less than the actual total quantity removed in periodic samples. In the case of ^{129}I, where only a single periodic sample was analyzed, that value was assumed as an estimate of the ^{129}I in all periodic samples. The "final solution" value is the quantity of the nuclide determined to be in the 250 mL of test solution at the end of a test cycle. For the actinides and ^{137}Cs, the "periodic solution" and "final solution" values are based on 0.4-μm filtered data. For ^{99}Tc, ^{90}Sr, ^{129}I, ^{126}Sn, and ^{14}C, the "periodic solution" and "final solution" values are based on unfiltered data. Concentration of the nuclide in the final solution is given in parentheses below the "final solution" value in the indicated units.

The "rinse" value is the quantity of the nuclide determined to be dissolved in the 600-mL rinse solutions when sampled the day after cycle termination. Rinse solution samples from bare-fuel tests were 0.4-μm filtered prior to analysis, while rinse solution samples from the clad-fuel tests were unfiltered. The "acid strip" value is the quantity of the nuclide determined to be dissolved in the 300 mL of 8 M HNO_3 used to strip the internal vessel hardware components at cycle termination. The "cycle total" values are the sum of the periodic samples, final solution, rinse, and acid strip values. The "+ 10^{-5} Inv." value is the cycle total value divided by 10^{-5} of the inventory of that nuclide calculated to be present in the initial spent fuel test specimen. The "% in solution" value is the sum of the periodic samples plus

the final solution values divided by the cycle total value times 100. "Less than" symbols indicate either: 1) the value was reported as below detection limits for the particular sample or 2) the value is a sum in which greater than 5% is based on "less than" values. A double dash (--) indicates that a value was not measured.

3.1.3 Qualifications for Certain Data Uses

The tabulated quantities of nuclides measured should not, in general, be directly related to release or amounts of actual fuel dissolution without considering certain qualifications. There is, in particular, a question of the significance of actinide quantities measured in the rinse and acid strip solutions from the bare-fuel tests where these data account for the majority of the nuclide content in the cycle total values.

Rinse Samples--Grains of undissolved fuel and quantities of precipitated secondary-phase materials were removed from the bare-fuel tests with the rinse solution. These phases partially dissolved in the fresh J-13 well water rinse solution during the day between cycle termination and rinse solution sampling. Actinide concentrations in the bare-fuel rinse solutions were usually equal to and often greater than in the final solution samples. Because of the relatively large (600-mL) volume, nuclide quantities measured in rinse solutions were, in some cases, a significant portion of the total cycle measured quantities.

Acid Strip--Ideally from a data evaluation point of view, the acid strip would contain all nuclides dissolved from the fuel that plated, precipitated, or otherwise did not remain in solution. However, in the bare-fuel tests, much of the precipitated secondary-phase material ended up undissolved in the rinse solution residue. An effort was made to remove all visible particles of fuel from the vessel components prior to stripping, but it is possible that microscopic particles of undissolved spent fuel were dissolved in the acid strip solution. In the Cycle 3 HBR/BF-85 acid strip sample, a rather large fuel particle was evidently dissolved.

10^{-5} Inventory--The tabulated "cycle total" values for the various nuclides were normalized to inventory by dividing by 10^{-5} of the ORIGEN-2 based specimen inventory for comparison. In the data discussions, the

resulting values are in some instances loosely referred to as "fractional release." Similarly for comparison, the solution activity level that would result if 10^{-5} of the specimen inventory were in solution is shown on various plots of the periodic solution sample data. The purpose of normalizing tabulated data to inventory and indicating relative inventory fraction levels on plots was to provide a means for comparison of these data. These values cannot be directly compared to the NRC release rate limit of one part in 10^5 per year of the 1,000-yr inventory (10 CFR 60.113).[11] For solubility-limited radionuclides, an assessment of the fractional release rate in the repository requires, at a minimum, knowledge of the amount of water that contacts the waste in a given year.

3.2 URANIUM

Except for a limited portion of certain fission products that diffuse out of the fuel matrix during irradiation, activation products associated primarily with cladding and fuel assembly structural components, and somewhat higher concentrations as a result of higher local burnup at the outer edge of the fuel pellets (rim effect), most of the radionuclide inventory in spent fuel is thought to be rather uniformly distributed in the UO_2 fuel matrix phase. In particular, the alpha-emitting actinides that account for the majority of the postcontainment period activity, and for which the most stringent U.S. Environmental Protection Agency (EPA) releases limits[12] apply, are thought to be contained in solid solution with the UO_2 matrix phase. In addition to dissolution from the fuel matrix phase, water soluble nuclides may be preferentially dissolved from sources such as grain boundaries where they may concentrate during irradiation. It was not possible to determine the relative amounts of matrix release versus preferential release for water soluble nuclides, or the amounts of fuel matrix dissolution, in the present tests because of the limited solubility of uranium and the other actinides. It has yet to be demonstrated that any of the nuclides that remain fully in aqueous solution after release from the fuel are not preferentially dissolved relative to the fuel matrix phase during such tests so as to provide a quantitative measure for matrix dissolution.

3.2.1 Uranium in Solution Samples

Uranium concentrations measured in 0.4-μm filtered solution samples from the six Series 3 tests are compared in Figure 3.1. In Cycle 1 of the bare-fuel tests, uranium concentrations reached a maximum in the initial samples at values on the order of about 10 mg/mL and then decreased to about 0.4 μg/mL in the TP/BF-85 test and about 0.2 μg/mL in the HBR/BF-25 test. The anomalous behavior exhibited during Cycle 1 of the HBR/BF-85 test is discussed later in Section 3.2.2 on vessel effects. Lower initial concentrations were observed in Cycles 2 and 3 of the bare-fuel tests. The initial Cycle 1 concentration peaks are thought to result from the dissolution of more readily dissolved oxidized fuel phases that form on the fuel surface as a result of handling and storing in air prior to testing. The oxidized surface film was apparently depleted by dissolution during Cycle 1, and very little additional surface oxidation appears to have occurred between cycles during which time the fuel was not allowed to dry.

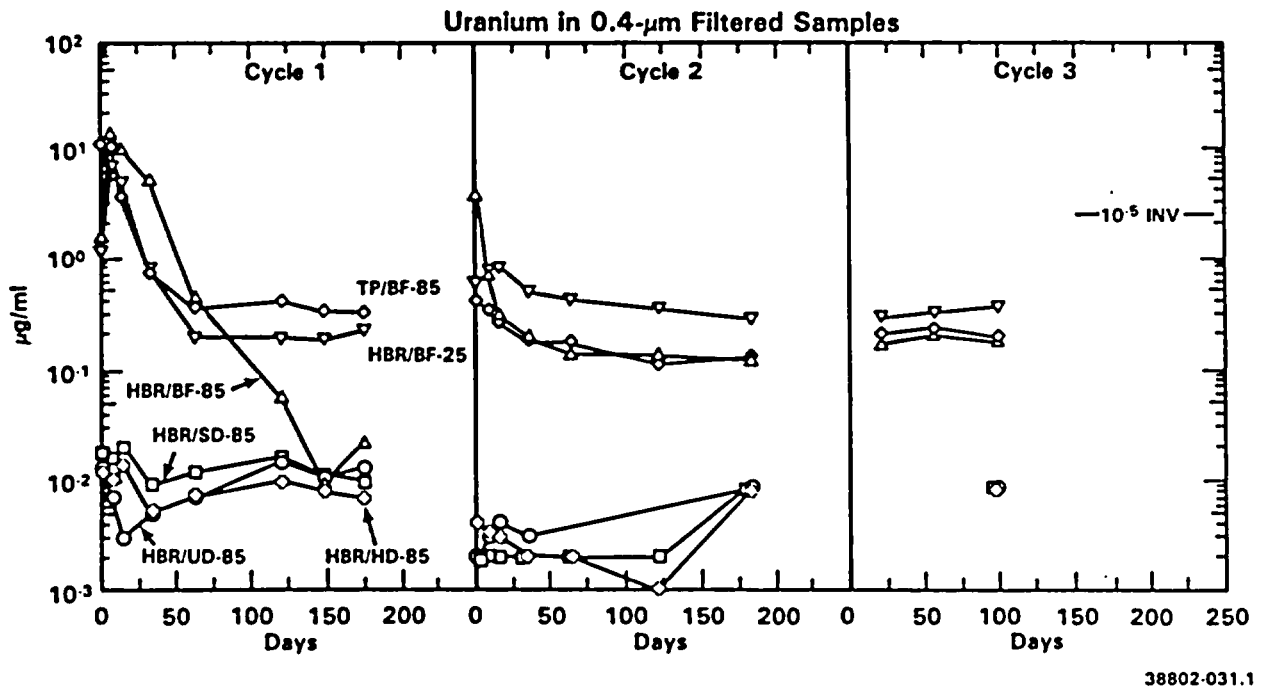

FIGURE 3.1. Uranium Concentrations Measured in 0.4-μm Filtered Samples

During both Cycles 2 and 3, the HBR/BF-25 test exhibited higher uranium concentrations than did the HBR/BF-85 and TP/BF-85 tests, which is the reverse of the temperature effect observed in Cycle 1, where the TP/BF-85 test showed higher uranium concentration than the HBR/BF-25 test. In later Cycle 2 samples and in Cycle 3 samples from the bare-fuel tests, uranium concentrations reached apparent steady-state values of about 0.1 to 0.2 μg/mL in the 85°C tests versus about 0.3 to 0.4 μg/mL in the 25°C test.

Much lower uranium concentrations were measured with the slit-defect and hole-defects specimens than with the bare-fuel specimens. In fact, no significant differences in uranium concentrations were observed for the HBR/SD-85, HBR/HD-85 or HBR/UD-85 specimens, suggesting the uranium release measured in these tests originated primarily from residual surface contamination on the cladding and not from the fuel within the specimens. A decrease in uranium concentrations measured initially in Cycle 2 of these three tests may be due to a depletion of soluble residual contamination on the cladding surface during Cycle 1. An increase in uranium concentrations in these three tests at the end of Cycle 2 and during Cycle 3 (only final solution samples were analyzed in Cycle 3) back to levels observed in Cycle 1 may be related to a degradation of the O-ring seals in the end-fittings. (End-fitting seal degradation was indicated by accelerated ^{137}Cs release from the undefected specimen starting with the 34-d Cycle 2 sample.)

Substantial reductions in uranium concentration as a result of filtration occurred in only a few samples, suggesting that uranium in most samples was in true solution and not present in fine suspended particles or colloidal phases. Uranium concentration measured in the unfiltered, 0.4-μm filtered, and 18-Å filtered fractions of the 119-d HBR/BF-85 Cycle 1 sample were 0.12, 0.055, and 0.028 μg/mL, respectively. This sample exhibited anomalous behavior in other respects and is discussed below under "Vessel Effects." A reduction from 1.67 μg/mL in the unfiltered aliquot to 0.41 μg/mL in the 0.4-μm filtered aliquot in the Day 1 sample from Cycle 2 of the TP/BF-85 test is another notable exception. One qualification for this data is that the laser fluorimetry method does not measure uranium contained in suspended solids. After filtration, the sample aliquots are acidified to 1% HNO_3 prior to analysis in order to dissolve any plate-out, colloids, or suspended

particles. There may be some question as to whether or not all suspended particles, such as undissolved fuel fines or uranium-containing secondary phases, are completely dissolved by this acidification step prior to analysis.

3.2.2 Vessel Effects

The 0.4-μm filtered uranium data from the Series 3 bare-fuel tests in sealed stainless steel vessels are compared to that from the Series 2 bare-fuel tests in unsealed silica vessels in Figure 3.2. After the initial Cycle 1 peak, lower uranium concentrations were observed in the Series 3 bare-fuel tests in comparison to those observed in the Series 2 bare-fuel tests. Local reactions between the stainless steel vessels and solution may be reducing U^{+6} to U^{+4} and limiting uranium solubility. Since the quantity of uranium in solution is not great, a small amount of vessel element oxidation may have a significant effect on uranium concentration. However, considering the low concentration of multivalent ions in J-13 water capable of providing effective Eh buffering, redox equilibrium was probably not well established in the Series 3 tests.

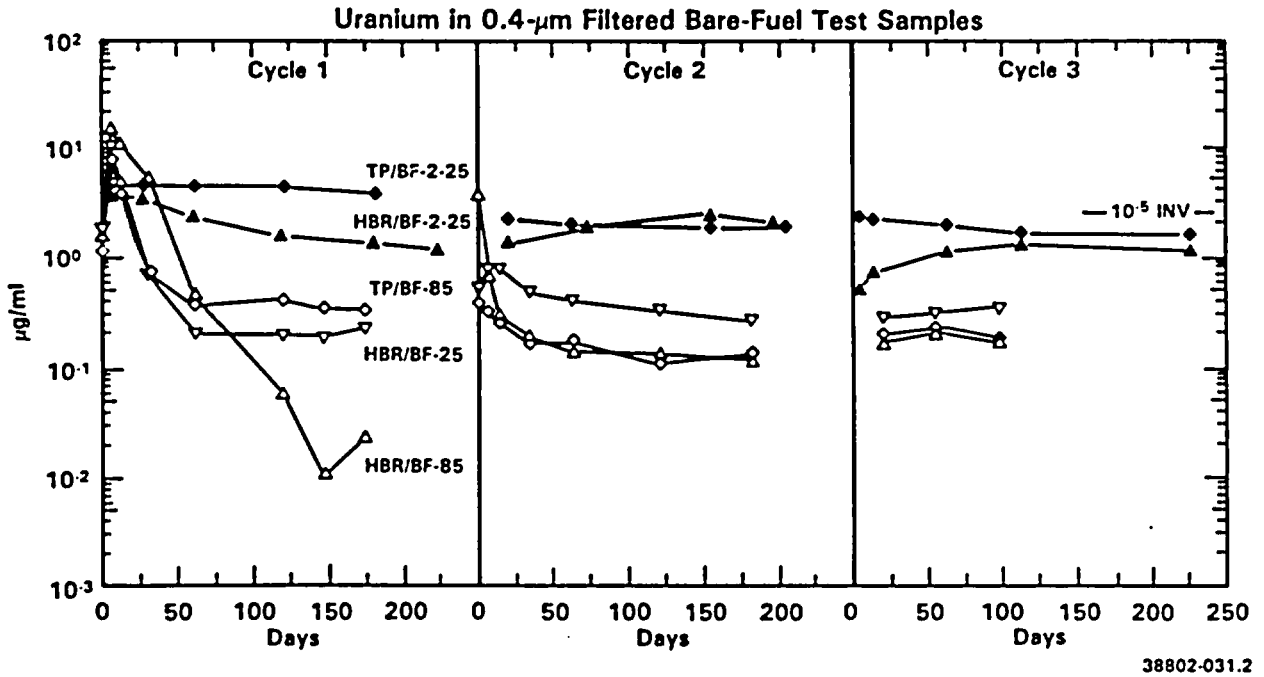

FIGURE 3.2. Comparison of Uranium Concentrations Measured in 0.4-μm Filtered Samples from the Three Series 3 and Two Series 2 Bare-Fuel Tests

The fact that stainless steel vessels are not completely inert relative to solutions containing Eh buffers was noted by Gray, who observed color changes with ZoBell's solution (an Eh standard based on the Fe^{+2}/Fe^{+3} reaction) in stainless steel containers, while no change was observed for the same ZoBell's solution in silica containers.[13] The $KMnO_4$ titration of equimolar $K_3Fe(CN)_6$ plus $K_4Fe(CN)_6$ solutions contained in 316 stainless steel under argon atmosphere for 3 days indicated that twice as much Fe^{+2} was present as in the starting solution, while no significant change in Fe^{+2}/Fe^{+3} ratio was observed for solutions contained in silica vessels. The additional Fe^{+2} in stainless steel resulted from reduction of the Fe^{+3}, from corrosion of the vessel (which contained a welded bottom), or from a combination of both.

The HBR/BF-85 Cycle 1 test exhibited anomalous behavior with uranium concentration decreasing to a minimum value of 0.01 μg/mL in the 147-d sample. The drop in uranium concentration (and also a drop in ^{99}Tc activity) is attributed to a combination of reduced solution oxygen potential in response to corrosion occurring within the vessel and scavenging of these elements by iron-bearing precipitates. A slight yellow turbidity was observed in the 119-d sample from this test, which was notable since solution samples are normally clear. The ICP data indicated 0.14 μg/mL Fe in 0.4-μm filtered solution on Day 33, increased to 0.45 μg/mL on Day 147, and dropped to 0.03 μg/mL on Day 174 at cycle termination. The 147-d sample was added in response to the observations on the 119-d sample from the HBR/BF-85 test. As indicated in Figure 3.3, the turbidity in the 119-d HBR/BF-85 sample appears to have been caused by the formation of iron-silicon containing flocs. The weld joining the bottom of the bare-fuel specimen basket to its cylindrical sides was considered a likely corrosion site, and several metallographic sections of this weld were examined after Cycle 1 termination. Figure 3.4(A) shows the etched microstructure at the boundary of the weld heat-affected zone and the bottom plate near the outer basket surface. This region would have been in a crevice region at the bottom of the narrow gap between the vessel and specimen basket. The more heavily etched appearance near the outer surface of the heat-affected zone suggests that some degree of intergranular corrosion may have occurred at this location. A stress crack shown in Figure 3.4(B) occurred at the weld intersection with the inner crevice

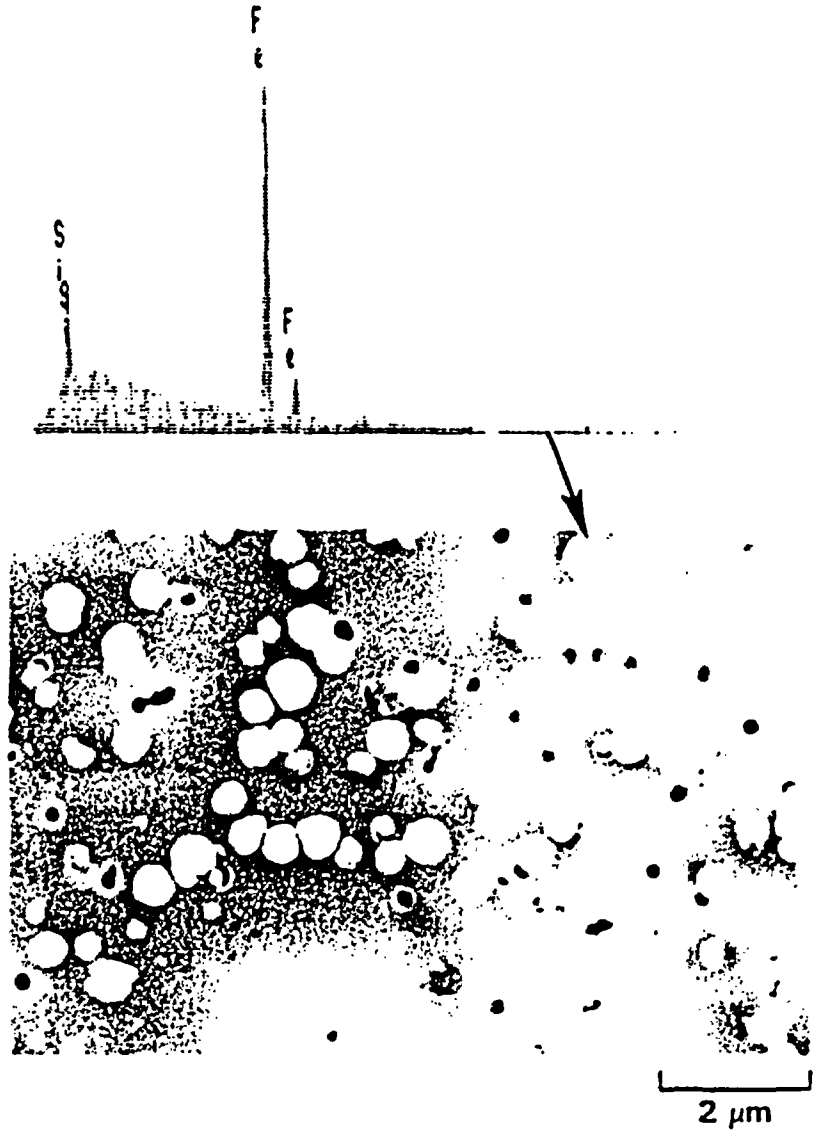

FIGURE 3.3. SEM Photograph Showing Flocs on 0.4-μm Filter Disk Used to Filter the 119-Day Sample from Cycle 1 of the HBR/BF-85 Test. (Accompanying EDX spectra indicates an iron-silicate floc composition.)

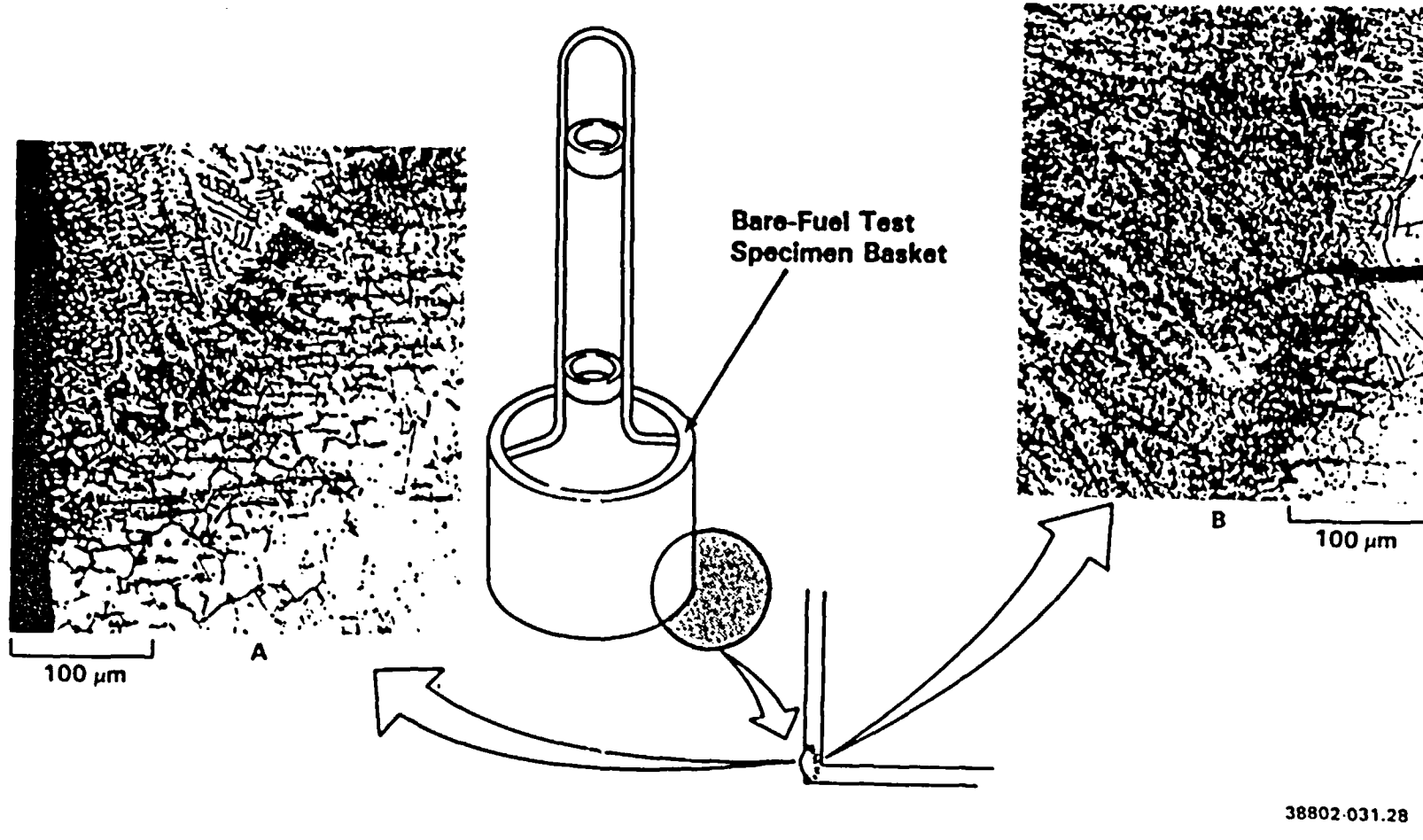

FIGURE 3.4. Metallographic Section of Bottom Weld in Specimen Basket from Cycle 1 of the HBR/BF-85 Test Etched with 10% Oxalic Acid (Neg. 8802279-1)

between the basket bottom plate and cylindrical side. Stress corrosion associated with this region may have been another source for iron dissolution.

Temperature/time conditions that allow precipitation of chromium-carbide phases at the grain boundaries may occur near the weld margins in austenitic stainless steel alloys such as 304. Transformation of the chromium-depleted austenitic stainless steel near the grain boundary to ferritic phase then sensitizes the grain boundaries to corrosion. Based on the apparent corrosion occurring in the 304 stainless steel HBR/BF-85 Cycle 1 vessel, it was decided to fabricate new vessels using 304L stainless steel for Cycle 2. Less of a tendency for such intergranular corrosion should occur with the lower carbon content 304L stainless steel. Data from Cycles 2 and 3 (especially ^{99}Tc data) suggest that corrosion-induced effects comparable to those observed in the HBR/BF-85 Cycle 1 test did not occur with the 304L stainless steel vessels.

3.2.3 Uranium Quantities in Sample Types

The quantities of uranium measured in the various liquid sample types are given in Table 3.1. The largest effect shown by these data is the much greater apparent release from bare-fuel in comparison to that from fuel still tightly confined in defected cladding. Much of the difference comes from the uranium measured in the rinse and strip samples in the bare-fuel tests that, as previously discussed in Section 3.1.3, are of questionable significance, since the portion of precipitated secondary uranium phases undissolved in the rinse solutions and the quantity of previously undissolved fuel fines dissolved in the strip solutions are not known. There was no evidence that grains of undissolved fuel or significant amounts of nuclide-containing secondary-phase particles were contained in the rinse or strip solutions from the three clad-specimen tests. Another observation on the bare-fuel rinse and strip sample data is that a greater portion of the measured uranium in these samples was contained in the rinse samples at 25°C in comparison to the 85°C tests. This correlation was also noted for the other actinides. This effect is explained by the hypothesis that actinides precipitated from the 85°C tests transformed to more stable crystalline phases exhibiting lower solubility in the rinse solution versus the 25°C test where less secondary-phase formation occurred, and the phases that did form may not have completely transformed to the more stable mineral states.

TABLE 3.1. Quantities of Uranium Measured in Samples (μg)

	HBR/BF-25	TP/BF-85	HBR/BF-85	HBR/SD-85	HBR/HD-85	HBR/UD-85
Cycle 1						
Periodic Samples	485	263	643	2.02	1.30	1.21
Final Solution	57.5	82.5	5.5	2.50	1.75	3.25
[U (ppm)]	(0.23)	(0.33)	(0.02)	(0.010)	(0.007)	(0.013)
Rinse	396	108	330	<0.6	66	0.6
Acid Strip	405	6330	4950	30	4.8	2.4
Cycle Total	1343	6784	5928	35.1	74	7.5
+ 10^{-5} Inv.	1.86	9.35	8.75	0.05	0.11	0.01
% in Solution	40.4	5.1	10.9	12.9	4.1	59.8
Cycle 2						
Periodic Samples	76.9	29.6	90.0	0.26	0.32	0.29
Final Solution	70.0	32.5	30.0	2.25	2.00	2.00
[U (ppm)]	(0.28)	(0.13)	(0.12)	(0.009)	(0.008)	(0.008)
Rinse	576	66	78	4.2	2.4	3.6
Acid Strip	159	810	1860	3.9	3.3	3.6
Cycle Total	882	938	2058	10.6	8.0	9.5
+ 10^{-5} Inv.	1.24	1.31	3.09	0.015	0.012	0.013
% in Solution	16.7	6.6	5.8	23.7	28.9	24.1
Cycle 3						
Periodic Samples	15.8	10.8	9.5	--	--	--
Final Solution	95.0	47.5	45.0	2.25	2.25	2.00
[U (ppm)]	(0.38)	(0.19)	(0.18)	(0.009)	(0.009)	(0.008)
Rinse	660	78	84	--	--	--
Acid Strip	24.9	480	(a)	--	--	--
Cycle Total	769	616	(a)	--	--	--
+ 10^{-5} Inv.	1.13	0.87	(a)	--	--	--
% in Solution	13.9	9.5	(a)	--	--	--
Sum of Cycles 1, 2 & 3						
Σ Cycle Totals	3021	8338	>8125	45.7[b]	82[b]	17[b]
+ 10^{-5} Inv.	4.23	11.53	>12.04	0.063[b]	0.12[b]	0.023[b]

(a) Cycle 3 HBR/BF-85 acid strip appears to have been contaminated by fuel particles.
(b) Cycles 1 and 2 only.
NOTE: Periodic samples, final solution and bare fuel rinse values are based on 0.4-μm filtered data. Other values are based on unfiltered data.

The acid strip solution from Cycle 3 of the HBR/BF-85 test in particular was anomalous in its high nuclide content. On first analysis, 18.3 mg of uranium were indicated as being dissolved in this solution. A second aliquot taken and analyzed a few weeks later indicated that 116 mg of uranium had dissolved in this solution. Since the average bare-fuel particle in the test weighed 100 to 200 mg, it appears likely that one of these particles was left in the vessel when it was acid-stripped and was not yet completely dissolved when the first aliquot was taken for analysis.

3.3 SECONDARY PHASE CHARACTERIZATION

After removing the rinse solution sample for analysis, the remaining rinse solution was stirred to get settled particles temporarily into suspension and then filtered through a 0.4-μm filter. The weights of solid residues collected on the filters are given in Table 3.2 along with identification of the filters that were examined by SEM and XRD. The SEM examination included energy dispersive X-ray (EDX) analysis of observed particles and residues. The most abundant phase observed on rinse filters from the bare-fuel tests was individual grains or small particles of fuel. Grains at the fuel particle surfaces were apparently loosened as a result of grain boundary dissolution during the tests and removed by the rinsing procedure.

Quantities of acicular crystalline phases (Figure 3.5) indicated by EDX analyses to have a calcium-uranium-silicate composition were observed on rinse filters from Cycles 1 and 2 of the TP/BF-85 test and on the rinse filter from Cycle 2 of the HBR/BF-85 test. Flakes of material indicated as having different calcium-uranium-silicate composition richer in silicon (Figure 3.6)

TABLE 3.2. Residues Collected on Rinse Filters (mg)

Cycle	HBR/BF-25	TP/BF-85	HBR/BF-85	HBR/SD-85	HBR/HD-85	HBR/UD-85
1	6.1	10.0s,x	8.8s	0.4	0.8	1.2s
2	4.7s	20.8s,x	11.5s,x	1.2	0.7	1.9s
3	6.2	9.9	8.5			

s = examined by SEM
x = examined by XRD

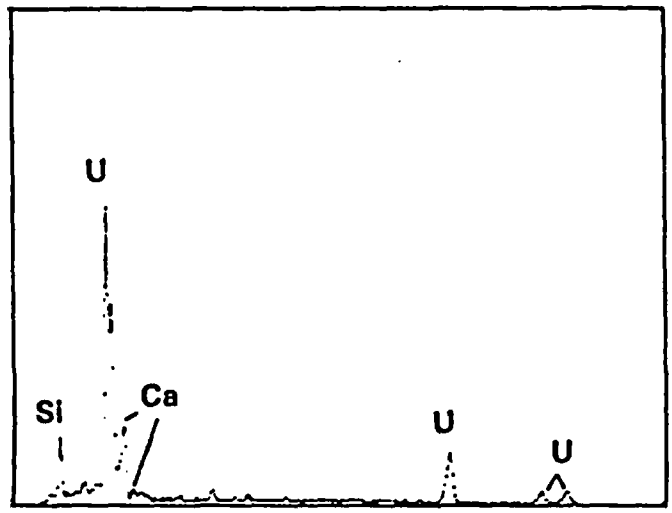

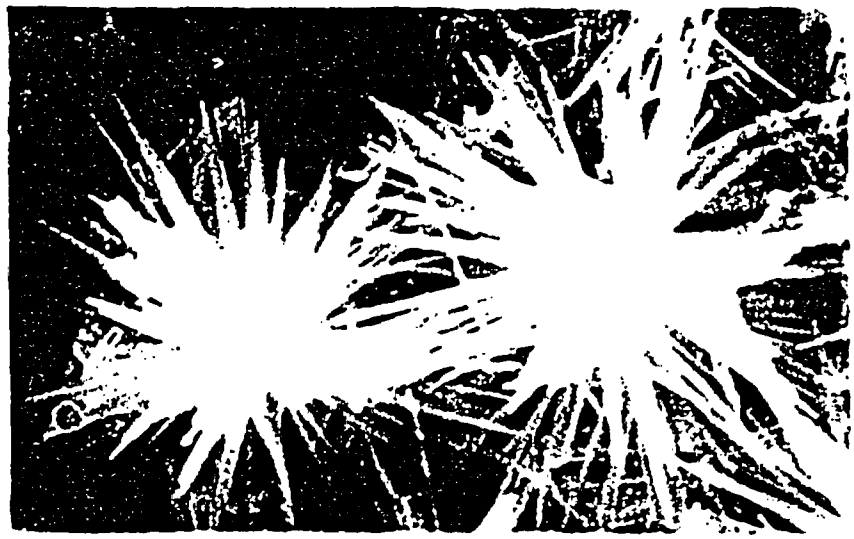

FIGURE 3.5. SEM Photograph and EDX Spectrum of Calcium-Uranium-Silicate Phase with Acicular Crystal Morphology on Rinse Filter from TP/BF-85 Cycle 1 Test (SEM Neg. 3085)

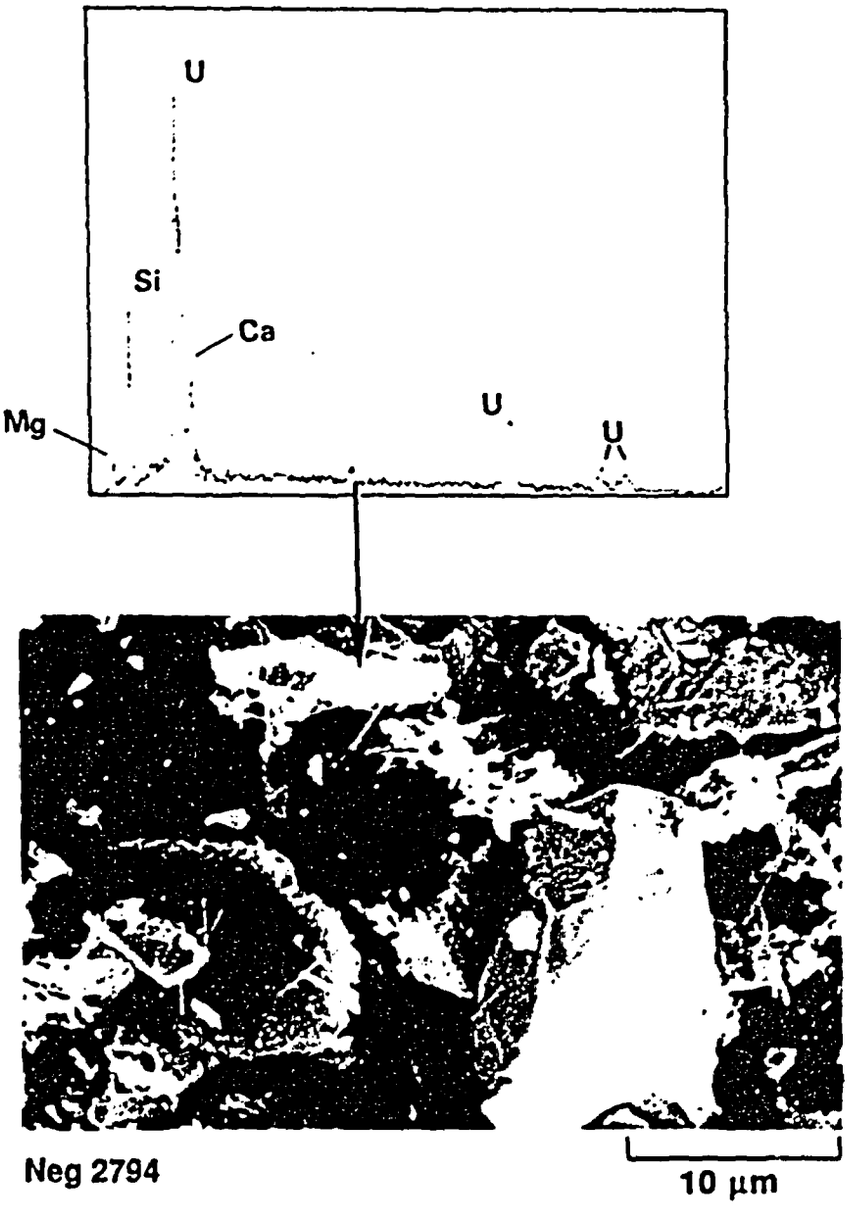

FIGURE 3.6. SEM Photograph and EDX Spectrum of Calcium-Uranium-Silicate Phase with Massive Flake Morphology on Rinse Filter from TP/BF-85 Cycle 2 Test (SEM Neg. 2794)

were also observed. The XRD patterns from these three rinse filters were extensively compared with reference Joint Committee on Powder Diffraction Standards (JCPDS) powder diffraction patterns for identification of possible uranium-containing secondary phases. Indexing data for lines identified in the XRD patterns by the diffractometer computer are tabulated in Appendix C. Confirmed and other possible uranium phases indicated by the XRD data are identified in Table 3.3. The acicular crystalline phase shown in Figure 3.5 is most likely uranophane and the higher silicon content phase shown in Figure 3.6 is likely a haiweeite phase.

The XRD pattern obtained from a piece of the HBR/BF-85 Cycle 2 rinse filter is shown in Figure 3.7 with reference stick patterns for uranophane and UO_2. The UO_2 lines are identified by a "U" and the uranophane lines by a "UP" in the sample pattern, providing an excellent match for all but one of the significant lines. The weak low-angle line identified as "H" was best matched by the 100% intensity 002 line (d = 9.30 Å) of the JCPDS No. 13-118 ranquilite pattern and was next closely matched by the 100% intensity line (d = 9.26 Å) in the JCPDS No. 12-721 haiweeite pattern. The symbol "H" was given to this low angle peak since ranquilite was renamed as haiweeite in the 1987 JCPDS files, and three of the four "haiweeite" patterns in the 1987 files have their most intense peak near this location.

The XRD pattern from the TP/BF-85 Cycle 1 rinse filter shown in Figure 3.8 was the weakest of the three patterns. There are two strong non-UO_2 lines in this pattern. The lower angle line identified as "H" is at the same position as the "H" line discussed above in the HBR/BF-85 Cycle 2 rinse filter pattern and is most closely matched by the 002 line of the JCPDS No. 13-118 ranquilite pattern. The position of the higher angle non-UO_2 line corresponds to a lattice spacing of d = 3.36 Å. Possible matches for this line are the 30% intensity 042 line of the JCPDS 13-118 ranquilite pattern and the 80% intensity 220 line in the JCPDS 26-1392 soddyite pattern, both with d = 3.34 Å. Another possible match is the 100% intensity line at d = 3.38 Å in the JCPDS 17-462 calcium-ursilite pattern. Major lines in all of these patterns are, however, missing from the sample pattern. A possible explanation for the missing lines would be preferred orientation on the filter

TABLE 3.3. Probable Phases Indicated by XRD on Bare-Fuel Rinse Filters

Mineral Name	Chemical Formula	JCPDS No.[a]	Status[b]
Uraninite	UO_2	5-550[i]	C
Uranophane	$CaO \cdot 2UO_3 \cdot 2SiO_2 \cdot 6H_2O$	8-442[i]	C
Ranquilite[c]	$1.5CaO \cdot 2UO_3 \cdot 5SiO_2 \cdot 12H_2O$	13-118[i]	L
Haiweeite	$CaO \cdot 2UO_3 \cdot 6SiO_2 \cdot 5H_2O$	12-721[o]	P
Ursilite[c]	$2CaO \cdot 2UO_3 \cdot 5SiO_2 \cdot 9H_2O$	17-462[o]	P
Soddyite	$2UO_3 \cdot SiO_2 \cdot 2H_2O$	26-1392*	P

(a) JCPDS data quality ratings: * = Best, i = Intermediate, o = Low.
(b) C = Confirmed, L = Likely, P = Possible.
(c) Renamed as haiweeite in the 1987 JCPDS files.

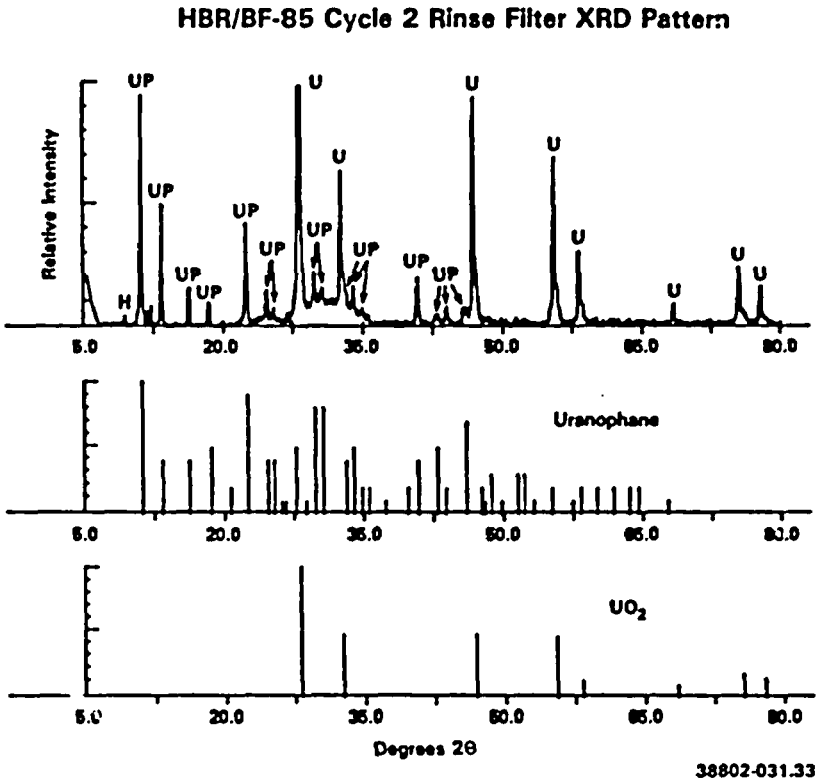

FIGURE 3.7. XRD Pattern of Rinse Filter from HBR/BF-85 Cycle 2 Test. (UP = Uranophane, U = UO_2, and H = Haiweeite.) (Neg. 90032144-14)

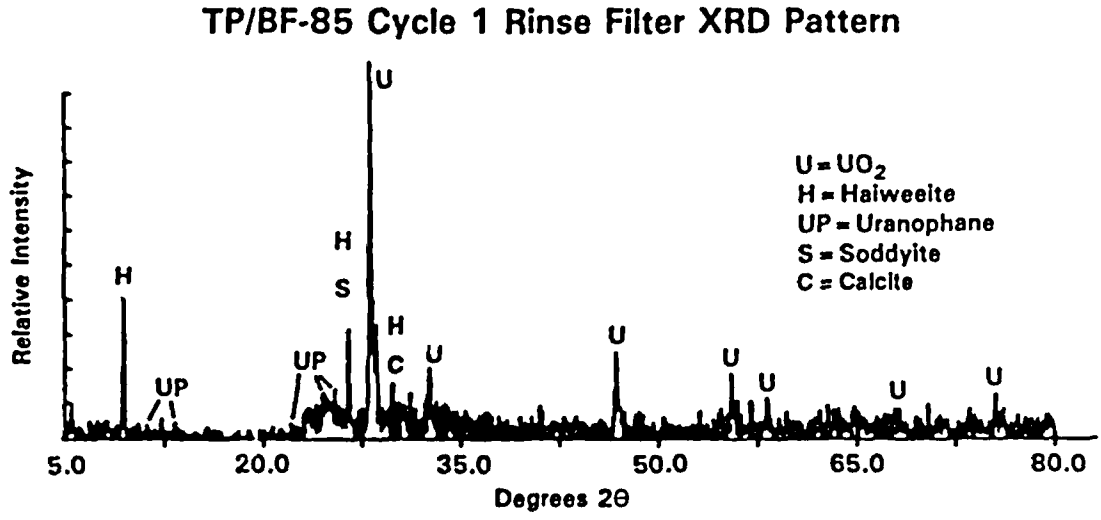

FIGURE 3.8. XRD Pattern of Rinse Filter from TP/BF-85 Cycle 1 Test. (UO_2 lines are identified as "U" and a haiweeite line as "H". The "HS" line may be haiweeite and/or soddyite.) (Neg. 90032144-16)

sample. The higher angle line has tentatively been labeled "H" and "S" because it could result from one of the "haiweeite" phases, soddyite, or some combination of these phases. Soddyite formation in this test would correlate with the lower solution calcium concentrations measured (1.1 μg/mL) and may explain why uranium concentrations stabilized at higher levels than in Cycles 2 and 3. A weaker non-UO_2 line identified at d = 3.121 Å could be a haiweeite or calcite line. The location of possible uranophane lines too weak for identification by the diffractometer computer are also shown.

The XRD pattern from the TP/BF-85 Cycle 2 rinse filter is shown in Figure 3.9. The same low angle "haiweeite" line observed in the HBR/BF-85 Cycle 2 and TP/BF-85 Cycle 1 rinse filters is present. Three other weak lines marked "H" correspond to line positions in the JCPDS 13-118 ranquilite pattern. Most of the remaining significant lines appear to be from uranophane or UO_2. In general, the XRD evidence for haiweeite formation in the 85°C bare-fuel tests is not as convincing as that for uranophane.

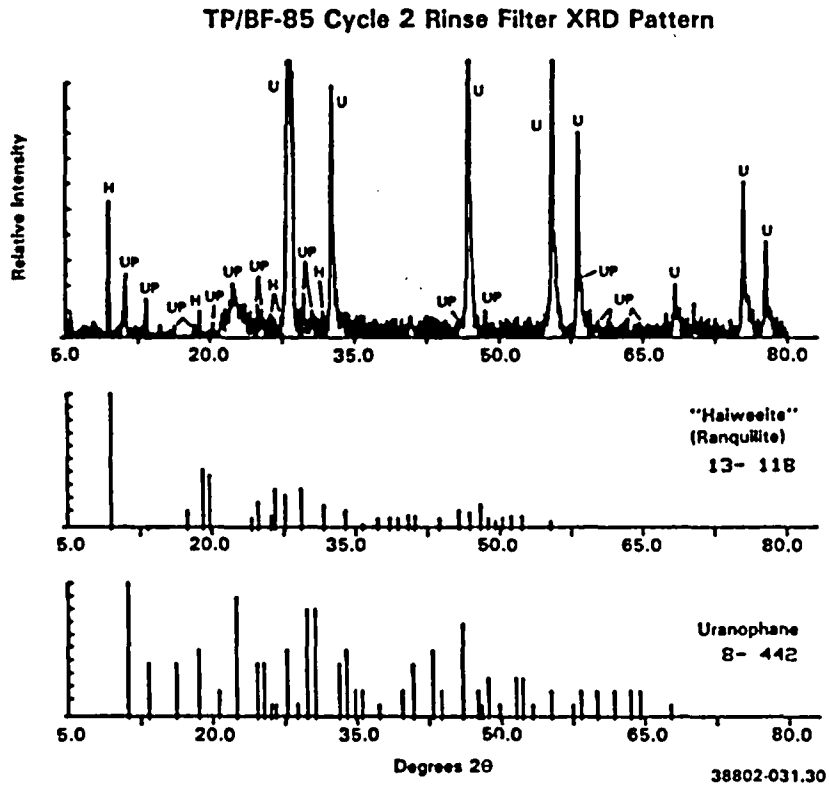

FIGURE 3.9. XRD Pattern of Rinse Filter from TP/BF-85 Cycle 2 Test. (UO_2 lines are identified as "U", uranophane lines as "UP," and haiweeite lines tentatively as "H." JCPDS patterns for uranophane and the "haiweeite" mineral ranquilite are shown below.) (Neg. 90032144-13)

Other phases such as calcite, dolomite, and SiO_2 (possibly as amorphous gel) also appear to be likely in all the rinse filters based on the SEM data and probably account for most of the rinse filter residue mass in the three clad fuel-specimen tests. White scale formation at the waterline was noted in all of the 85°C tests at cycle termination. No waterline scale formation was observed in the HBR/BF-25 test. As indicated by the solution chemistry data tabulated in Appendix B, significant drops in calcium, magnesium, silicon, and HCO_3 concentrations occurred in the five 85°C tests but not in the HBR/BF-25 test.

Formation of the secondary phases dolomite, calcite, quartz, haiweeite, and soddyite during spent-fuel dissolution in J-13 well water has been

predicted by the EQ3/6 geochemical model.[14] Thermodynamic properties of uranophane need yet to be determined for addition to the EQ3/6 database. There was no evidence in the examined rinse filters of schoepite ($UO_3 \cdot 2H_2O$) formation, which is predicted to occur eventually as fuel dissolution progresses. Further depletion of silicon concentration followed by increasing uranium concentration (expected prior to schoepite formation) was not observed. The observed uranium concentrations, solution chemistry data, and secondary-phase formation data are relatively consistent with EQ3/6 predictions. However, the solids characterizations data to date are considered limited. In particular, phases containing other important nuclide elements such as plutonium, americium, and curium, which either did not dissolve or dropped out of solution, have not been confirmed or identified.

3.4 PLUTONIUM

Plutonium isotopes account for about 45% of the ORIGEN-2 calculated activity of spent fuel at 1,000 yr and about 90% of the activity at 10,000 yr. Plutonium is thought to be in solid solution at a concentration on the order of 1% in the spent fuel UO_2 matrix phase. The principal isotopes accounting for most of the postcontainment period plutonium alpha activity are ^{239}Pu (24,000-yr half-life) and ^{240}Pu (6,570-yr half-life) that, because of their very similar alpha decay energies, are measured together as $^{239+240}Pu$ activity. In the relatively young spent fuel used in the current testing, ^{241}Pu (14.4-yr half-life) accounts for about 92% of the total actinide activity and about 22% of the total actinide plus fission product activity.

Activities of $^{239+240}Pu$ measured in 0.4-μm filtered solution samples are plotted in Figure 3.10. During Cycle 1 of the bare-fuel tests, plutonium rapidly reached maximum activities and then dropped out of solution, with the greatest decreases in activity occurring in the 85°C tests. Relatively stable steady-state activities on the order of 100 pCi/mL (~1 ppb or $10^{-8.4}$ M plutonium) were measured at 25°C in Cycles 2 and 3 of the bare-fuel tests versus much lower activities on the order of 1 pCi/mL (~0.01 ppb or $10^{-10.4}$ M plutonium) measured at 85°C. Lower actinide activities in solution at 85°C are attributed to faster kinetics for formation of solubility-limiting secondary phases at the higher temperature. Even lower activities ranging from about

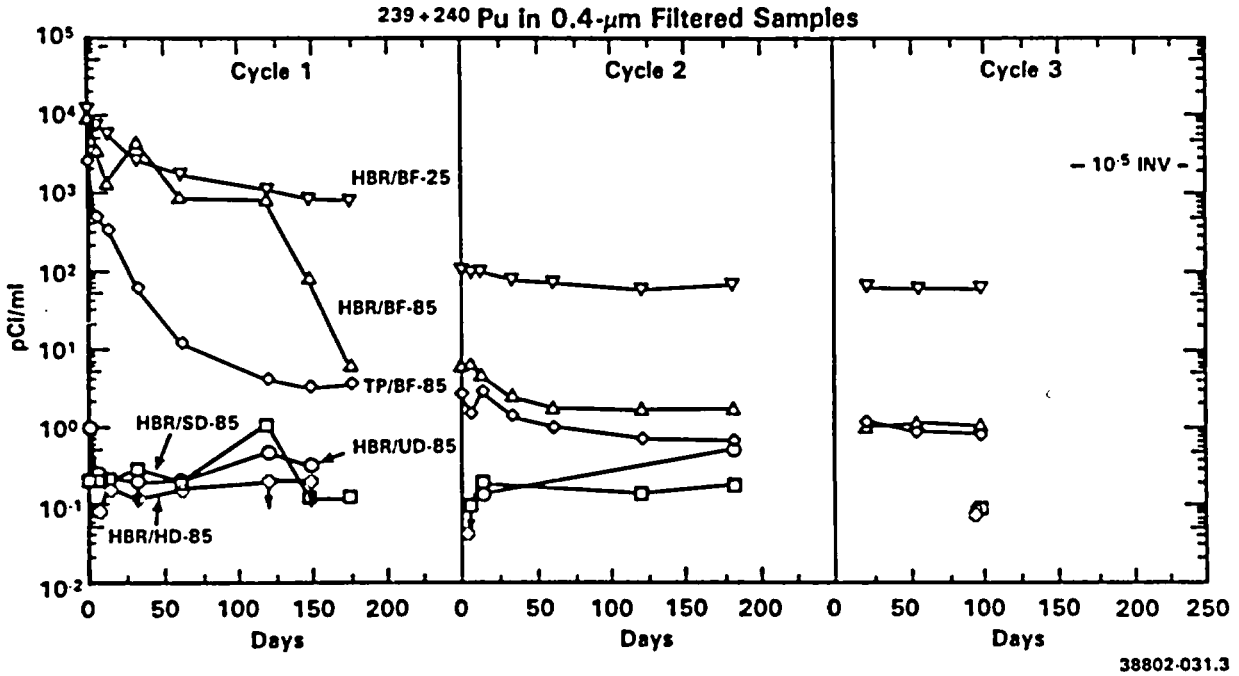

FIGURE 3.10. Activity of $^{239+240}Pu$ in 0.4-μm Filtered Solution Samples

0.1 to 1 pCi/mL, which were not much above the $^{239+240}Pu$ detection limit, were measured in the 85°C tests using fuel in defected cladding and undefected cladding.

The 0.4-μm filtered $^{239+240}Pu$ solution sample data from the Series 3 bare-fuel tests are compared to that from the Series 2 bare-fuel tests in Figure 3.11. The effects of sealed stainless steel versus unsealed silica vessels are relatively small compared to the effect of temperature. Activities measured near the end of each cycle of three 25°C bare-fuel tests ranged from about 900 pCi/mL ($10^{-7.4}$ M plutonium) in Cycle 1 of the Series 3 test down to about 30 pCi/mL ($10^{-8.9}$ M plutonium) in Cycle 2 of the HBR Series 2 test. These results agree very well with those reported by Rai and Ryan[15], who measured the solubility of PuO_2 and hydrous $PuO_2 \cdot xH_2O$ in deionized water suspensions aged for up to 1,300 d at 25°C. At a pH of 8, which was the extrapolated lower limit of their data and the approximate pH in the Series 2 and 3 tests, they report that plutonium concentration ranged from about

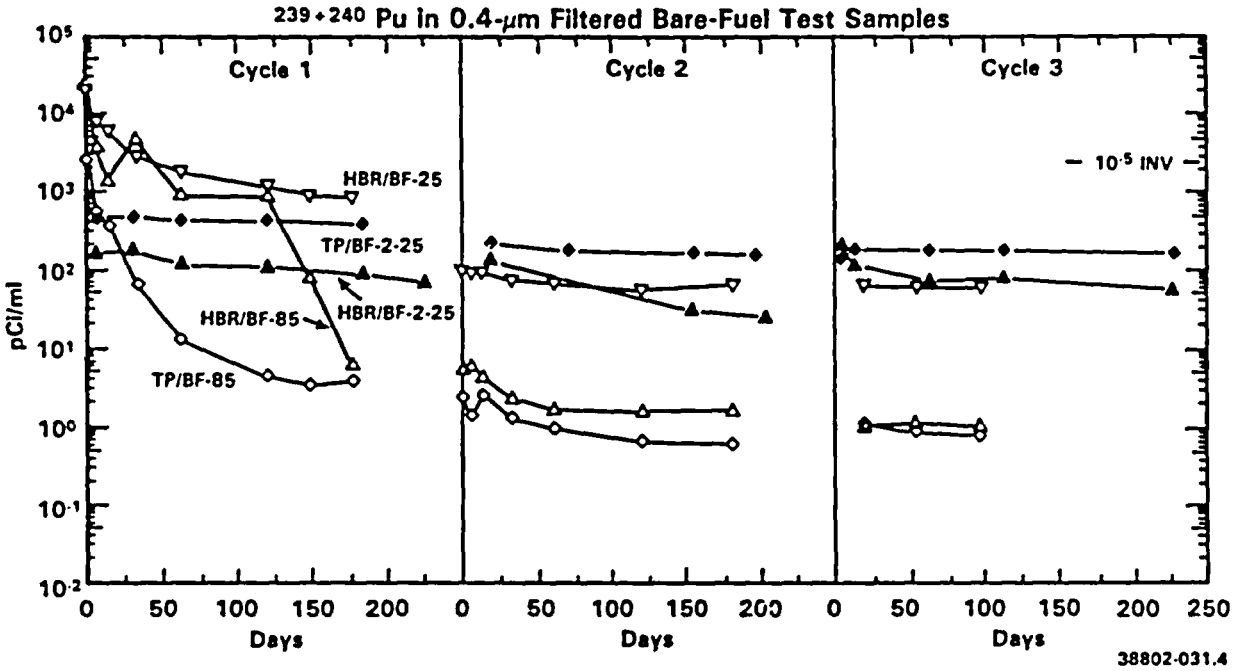

FIGURE 3.11. Comparison of $^{239+240}Pu$ Activities Measured in 0.4-μm Filtered Samples from the Three Series 3 and Two Series 2 Bare-Fuel Tests

$10^{-7.4}$ M, where amorphous $PuO_2 \cdot xH_2O$ was thought to be controlling concentration, down to about 10^{-9} M, where aging to a more crystalline PuO_2 was thought to reduce Pu concentration. Samples were 0.015 μm or 18-Å filtered.

The effect of sample filtration on $^{239+240}Pu$ activities measured in solution samples from the bare-fuel tests are shown in Figure 3.12. The effect of 0.4-μm filtration was generally slight, except in Cycle 3 of the 85°C tests, where the effect diminished with time. The 18-Å filtration was conducted only through the 34-d Cycle 2 sample. Approximately 80% of the activity in the later HBR/BF-25 Cycle 1 0.4-μm filtered samples was retained by the 18-Å filters, with this percentage dropping to about 40% in Cycle 2. The greatest filtration effect was observed during the HBR/BF-85 Cycle 1 test, where 99.86% of the 0.4-μm filtered activity in the 119-d sample was retained by the 18 Å filter, which may be another anomaly of the vessel corrosion that occurred in this test. Plutonium may have been adsorbed on a finely dispersed iron-silica phase that formed in this test, floccules of which were shown in Figure 3.3. An order of magnitude reduction in activity was also observed for

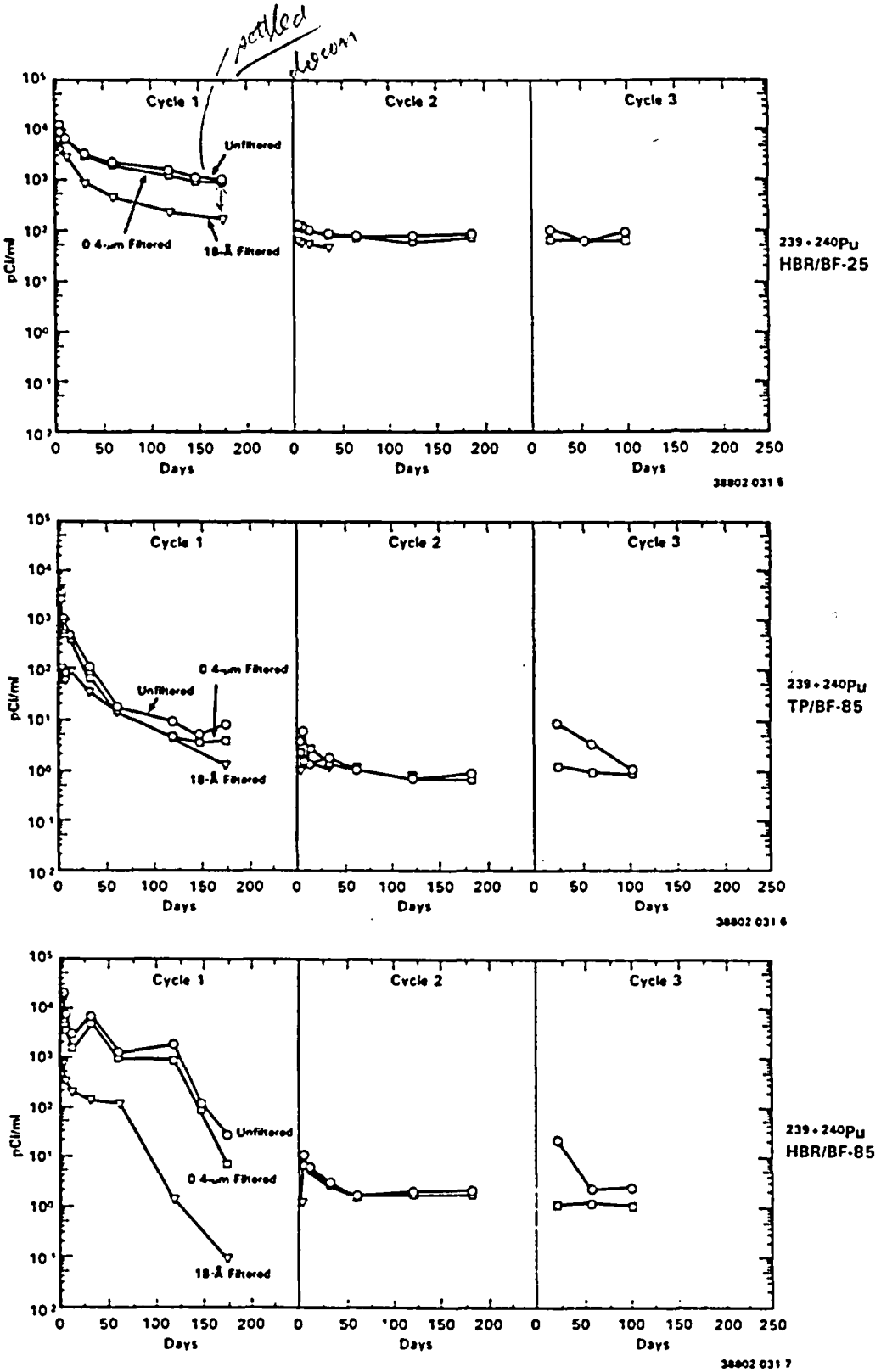

FIGURE 3.12. Effects of Filtration on Measured $^{239+240}Pu$ Activity in Solution Samples from the Bare-Fuel Tests

the initial 18-Å filtered samples from the TP/BF-85 Cycle 1 test. Except as noted, the effects of filtration on measured plutonium activities were in general relatively small. The filtration effects were particularly small during Cycle 2.

Although stable plutonium colloid formation in aqueous systems has been well documented,[15,16] the filtration data do not strongly support colloid formation as a primary factor contributing to solution plutonium content over an extended period. The actual quantities of plutonium released by fuel dissolution during Cycles 2 and 3 were probably on the order of a few micrograms. This relatively small amount of plutonium could have been incorporated in the uranium secondary phases as they formed or may have been associated with other phases that either precipitated or plated out of solution. The data given in Table 3.4 indicate that the majority of the plutonium was measured in the acid strip samples. The greater quantities of plutonium in acid strip solutions from the 85°C bare-fuel tests relative to the 25°C test are probably indicative of a greater amount of fuel dissolution and actinide precipitation at the higher temperature.

3.5 AMERICIUM

At 1,000 yr, ^{241}Am accounts for about half of the gross activity in spent fuel. Americium-241 activity in spent fuel increases during the first ~100 yr after discharge as a result of ^{241}Pu decay and then decreases by alpha decay (432-yr half-life) to ^{237}Np. By 10,000 yr, the only remaining significant americium isotope is ^{243}Am, which accounts for ~3% (including a short-lived ^{239}Np daughter) of the gross 10,000-yr activity. Americium concentration in the spent fuel matrix phase is ~6×10^{-4} g per g of fuel, which is thought to be in solid solution with the matrix phase.

Activity of ^{241}Am measured in 0.4-μm filtered solution samples is plotted in Figure 3.13. The effect of temperature on americium activity in solution is even greater than with plutonium. Relatively stable steady-state ^{241}Am activities on the order of 100 pCi/mL were measured during Cycles 2 and 3 of the 25°C bare-fuel test, which is about the activity level measured for $^{239+240}Pu$ in this test. Activity levels during Cycles 2 and 3 of the 85°C bare-fuel tests dropped to an approximate range of about 0.1 to 0.5 pCi/mL,

TABLE 3.4. Quantities of $^{239+240}Pu$ Measured in Samples (nCi)

	HBR/BF-25	TP/BF-85	HBR/BF-85	HBR/SD-85	HBR/HD-85	HBR/UD-85
Cycle 1						
Periodic Samples	629	57.1	580	<0.078	<0.022	<0.038
Final Solution	229	1.01	1.7	0.034	<0.056	~0.05
[Pu (pg/mL)]	(9660)	(43.2)	(71.4)	(1.43)	(<2.4)	(~2)
Rinse	188	24.3	97	0.081	0.01	~0.6
Acid Strip	1527	3554	5392	37.3	6.0	7.8
Cycle Total	2573	3636	6071	37.5	6.0	8.0
+ 10^{-5} Inv.	4.01	6.04	10.11	0.059	0.01	0.013
% in Solution	33.3	1.60	9.6	0.03	<1.2	~1
Cycle 2						
Periodic Samples	11.2	0.22	0.46	~0.01	--	--
Final Solution	17.7	0.16	0.43	0.045	<0.02	0.135
[Pu (pg/mL)]	(747)	(6.7)	(18.1)	(1.90)	(<1)	(5.7)
Rinse	216	17.0	33.5	0.054	0.08	0.054
Acid Strip	430	1224	1581	6.76	2.4	7.30
Cycle Total	675	1242	1615	6.87	2.5	7.49
+ 10^{-5} Inv.	1.07	2.09	2.74	0.011	0.004	0.012
% in Solution	4.3	0.03	0.05	0.79	--	>1.8
Cycle 3						
Periodic Samples	3.24	0.05	0.06	--	--	--
Final Solution	16.1	0.20	0.26	0.022	0.022	0.022
[Pu (pg/mL)]	(681)	(8.6)	(11.0)	(0.95)	(0.95)	(0.95)
Rinse	233	30.8	26.5	--	--	--
Acid Strip	511	819	(a)	--	--	--
Cycle Total	573	850	(a)	--	--	--
+ 10^{-5} Inv.	1.21	1.44	(a)	--	--	--
% in Solution	2.6	0.03	(a)	--	--	--
Sum of Cycles 1, 2 & 3						
Σ Cycle Totals	4000	5728	>7713	44.3(b)	9.1(b)	15.4(a)
+ 10^{-5} Inv.	6.29	9.57	>12.89	0.07(b)	0.02(b)	0.025(a)

(a) Cycle 3 HBR/BF-85 acid strip appears to have been contaminated by fuel particles.
(b) Cycles 1 and 2 only.
NOTE: Periodic samples, final solution and bare fuel rinse values are based on 0.4-μm filtered data. Other values are based on unfiltered data.

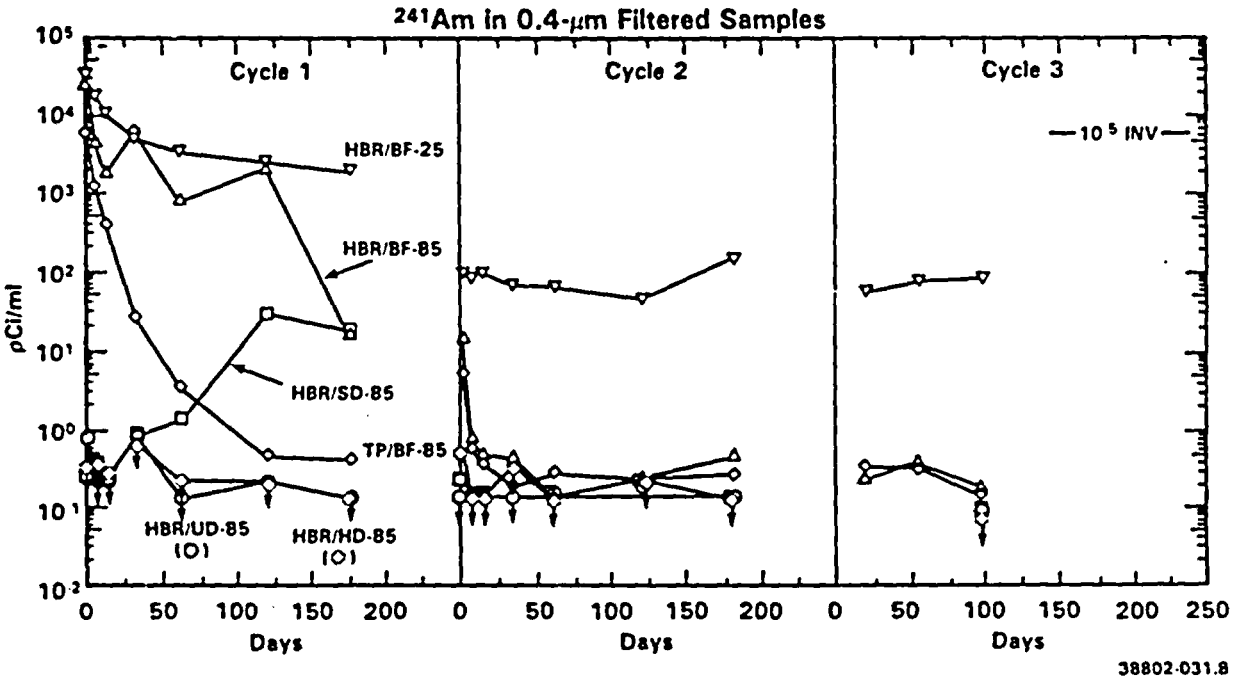

FIGURE 3.13. Activity of ^{241}Am Measured in 0.4-μm Filtered Solution Samples

which was barely above the detection limit. Except for Cycle 1 of the slit-defect test, ^{241}Am activities were generally below detection in the slit-defect, hole-defects, and undefected clad fuel tests. Activity in the slit-defect test reached a maximum value of 31 pCi/mL in the 119-d Cycle sample. Most of this activity was apparently present in solution as fine suspended particles since the 18-Å filtered activity increased only to a barely detectable 0.45 pCi/mL during Cycle 1 of this test.

The 0.4-μm filtered ^{241}Am solution sample data from the Series 3 bare-fuel tests are compared to that from the Series 2 bare-fuel tests in Figure 3.14. As with the plutonium data, these data show very little effect of sealed stainless steel versus unsealed silica vessels on the 25°C americium activity. However, the effect of temperature is again clearly shown. Although relatively stable steady-state activities appeared to be established during individual test cycles at 25°C, these activity levels varied from about 2,000 pCi/mL at the end of Cycle 1 of the Series 3 test down to 11 pCi/mL at the end of Cycle 2 of the Series 2 HBR test. Excluding the Cycle 1 data and the Series 2 Cycle 2 HBR data, the 25°C activities tended to stabilize at

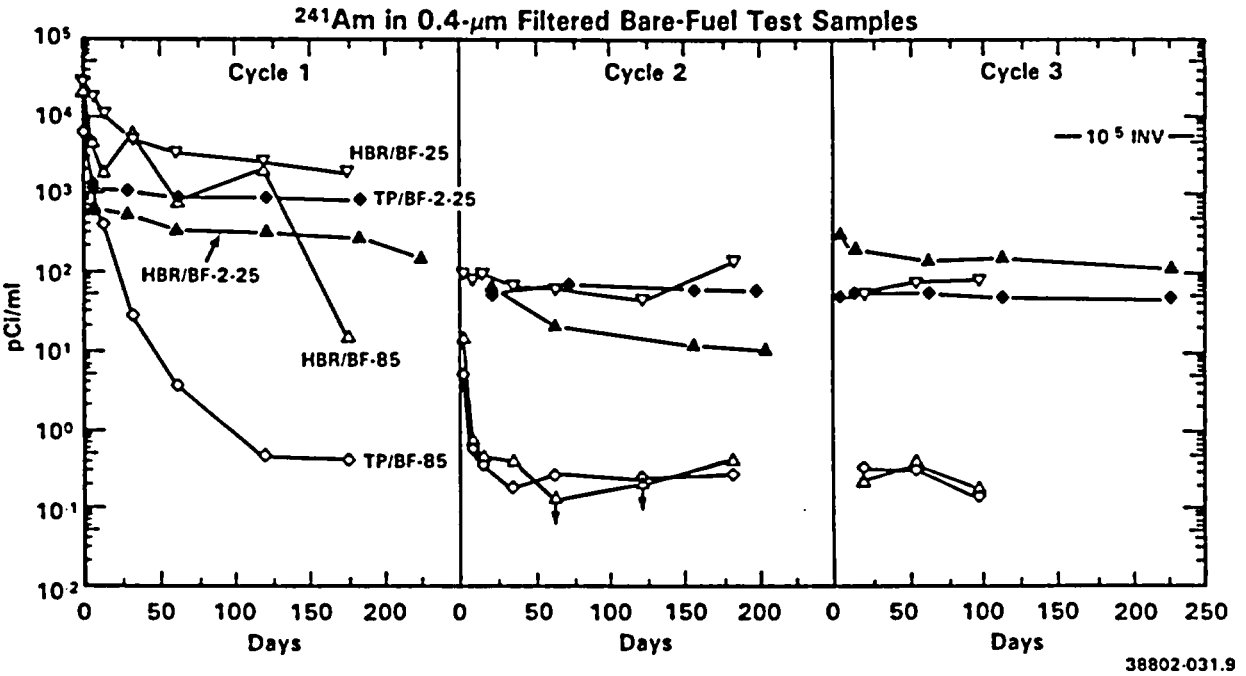

FIGURE 3.14. Comparison of ^{241}Am Activities Measured in 0.4-μm Filtered Samples from the Three Series 3 and Two Series 2 Bare-Fuel Tests

levels on the order of 100 pCi/mL, which corresponds to an americium concentration of $10^{-9.8}$ M. The 85°C activities during Cycles 2 and 3 tended to stabilize at more consistent levels around 0.2 pCi/mL, corresponding to an americium concentration of $10^{-12.5}$ M.

The effects of filtration on ^{241}Am activity measured in solution samples are shown in Figure 3.15 for the bare-fuel tests. The effects of 0.4-μm filtration were small in the 25°C test. However, only a few percent of the 0.4-μm filtered activity was passed by the 18-Å filters in the 25°C test, suggesting that ^{241}Am may have been associated with a colloidal phase at 25°C. The generally much lower ^{241}Am activities reached in all filter fractions at 85°C suggest that a different mechanism may be controlling americium concentrations in the 85°C tests. Americium association with a colloidal phase is also suggested for Cycle 1 of the HBR/BF-85 test in which vessel corrosion anomalies were indicated. Differences between unfiltered and 0.4-μm filtered data in the other 85°C test cycles could indicate formation of low-density suspended floccules or gel structures.

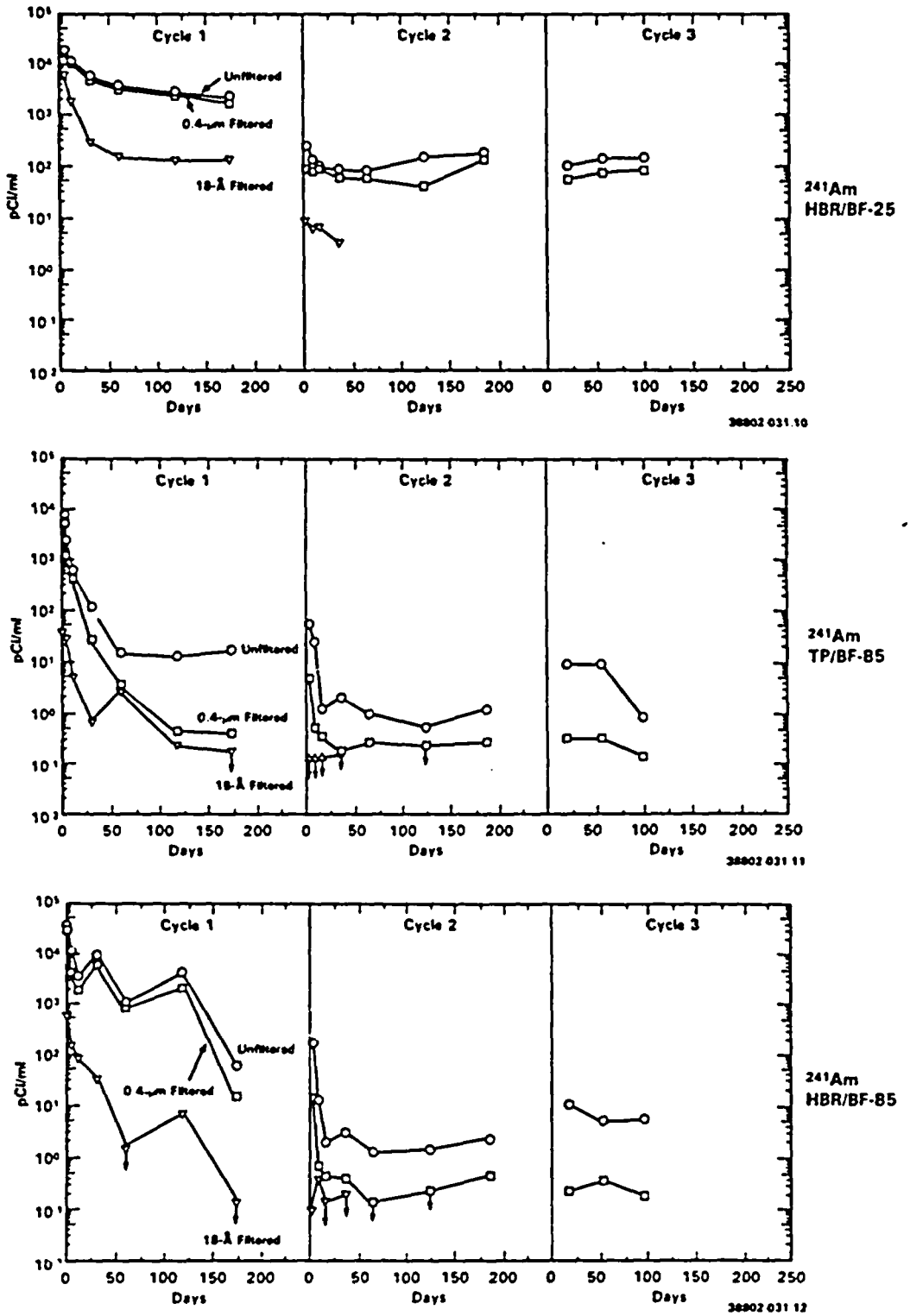

why decrease in unfiltered

FIGURE 3.15. Effects of Filtration on Measured ^{241}Am Activity in Solution Samples from the Bare-Fuel Tests

The data for quantities of ^{241}Am activity measured in the various liquid sample types tabulated in Table 3.5 are somewhat similar in appearance to the data for uranium and $^{239+240}Pu$. Greater ^{241}Am activity was measured in periodic, final solution, and rinse solution samples from the HBR/BF-25 test than in the same samples from the 85°C bare-fuel tests. Lower actinide concentrations in solution at 85°C are attributed primarily to kinetic factors involved in the nucleation and precipitation of stable secondary phases or colloids. The amount of ^{241}Am measured in the HBR/BF-85 Cycle 1 acid strip (15,811 nCi, the largest quantity of ^{241}Am measured) corresponds to only ~5 μg of americium (the americium content of ~9 mg of fuel). Due to the small quantities involved, separation and characterization of secondary phases containing americium in a high concentration would be difficult. If americium is contained in dilute concentration in the more abundant uranium secondary phases, it may be possible to measure ^{241}Am activity in these phases, if they can be separated. The 102 nCi of ^{241}Am measured in the HBR/SD-85 Cycle 1 acid strip indicates that some precipitation or plate-out did occur in response to the increasing ^{241}Am activity observed in unfiltered and 0.4-μm samples in Cycle 1 of this test.

3.6 CURIUM

Curium-244 is one of the five principal alpha-emitting nuclides (along with ^{241}Am, ^{238}Pu, ^{239}Pu, and ^{240}Pu) in the spent fuel specimens tested. One other high-activity actinide isotope in young spent fuel is ^{241}Pu, which beta-decays with a 14.4-yr half-life to ^{241}Am. Of these six principal actinide nuclides occurring in young spent fuel, ^{244}Cm is the second shortest lived, decaying with a 18.1-yr half-life to ^{240}Pu. (Plutonium-238 is the next shortest lived, decaying with a 88-yr half-life to ^{234}U.) After ^{244}Cm has decayed out, the alpha activity contributed by other curium isotopes is minor in comparison to that contributed by americium and plutonium decay. The curium concentration (93% ^{244}Cm) in the spent fuel specimens was about 2×10^{-5} g/g of fuel.

The activity of ^{244}Cm measured in 0.4-μm filtered solution samples is plotted in Figure 3.16. The 0.4-μm filtered ^{244}Cm data from the bare-fuel tests are compared to those from the two Series 2 bare-fuel tests in

TABLE 3.5. Quantities of ^{241}Am Measured in Samples (nCi)

	HBR/BF-25	TP/BF-85	HBR/BF-85	HBR/SD-85	HBR/HD-85	HBR/UD-85
Cycle 1						
Periodic Samples	1241	114.0	926	<0.88	<0.05	<0.06
Final Solution	492	0.10	13.72	4.62	<0.034	<0.034
[Am (pg/mL)]	(724)	(0.15)	(5.5)	(6.8)	(<0.05)	(<0.05)
Rinse	243	47.0	151	0.19	0.14	0.19
Acid Strip	8365	9757	15811	102	5.0	3.5
Cycle Total	10341	9918	16892	107	5.2	3.8
+ 10^{-5} Inv.	6.78	7.68	11.83	0.071	0.004	0.003
% in Solution	16.8	1.15	5.5	5.1	<1.6	<2.4
Cycle 2						
Periodic Samples	10.2	0.104	0.27	<0.027	<0.032	<0.013
Final Solution	38.7	0.068	0.11	<0.034	<0.034	<0.034
[Am (pg/mL)]	(57)	(0.10)	(0.17)	(<0.05)	(<0.05)	(<0.05)
Rinse	239	28.6	63.8	0.24	0.16	0.16
Acid Strip	2027	2784	4608	2.84	2.43	2.7
Cycle Total	2315	2813	4672	3.14	2.66	2.9
+ 10^{-5} Inv.	1.54	2.21	3.32	0.002	0.002	0.002
% in Solution	2.1	0.006	0.008	<2	<2.5	<1.6
Cycle 3						
Periodic Samples	3.42	0.016	0.015	--	--	--
Final Solution	22.0	0.034	0.045	<0.02	<0.022	<0.022
[Am (pg/mL)]	(32)	(0.05)	(0.07)	(<0.03)	(<0.03)	(<0.03)
Rinse	319	61.1	62.7	--	--	--
Acid Strip	1635	1811	(a)	--	--	--
Cycle Total	1979	1872	(a)	--	--	--
+ 10^{-5} Inv.	1.34	1.48	(a)	--	--	--
% in Solution	1.3	0.003	(a)	--	--	--
Sum of Cycles 1, 2 & 3						
& Cycle Totals	14635.	14602	<21627	110(b)	7.8(b)	6.7(b)
+ 10^{-5} Inv.	9.66	11.37	>15.20	0.073(b)	0.006(b)	0.004(b)

(a) Cycle 3 HBR/BF-85 acid strip appears to have been contaminated by fuel particles.
(b) Cycles 1 and 2 only.
NOTE: Periodic samples, final solution and bare fuel rinse values are based on 0.4-μm filtered data. Other values are based on unfiltered data.

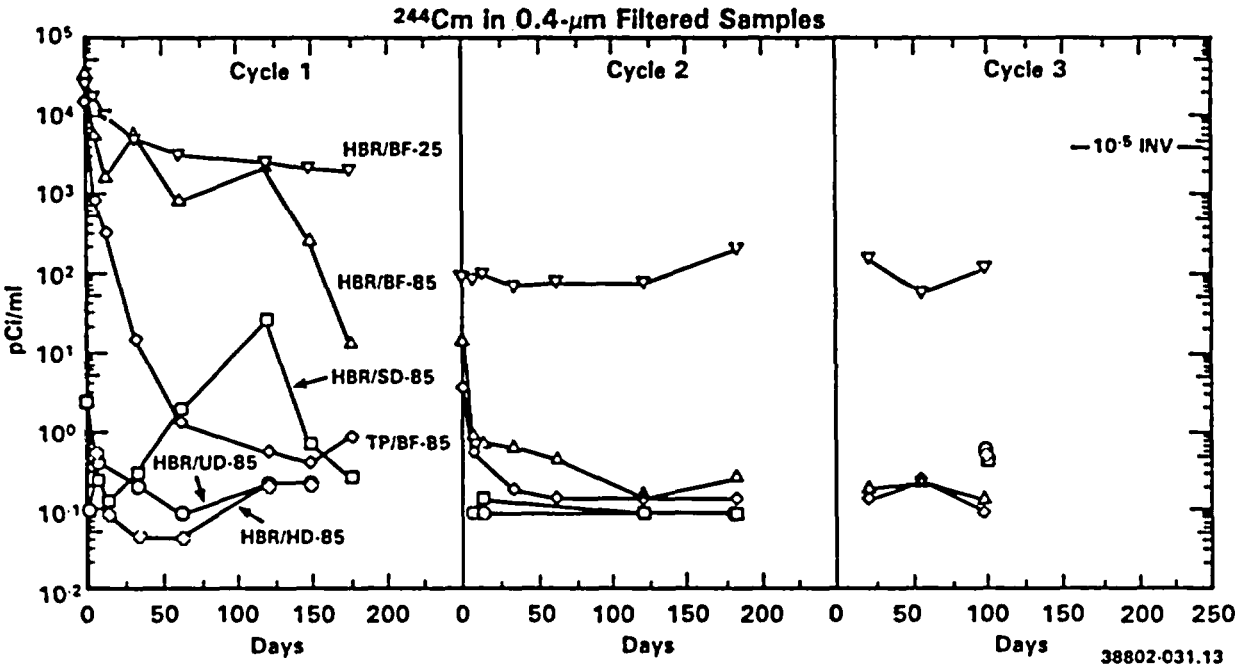

FIGURE 3.16. Activity of ^{244}Cm Measured in 0.4-μm Filtered Solution Samples

Figure 3.17. The effects of filtration on ^{244}Cm measured in solution samples from the bare-fuel tests are shown in Figure 3.18. Quantities of ^{244}Cm measured in different liquid sample types are tabulated in Table 3.6. In terms of activity levels, the ^{244}Cm data are quite similar in appearance to the ^{241}Am data. However, equivalent ^{244}Cm activities correspond to much lower concentrations in comparison to ^{241}Am. During Cycles 2 and 3 of the 25°C bare-fuel tests, ^{244}Cm activity tended to stabilize at levels on the order of 100 pCi/mL, corresponding to a curium concentration of about $10^{-11.1}$ M. At 85°C, ^{244}Cm activity dropped to about 0.1 pCi/mL, corresponding to a curium concentration of about $10^{-14.3}$ M.

During the HBR/SD-85 Cycle 1 test, the 0.4-μm filtered ^{244}Cm activity peaked in the 119-d sample at about 28 pCi/mL and then dropped to about 0.3 pCi/mL by the end of Cycle 1. The 0.4-μm filtered ^{241}Am activity similarly increased during this test but showed much less drop after the 119-d sample. However, the 18-Å filtered activities for both ^{241}Am and ^{244}Cm remained below 0.5 pCi/mL during all of Cycle 1, suggesting that americium and

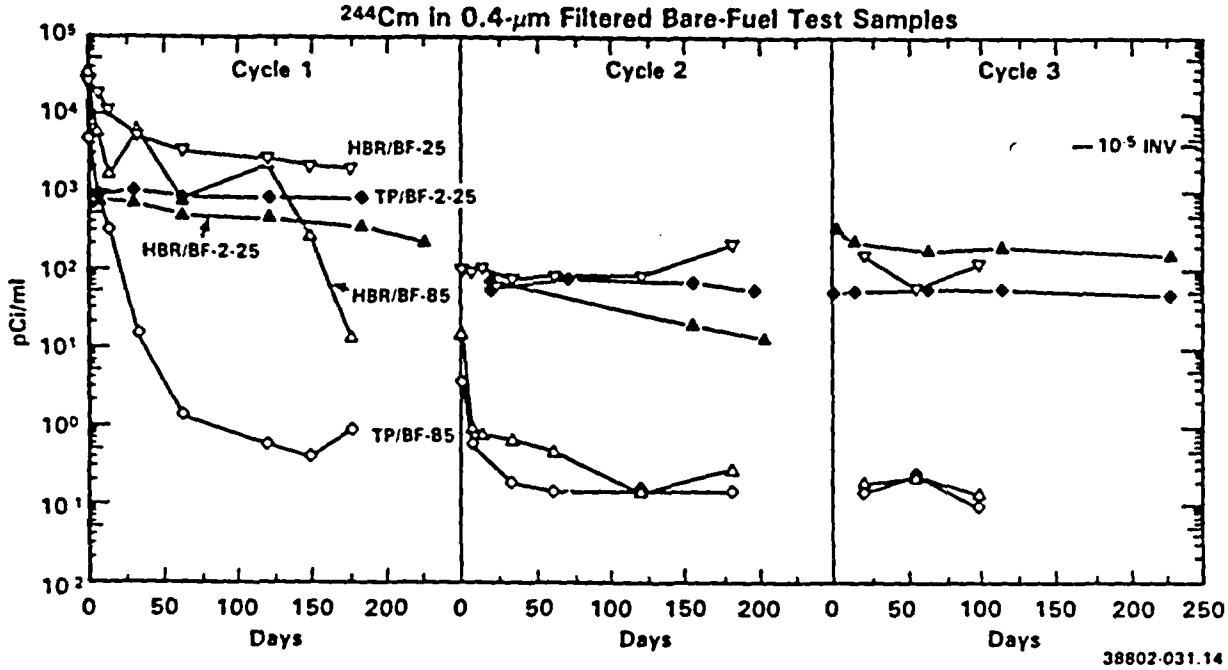

FIGURE 3.17. Comparison of ^{244}Cm Activities Measured in 0.4-μm Filtered Samples from the Three Series 3 and Two Series 2 Bare-Fuel Tests

curium may have been associated with separate finely suspended phases since only ^{244}Cm dropped out in the 0.4-μm filtered samples. In most other respects, the ^{244}Cm data were remarkably similar to the ^{241}Am data.

3.7 NEPTUNIUM

The primary neptunium isotope of concern for repository storage of spent fuel is ^{237}Np. Concentration of neptunium in spent fuel is about 4×10^{-4} g/g of fuel and, at this low concentration, likely remains in solid solution with the fuel matrix phase. With a 2,140,000-yr half-life, ^{237}Np activity is initially relatively low (about 0.24 μCi/g in the test specimens) but increases with time for several thousand years as the product of ^{241}Am decay (432-yr half-life). At 1,000 yr, ^{237}Np activity increases to about 1 μCi/g and accounts for about 0.06% of the total Ci activity in spent fuel. At 10,000 yr, ^{237}Np accounts for about 0.25% of total activity of spent fuel. Neptunium-239 represents a larger fraction of the spent fuel total activity (~0.9 % at 1,000 yr and ~1.4% at 10,000 yr). However, ^{239}Np, with its short

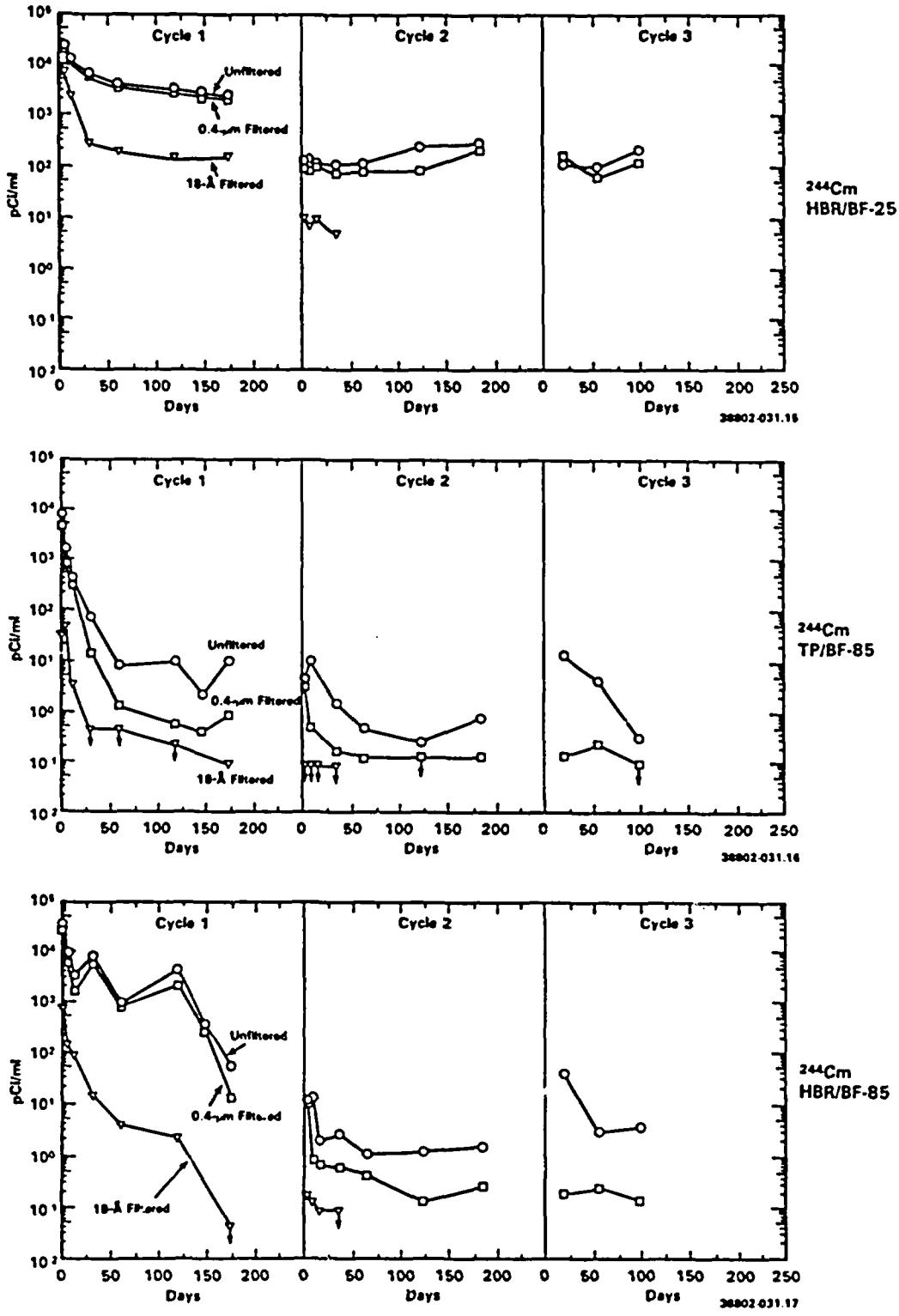

FIGURE 3.18. Effects of Filtration on Measured ^{244}Cm Activity in Solution Samples from the Bare-Fuel Tests

TABLE 3.6. Quantities of ^{244}Cm Measured in Samples (nCi)

	HBR/BF-25	TP/BF-85	HBR/BF-85	HBR/SD-85	HBR/HD-85	HBR/UD-85
Cycle 1						
Periodic Samples	1272	97.9	911	0.81	<0.02	<0.03
Final Solution	512	0.225	3.49	0.068	<0.034	<0.03
[Cm (pg/mL)]	(26)	(0.012)	(0.18)	(0.003)	(<0.002)	(<0.002)
Rinse	243	29.5	134	0.11	0.054	--
Acid Strip	9095	7622	15541	99	4.2	2.8
Cycle Total	11122	7949	16589	100	4.3	2.9
+ 10^{-5} Inv.	10.08	9.15	16.06	0.091	0.004	0.003
% in Solution	16.0	1.27	5.5	0.88	<1.2	<1.7
Cycle 2						
Periodic Samples	11.5	0.138	0.29	<0.007	--	--
Final Solution	53.8	0.034	0.068	<0.023	--	<0.023
[Cm (pg/mL)]	(2.8)	(0.002)	(0.003)	(<0.001)	--	(<0.001)
Rinse	189	22.2	63	0.054	0.1	0.054
Acid Strip	2284	2162	4324	2.84	1.8	2.57
Cycle Total	2538	2184	4388	2.92	1.9	2.64
+ 10^{-5} Inv.	2.34	2.62	4.32	0.0027	-0.002	0.0024
% in Solution	2.6	0.008	0.008	<1	--	<0.85
Cycle 3						
Periodic Samples	5.5	0.009	0.010	--	--	--
Final Solution	31.0	<0.023	0.034	0.11	0.13	0.146
[Cm (pg/mL)]	(1.6)	(<0.001)	(0.002)	(0.006)	(0.007)	(0.008)
Rinse	273	42.2	52.7	--	--	--
Acid Strip	1554	1239	(a)	--	--	--
Cycle Total	1863	1281	(a)	--	--	--
+ 10^{-5} Inv.	1.74	1.55	(a)	--	--	--
% in Solution	2.0	<0.003	(a)	--	--	--
Sum of Cycles 1, 2 & 3						
Σ Cycle Totals	15524	11215	21030	102(b)	6.2(b)	5.5(b)
+ 10^{-5} Inv.	14.16	13.32	20.43	0.094	0.006(b)	0.005(b)

(a) Cycle 3 HBR/BF-85 acid strip appears to have been contaminated by fuel particles.
(b) Cycles 1 and 2 only.
NOTE: Periodic samples, final solution and bare fuel rinse values are based on 0.4-μm filtered data. Other values are based on unfiltered data.

half-life (~2 d), is a transient state in the ^{243}Am to ^{239}Pu decay chain. Although a small portion of the total activity, neptunium is of concern because it has been predicted to be the most soluble of the alpha-emitting actinides under NNWSI repository conditions[17] and will be present for a very long time.

Activities of ^{237}Np measured in 0.4-μm filtered samples from the three bare-fuel tests are plotted in Figure 3.19. The effects of filtration on ^{237}Np activity are shown in Figure 3.20. Only data from the bare-fuel tests are plotted, since ^{237}Np activities were generally below detection in the tests using clad fuel. After an initial apparent supersaturation in Cycle 1, ^{237}Np activity drops to a range of about 0.1 to 0.5 pCi/mL during Cycles 2 and 3. The solution activity data do not show a significant dependence on temperature or filtration. Scatter in the data shown in Figures 3.19 and 3.20 is attributed primarily to counting statistics for the low activities being measured. A ^{237}Np activity of 0.2 pCi/mL, which is about the middle of the range measured in Cycles 2 and 3, corresponds to a neptunium concentration of

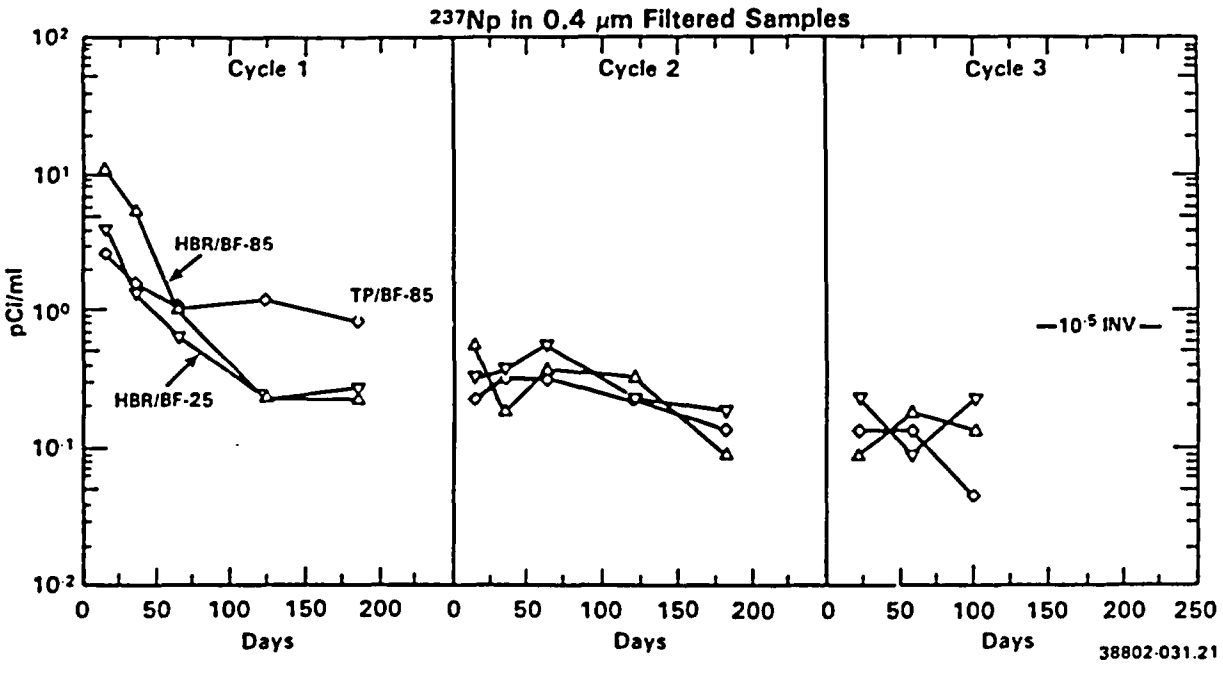

FIGURE 3.19. Activity of ^{237}Np Measured in 0.4-μm Filtered Solution Samples from the Bare-Fuel Tests

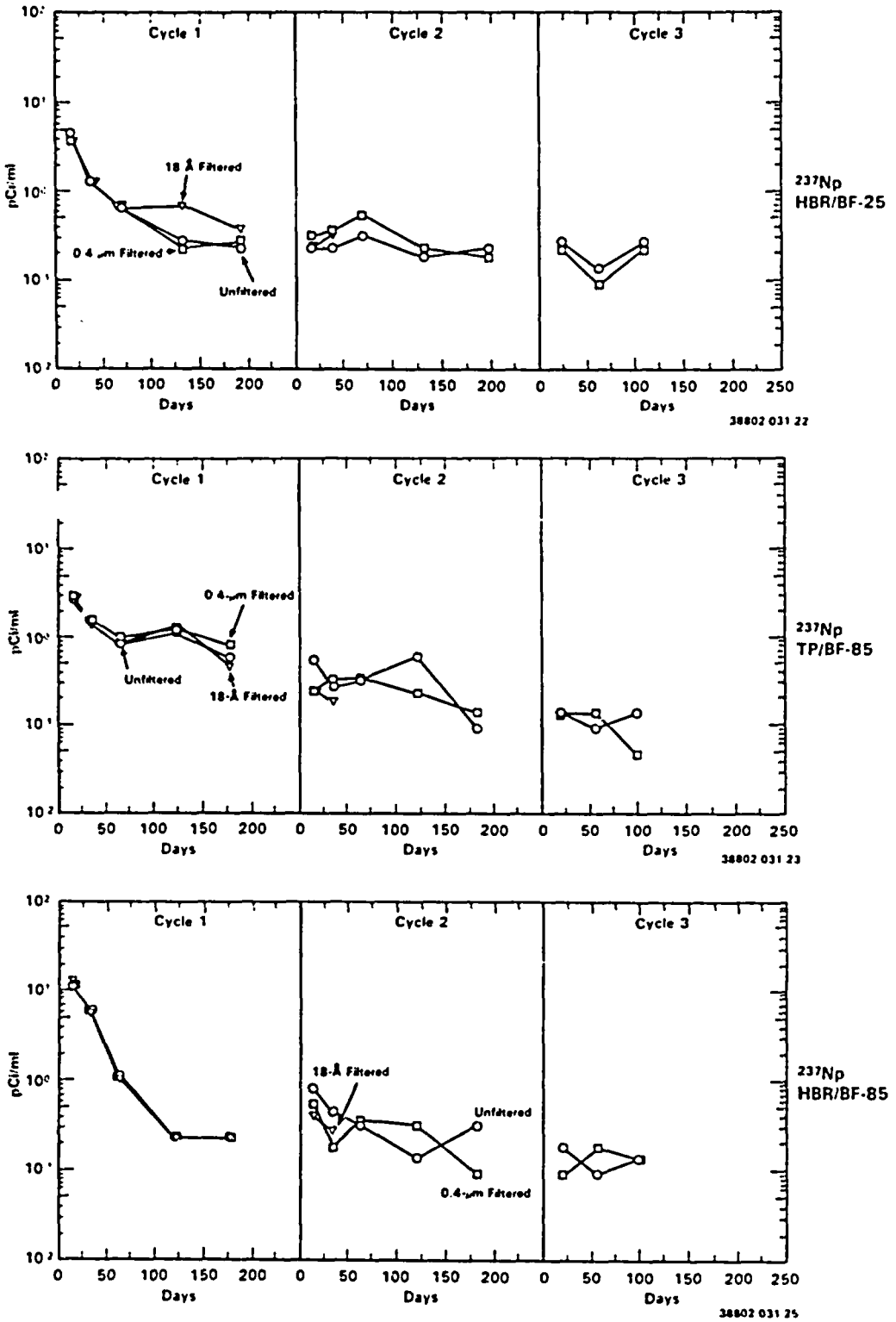

FIGURE 3.20. Effects of Filtration on Measured ^{237}Np Activity in Solution Samples from the Bare-Fuel Tests

about $10^{-8.9}$ M. The absense of significant effects of filtration on the activities of ^{237}Np measured in solution samples indicate that neptunium was not present as colloids or suspended phases in these samples.

Quantities of ^{237}Np measured in the various liquid sample types from the bare-fuel tests are tabulated in Table 3.7. (Note that these data are tabulated in pCi units whereas the $^{239+240}Pu$, ^{241}Am, and ^{244}Cm data were tabulated in nCi units.) As with the other actinides, it appears that neptunium-containing secondary phases from the 25°C tests redissolved in the rinse solutions to a greater extent than those from the 85°C tests. Generally larger quantities of ^{237}Np in acid strip solutions at 85°C is consistent with data for the other actinides suggesting greater fuel dissolution and subsequent removal of species from solution occurred at the higher temperature. The percentages of ^{237}Np measured in solution samples are generally somewhat higher than for the other actinides and much higher than measured for $^{239+240}Pu$, ^{241}Am, and ^{244}Cm in Cycles 2 and 3 of the 85°C bare-fuel tests.

3.8 TECHNETIUM

Technetium-99, which beta-decays with a 213,000-yr half-life, accounts for about 0.75% of the total activity of spent fuel at 1,000 yr and about 3% of the activity at 10,000 yr. Technetium is expected to be soluble as TcO_4^- in air-equilibrated water and may reach relatively high activities in water that contacts substantially degraded fuel. Only ^{99}Tc data from the bare-fuel tests are discussed in this report because ^{99}Tc activities in the other tests were generally below the detection limit.

Activities of ^{99}Tc measured in unfiltered samples from the three Series 3 bare-fuel tests and the Series 2 HBR bare-fuel tests are plotted as a linear plot in Figure 3.21. The most significant aspect of this data is that, with the exception of Cycle 1 of the HBR/BF-85 test, the ^{99}Tc activity in solution increases continuously with time and is not limited by solubility. At the beginning of Cycle 1, there was a rapid release on the order of 0.01% of the specimen inventory. In the TP/BF-85 test, the rapid release was followed by a continuous release of about 5×10^{-6} of specimen inventory per day. Most of the ^{99}Tc initially released to solution in the HBR/BF-85 test dropped out of solution following the 62-d sample, which was probably a result of

TABLE 3.7 Quantities of ^{237}Np Measured in Samples (pCi)

	HBR/BF-25	TP/BF-85	HBR/BF-85	HBR/SD-85	HBR/HD-85	HBR/UD-85
Cycle 1						
Periodic Samples	143	163	415	For these tests ^{237}Np activity was below the detection limit.		
Final Solution	68	203	<68			
[Np (ppb)]	(0.38)	(1.15)	(<0.32)			
Rinse	162	<135	<135			
Acid Strip	135	1243	1486			
Cycle Total	508	<1744	<2104			
+ 10^{-5} Inv.	2.43	<9.3	<10.7			
% in Solution	41.5	~21.0	~23			
Cycle 2						
Periodic Samples	36	<27	35			
Final Solution	45	34	22.5			
[Np (ppb)]	(0.26)	(0.19)	(0.13)			
Rinse	189	<54	<54			
Acid Strip	81	500	662			
Cycle Total	351	<615	<774			
+ 10^{-5} Inv.	1.70	<3.4	<4.0			
% in Solution	23.0	~10	~7.5			
Cycle 3						
Periodic Samples	7.9	6.8	6.8			
Final Solution	56.3	11.3	33.8			
[Np (ppb)]	(0.32)	(0.06)	(0.20)			
Rinse	216	27	<27			
Acid Strip	95	149	(a)			
Cycle Total	375	194	(a)			
E 10^{-5} Inv.	1.85	1.06	(a)			
% in Solution	17.1	9.3	(a)			
Sum of Cycles 1, 2 & 3						
Σ Cycle Totals	1234	<2553	2945(b)			
+ 10^{-5} Inv.	5.97	<13.7	~15.1(b)			

(a) Cycle 3 HBR/BF-85 acid strip appears to have been contaminated by fuel particles.
(b) Cycles 1 and 2 only.
NOTE: Periodic samples, and final solution and rinse values are based on 0.4-μm filtered data.

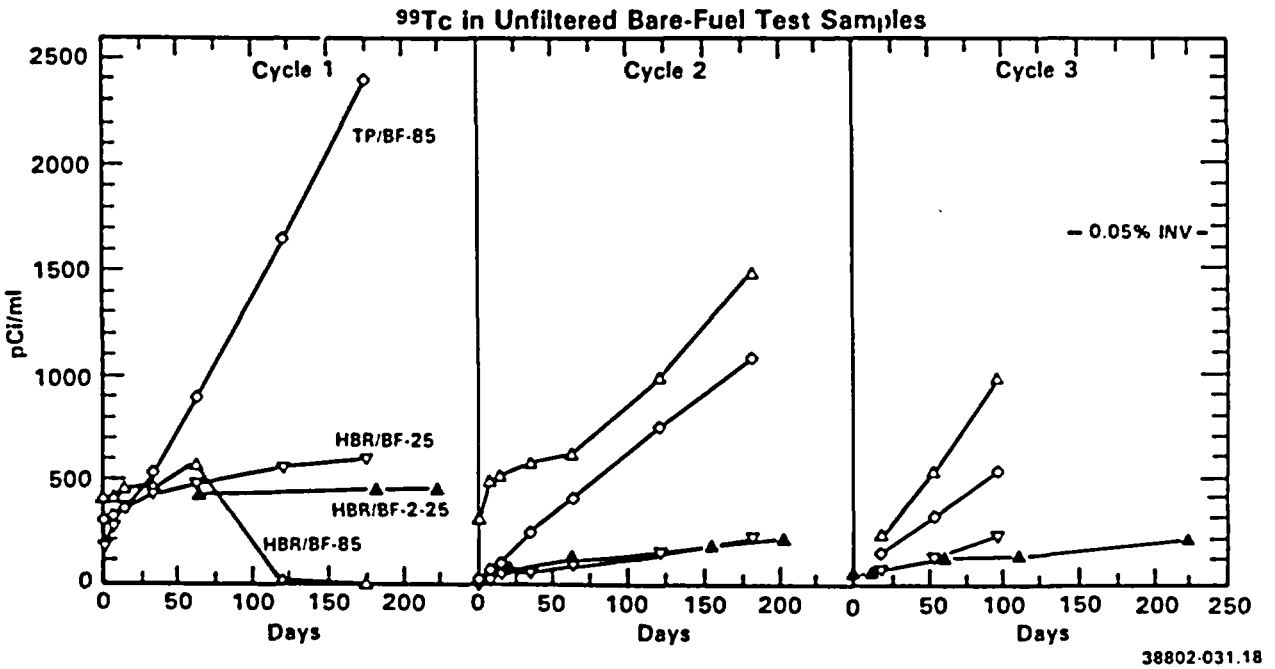

FIGURE 3.21. Technetium-99 Activities Measured in Unfiltered Samples from the Series 3 Bare-Fuel Tests and the Series 2 HBR Bare-Fuel Test

reducing conditions caused by the vessel corrosion anomaly indicated to have occurred in this test, and also correlates with the drop in uranium concentration observed in this test. There was an enhanced initial release from this test in Cycle 2, which likely resulted from dissolution of technetium-bearing phases (TcO_2, technetium adsorbed on precipitates, etc.) that precipitated during Cycle 1 and were not completely removed from the fuel surface during the cycle termination rinsing procedure. The ^{99}Tc continuous release rate showed a significant dependence on temperature.

During Cycles 2 and 3, ^{99}Tc was continuously released at a rate of about 2.5×10^{-6} of specimen inventory per day in both the HBR/BF-85 and TP/BF-85 tests. Continuous release rate during Cycle 2 of both the HBR/BF-25 and HBR/BF-2-25 tests was about 5×10^{-7} of specimen inventory per day. The continuous ^{99}Tc release to solution with time is presumably the additive result of congruent dissolution of the fuel matrix plus preferential release from grain boundaries (or other phases) where technetium may be concentrated. However, the relative contributions of these two sources of release could not

be determined. Technetium-99, which segregates from the fuel matrix during irradiation, is known to combine with fission products molybdenum, ruthenium, rhodium, and palladium forming finely dispersed "five metal" particles in the fuel. These particles are very difficult to dissolve even in nitric acid and may remain undissolved even during fuel reprocessing. Therefore, the mechanism by which ^{99}Tc would be preferentially released during dissolution tests in water is uncertain.

Quantities of ^{99}Tc measured in the different sample types are tabulated in Table 3.8. Except for the HBR/BF-85 Cycle 1 test, most of the measured ^{99}Tc (>90%) was in solution. The ^{99}Tc fractional releases represented by the Cycle Total values divided by 10^{-5} of specimen inventory were generally much greater than those for the actinides, indicating either a large component of preferential release of ^{99}Tc or a large amount of actinide secondary phase material unaccounted for in the rinse and strip samples. The 708 nCi of ^{99}Tc measured in solution in the TP/BF-85 Cycle 1 test would correspond to about 62 mg of congruent uranium dissolution if ^{99}Tc were not preferentially released. The fact that only about 6.8 mg of uranium was accounted for in the Cycle Total value, and that only 10 mg of material was retained on the rinse filter (most of which was undissolved fuel grains), implies that about 50 mg uranium in secondary phase material was not accounted for in this test if ^{99}Tc was not preferentially released. By the same estimate, about 20 mg of secondary phase uranium would have been missed in Cycle 2 of the TP/BF-85 test. That such quantities of secondary phases remained attached to the fuel particle surfaces, or otherwise escaped observation, is unlikely but possible. These data support the hypothesis that preferential release from grain boundaries or other secondary fuel phases is likely a significant component of the ^{99}Tc release. Unfortunately, the data are not sufficient to derive quantitative estimates of the relative fractions of ^{99}Tc (or any other nuclide) release originating from congruent matrix dissolution versus preferential dissolution.

By assuming that all of the ^{99}Tc measured in acid strip samples originates from previously undissolved fuel fines, one can estimate the portion of other nuclides in the acid strip samples originating from previously undissolved fuel fines. The percentages of uranium, $^{239+240}Pu$, ^{241}Am, ^{237}Np, ^{137}Cs, and ^{90}Sr in acid strip samples thereby calculated to have originated

TABLE 3.8. Quantities of ^{99}Tc Measured in Samples (nCi)

	HBR/BF-25	TP/BF-85	HBR/BF-85	HBR/SD-85	HBR/HD-85	HBR/UD-85
Cycle 1						
Periodic Samples	60.1	109	54	<2.4	<1.7	<1.5
Final Solution	153	599	<2	<2.3	<2.3	<2.3
[Tc (ppb)]	(36)	(141)	(<0.5)	(<0.5)	(<0.5)	(<0.5)
Rinse	10.3	24	22.4	<5.4	<12.2	<5.4
Acid Strip	4.6	12.3	24.3	<2.7	<2.7	<2.7
Cycle Total	228	745	103	<12.7	<18.9	<11.8
+ 10^{-5} Inv.	25.2	89.4	12.2	<1.4	<2.2	<1.3
% in Solution	93.5	95.1	54.6	--	--	--
Cycle 2						
Periodic Samples	8.4	34.2	78	In Cycles 2 and 3 these values were below the detection limit.		
Final Solution	56.3	270	372			
[Tc (ppb)]	(13)	(63)	(87)			
Rinse	4.0	6.5	11.9			
Acid Strip	<1.4	6.5	10.1			
Cycle Total	70.1	317	471			
+ 10^{-5} Inv.	7.9	38.6	56.5			
% in Solution	~93	95.9	95.3			
Cycle 3						
Periodic Samples	4.8	11.8	19.4			
Final Solution	58.6	135	248			
[Tc (ppb)]		(32)	(58)			
Rinse	<5.4	<54	10.8			
Acid Strip	<2.7	5.4	(a)			
Cycle Total	<71.5	158	278			
+ 10^{-5} Inv.	<8.1	19.4	33.7			
% in Solution	>88.7	93.1	>96			
Sum of Cycles 1, 2 & 3						
Σ Cycle Total	370	1220	852			
+ 10^{-5} Inv.	41.2	147.4	102.2			

(a) Cycle 3 HBR/BF-85 acid strip appears to have been contaminated by fuel particles.

NOTE: Bare fuel test rinse samples were 0.4-μm filtered. All other values are based on unfiltered data.

from previously undissolved fuel fines are given in Table 3.9 for test cycles in which significant ^{99}Tc values were measured in the acid strip samples. The relatively high fraction of the uranium in the Cycle 1 HBR/BF-25 acid strip sample attributed to previously undissolved fuel fines and is consistent with the observation that very little uranium-bearing secondary phase material was found in rinse filter residues from this test. The fact that the Table 3.9 values are not particularly high for the HBR/BF-85 Cycle 1 test indicates that little of the ^{99}Tc that dropped out of solution in this test remained attached to the vessel components after the rinse procedure. An interesting result is the portions of ^{137}Cs and ^{90}Sr measured in acid strip solutions that would appear to originate from plate-out or precipitated secondary phases.

3.9 CESIUM

The fission product cesium nuclides, ^{134}Cs (2.06-yr half-life) and ^{137}Cs (30.2-yr half-life), plus ^{137m}Ba (short-lived ^{137}Cs daughter), account for about 38% of the total activity of the tested fuel and for a significant portion of the decay heat during the thermal period. The longer lived ^{135}Cs nuclide (2,300,000-yr half-life) had a much lower inventory (0.3 μCi/g versus 6×10^4 μCi/g for ^{137}Cs) and was not measured in the current tests. Cesium is relatively mobile under temperature and oxygen potential conditions present in the fuel during irradiation due to its ~670°C boiling point in the metallic

TABLE 3.9. Percent Nuclide Fractions in Acid Strip Samples Attributed to Previously Undissolved Fuel Fines Based on ^{99}Tc Data[a]

Test	Cycle	U	$^{239+240}Pu$	^{241}Am	^{237}Np	^{137}Cs	^{90}Sr
HBR/BF-25	1	90.9	21.3	9.3	78.9	32.4	49.4
TP/BF-85	1	16.9	25.0	19.5	22.1	3.1	4.6
	2	69.9	38.4	36.2	29.1	48.6	34.0
HBR/BF-85	1	39.3	31.9	25.9	37.8	8.9	15.7
	2	43.4	45.3	36.9	35.3	42.8	8.9

(a) Assumes 100% of ^{99}Tc measured in acid strip samples was from previously undissolved fuel fines.

state. As a result, the cesium inventory fraction in the gap may approach that of fission gases xenon and krypton.

The ^{137}Cs activities measured in 0.4-μm filtered solution samples are plotted in Figure 3.22. Gap releases of 0.66% in the HBR/BF-25 test, 0.84% in the HBR/BF-85 test, and 0.36% in the TP/BF-85 test were measured in the 1-d Cycle 1 solution samples. The Cycle 2 bare-fuel releases were on the order of a few percent of those measured in Cycle 1. Release from the HBR/HD-85 specimen was much slower than from the HBR/SD-85 and bare-fuel specimens, and release of a portion of the ^{137}Cs gap inventory from this specimen appears to have been delayed into Cycle 2.

The O-ring in the end fittings of the HBR/UD-85 test specimen apparently started leaking after the 14-d Cycle 2 sample. The O-ring seals in this test appear to have substantially failed during Cycle 3 with most of the initial gap inventory being released during this cycle. The O-ring failure was likely a result of radiation exposure and simultaneous O-ring failure in the HBR/HD-85 and HBR/SD-85 tests is likely. The O-ring failures did not appear

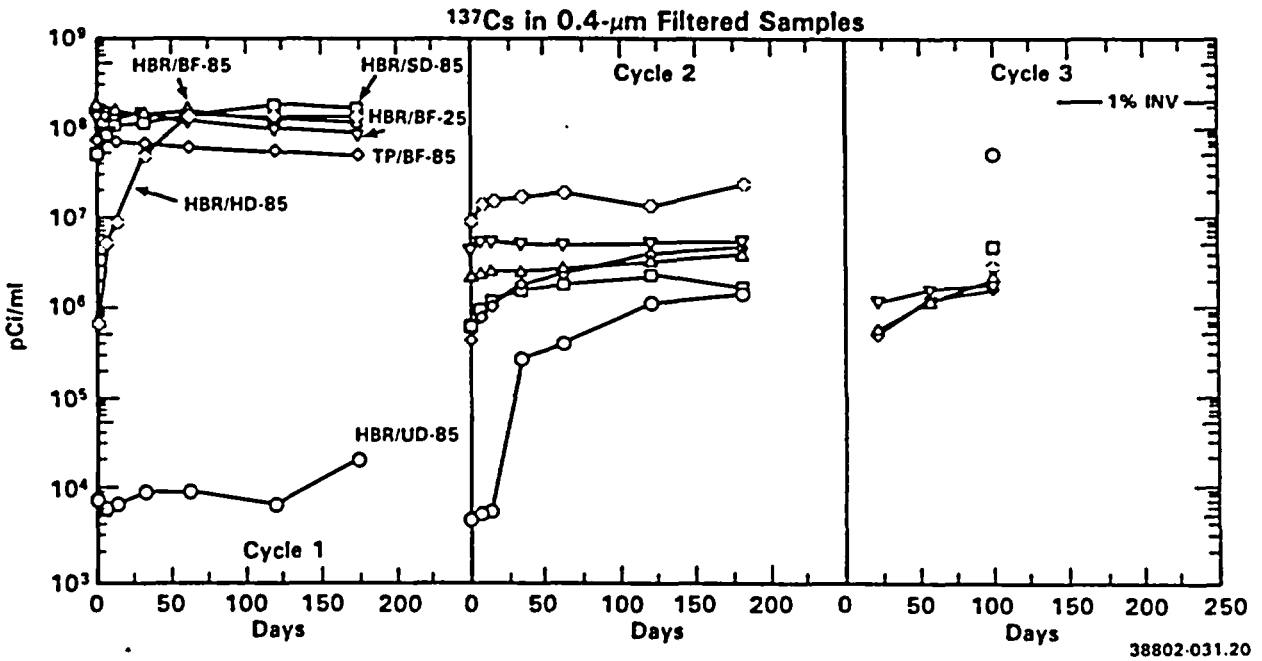

FIGURE 3.22. Activity of ^{137}Cs in 0.4-μm Filtered Solution Samples

state. As a result, the cesium inventory fraction in the gap may approach that of fission gases xenon and krypton.

The ^{137}Cs activities measured in 0.4-μm filtered solution samples are plotted in Figure 3.22. Gap releases of 0.66% in the HBR/BF-25 test, 0.84% in the HBR/BF-85 test, and 0.36% in the TP/BF-85 test were measured in the 1-d Cycle 1 solution samples. The Cycle 2 bare-fuel releases were on the order of a few percent of those measured in Cycle 1. Release from the HBR/HD-85 specimen was much slower than from the HBR/SD-85 and bare-fuel specimens, and release of a portion of the ^{137}Cs gap inventory from this specimen appears to have been delayed into Cycle 2.

The O-ring in the end fittings of the HBR/UD-85 test specimen apparently started leaking after the 14-d Cycle 2 sample. The O-ring seals in this test appear to have substantially failed during Cycle 3 with most of the initial gap inventory being released during this cycle. The O-ring failure was likely a result of radiation exposure and simultaneous O-ring failure in the HBR/HD-85 and HBR/SD-85 tests is likely. The O-ring failures did not appear

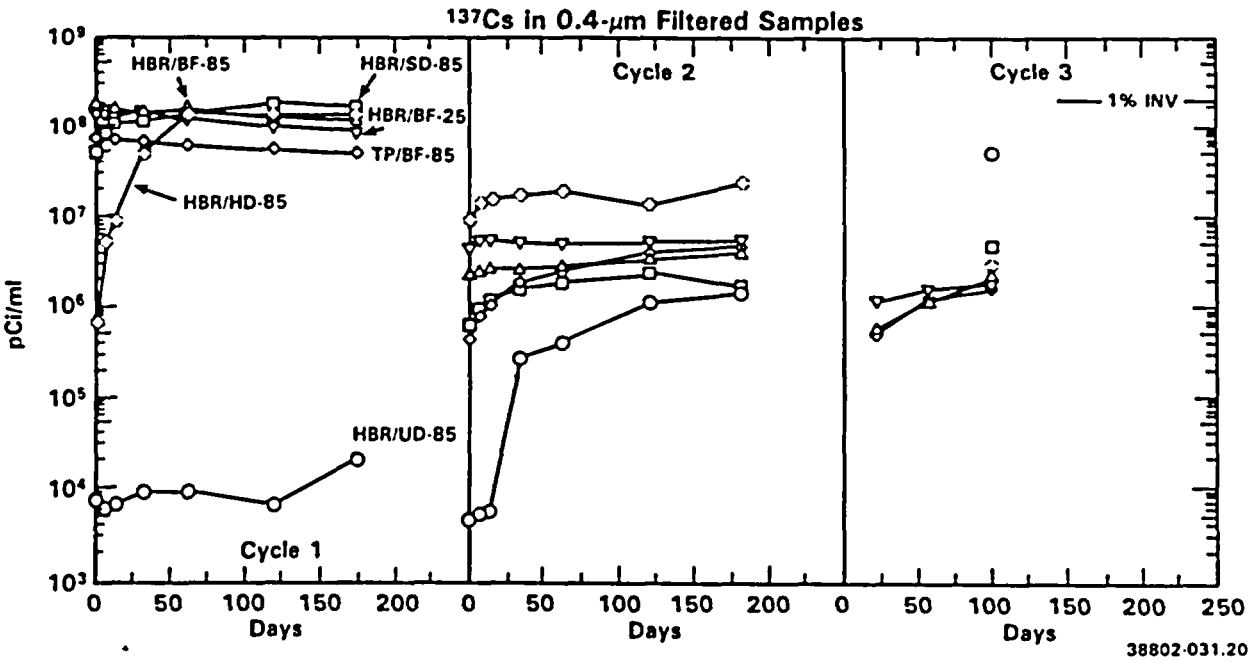

FIGURE 3.22. Activity of ^{137}Cs in 0.4-μm Filtered Solution Samples

to be a significant factor in the delayed release of nuclides other than ^{137}Cs. The fact that the O-rings seals did not fail over two complete test cycles in the Series 2 tests may be related to the lower 25°C temperature of these tests.

The quantities of ^{137}Cs measured in the various sample types are tabulated in Table 3.10. The total measured fractional releases for Cycles 1, 2, and 3 from the HBR specimens were about 1% at 85°C and about 0.8% at 25°C. The total measured fractional release for the TP specimen at 85°C was about 0.5%. If the assumption is valid that all the ^{99}Tc in the acid strip samples originated from previously undissolved fuel fines, the Table 3.9 data suggest that much of the ^{137}Cs in acid strip solutions (particularly in Cycle 1 of the 85°C tests) was associated with plate-out or other secondary phases. Cesium may have been adsorbed onto colloids or by silica gel that dropped from solution in these tests. However, cesium association with any particular phase has not been confirmed.

3.10 STRONTIUM

Strontium-90 beta-decays (28.6-yr half-life) to a short-lived ^{90}Y daughter, which then beta-decays (64-hour half-life) to stable ^{90}Zr. Strontium-90 plus ^{90}Y activity accounts for about 28% of the total activity of the specimens tested and, along with ^{137}Cs and its ^{137m}Ba daughter, account for a substantial portion of the decay heat during the repository thermal period.

Analyses for ^{90}Sr were conducted on selected samples during Cycles 1 and 2 and on all Cycle 3 solution samples. Only unfiltered aliquots were analyzed for ^{90}Sr, except for the Cycle 3 final solution samples from the bare-fuel tests, where unfiltered and 0.4-μm filtered aliquots were also analyzed. No significant differences were found between the unfiltered and the 0.4-μm filtered results in the three samples on which both filter fractions were analyzed. The ^{90}Sr activities measured in the unfiltered samples are plotted in Figure 3.23. Quantities of ^{90}Sr measured in different sample types are given in Table 3.11.

Strontium-90 was rapidly released to solution in Cycle 1 of the bare-fuel tests but then appeared to saturate and drop out of solution. Solution

TABLE 3.10. Quantities of ^{137}Cs Measured in Samples (μCi)

	HBR/BF-25	TP/BF-85	HBR/BF-85	HBR/SD-85	HBR/HD-85	HBR/UD-85
Cycle 1						
Periodic Samples	17718	8820	19908	15858	9019	1.1
Final Solution	21734	11712	27590	39640	31419	5.3
[Cs (ppb)]	(2521)	(1359)	(3200)	(4600)	(3645)	(0.6)
Rinse	1368	719	1084	381	473	1
Acid Strip	86	2446	1649	70	45	0.14
Cycle Total	40906	23696	50230	55949	40956	7.6
+ 10^{-5} Inv.	745	459	977	1024	802	0.14
% in Solution	96.5	86.6	94.6	99.2	98.7	84.7
Cycle 2						
Periodic Samples	686	239	352	192	1966	8.6
Final Solution	1329	1239	1032	418	5709	367
[Cs (ppb)]	(154)	(144)	(120)	(48)	(662)	(42.6)
Rinse	128	55	56	78	130	36.2
Acid Strip	22	83	143	0.3	23	0.29
Cycle Total	2166	1616	1582	688	7828	412
+ 10^{-5} Inv.	40.1	37.7	31.3	12.6	153	7.61
% in Solution	93.0	91.5	87.4	88.7	98.1	91.2
Cycle 3						
Periodic Samples	70	42	45	--	--	--
Final Solution	476	428	528	1227	698	12950
[Cs (ppb)]	(55)	(50)	(61)	(142)	(81)	(1502)
Rinse	64	32	26	--	--	--
Acid Strip	22	57	(a)	--	--	--
Cycle Total	633	559	600	1227	698	12950
+ 10^{-5} Inv.	11.9	11.1	12.0	23	13.7	240
% in Solution	86.4	84.1	<95.6	--	--	--
Sum of Cycles 1, 2 & 3						
Σ Cycle Totals	43704	25871	52412	57864	49482	13370
+ 10^{-5} Inv.	797	501	1020	1059	969	248

(a) Cycle 3 HBR/BF-85 acid strip appears to have been contaminated by fuel particles.

NOTE: Periodic samples, final solution and bare fuel rinse values are based on 0.4-μm filtered data. Other values are based on unfiltered data.

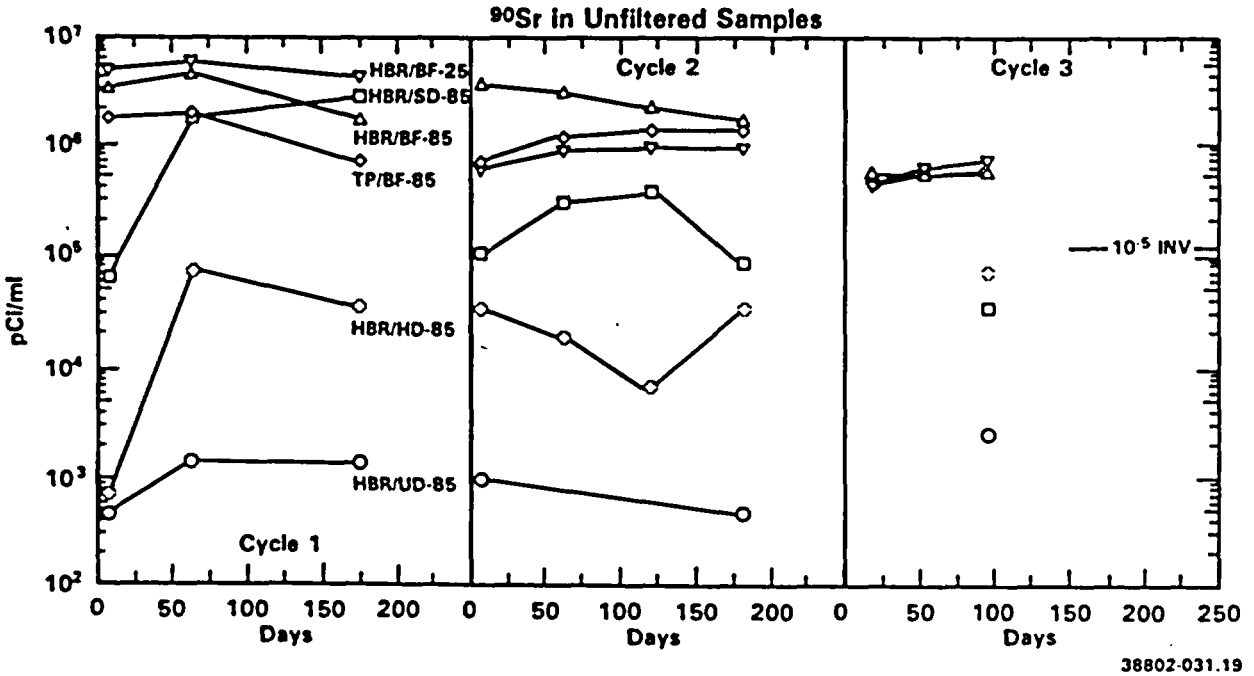

FIGURE 3.23. Activity of ^{90}Sr in Unfiltered Solution Samples

activities in the 174-d Cycle 1 samples from both the HBR/BF-85 and TP/BF-85 tests were only about 40% as high as measured in the 62-d samples. A significant drop in ^{90}Sr activity also occurred during Cycle 2 of the HBR/BF-85 test. That ^{90}Sr is controlled to a degree by secondary phases in these test cycles is supported by the relatively small fraction of the ^{90}Sr activity in the acid strip samples calculated to have originated from previously undissolved fuel fines (see Table 3.9). Strontium may be partially substituting for calcium in secondary phases such as uranophane, haiweeite, calcite, or dolomite at concentrations below those that would have been detected during SEM-EDX examination of solid residues from these tests.

The calculated "fractional release" values for ^{90}Sr (+ 10^{-5} Inv. values in Table 3.11) were significantly greater than those for calculated for the actinides, suggesting that ^{90}Sr is preferentially released. The fractional release values were particularly greater in the HBR/SD-85 test. Although release was delayed in the HBR/SD-85 test, by the end of Cycle 1, the ^{90}Sr level in solution in this test was greater than that in the two 85°C bare-fuel

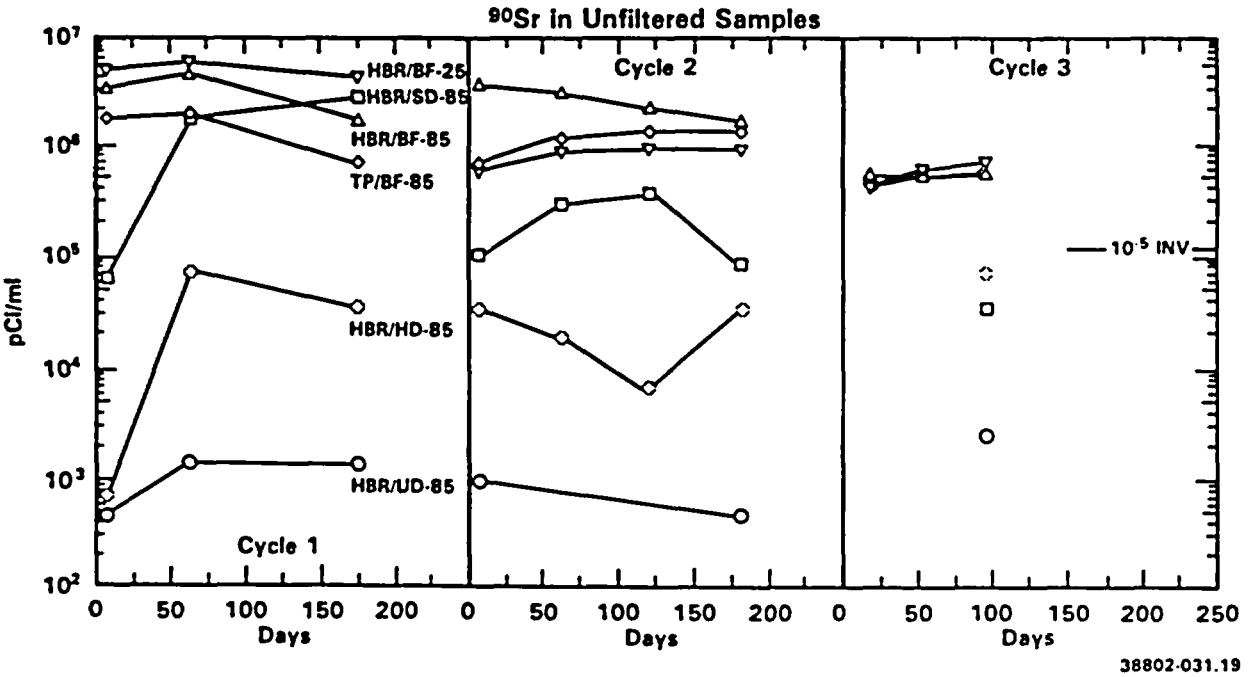

FIGURE 3.23. Activity of ^{90}Sr in Unfiltered Solution Samples

activities in the 174-d Cycle 1 samples from both the HBR/BF-85 and TP/BF-85 tests were only about 40% as high as measured in the 62-d samples. A significant drop in ^{90}Sr activity also occurred during Cycle 2 of the HBR/BF-85 test. That ^{90}Sr is controlled to a degree by secondary phases in these test cycles is supported by the relatively small fraction of the ^{90}Sr activity in the acid strip samples calculated to have originated from previously undissolved fuel fines (see Table 3.9). Strontium may be partially substituting for calcium in secondary phases such as uranophane, haiweeite, calcite, or dolomite at concentrations below those that would have been detected during SEM-EDX examination of solid residues from these tests.

The calculated "fractional release" values for ^{90}Sr (+ 10^{-5} Inv. values in Table 3.11) were significantly greater than those for calculated for the actinides, suggesting that ^{90}Sr is preferentially released. The fractional release values were particularly greater in the HBR/SD-85 test. Although release was delayed in the HBR/SD-85 test, by the end of Cycle 1, the ^{90}Sr level in solution in this test was greater than that in the two 85°C bare-fuel

TABLE 3.11. Quantities of ^{90}Sr Measured in Samples (μCi)

	HBR/BF-25	IP/BF-85	HBR/BF-85	HBR/SD-85	HBR/HD-85	HBR/UD-85
Cycle 1						
Periodic Samples	254	86	51	56	2.3	<0.05
Final Solution	1089	180	441	707	8.7	0.33
[Sr (ppb)]	(56.4)	(9.4)	(23)	(36)	(0.45)	(0.02)
Rinse	92	104	119	22	13.9	0.22
Acid Strip	37	1116	615	48	1.1	0.135
Cycle Total	1472	1486	1366	834	26.0	0.725
+ 10^{-5} Inv.	41.0	43.1	40.6	23.3	0.78	0.02
% in Solution	91.3	17.9	46.2	91.5	42.3	-50
Cycle 2						
Periodic Samples	50	62	162	15.5	1	--
Final Solution	248	348	419	22.8	8.67	0.11
[Sr (ppb)]	(12.8)	(18.1)	(21.7)	(1.15)	(0.45)	(0.006)
Rinse	31.3	41	71	2.03	1	<0.27
Acid Strip	14.5	79	450	0.72	5.77	<0.11
Cycle Total	343	530	1102	40.5	16.5	<0.49
+ 10^{-5} Inv.	12.8	15.6	33.3	1.13	0.49	<0.02
% in Solution	86.7	77.3	52.8	93.2	58.9	--
Cycle 3						
Periodic Samples	28.1	25	28	--	--	--
Final Solution	196	157	153	8.9	18.2	0.63
[Sr (ppb)]	(10.2)	(8.1)	(7.9)	(0.46)	(0.94)	(0.033)
Rinse	23.3	24	23	--	--	--
Acid Strip	15.7	84	(a)	--	--	--
Cycle Total	263	290	205	>8.9	>18.2	>0.63
+ 10^{-5} Inv.	7.5	8.6	6.2	>0.25	>0.55	>0.01
% in Solution	85.2	62.6	>88.6	--	--	--
Sum of Cycles 1, 2 & 3						
Σ Cycle Total	2078	2307	2673	883	60.7	1.85
+ 10^{-5} Inv.	58.2	67.3	80.1	24.7	1.82	-0.03

(a) Cycle 3 HBR/BF-85 acid strip appears to have been contaminated by fuel particles.

NOTE: Bare fuel test rinse samples were 0.4-μm filtered. All other values are based on unfiltered data.

tests. Another indication that ^{90}Sr may be present as gap inventory, or otherwise concentrated in the fuel so as to be available for preferential release, is that the inventory fractions in solution early in Cycle 1 of HBR/BF-25 and HBR/BF-85 tests were significantly greater than that of ^{99}Tc, whose activity did not appear to be solubility limited. (This is shown in the following chapter where fission inventory fractions in solution are compared in the same plot.) Although the release and solubility control mechanisms are not clear, ^{90}Sr appears to be initially released preferentially and then subject to some form of solution concentration control.

3.11 IODINE

Iodine-129 beta-decays with a 17,000,000-yr half-life to stable ^{129}Xe. With an inventory of about 0.025 μCi/g of fuel (~30 Ci/1,000 MTHM) in the tested specimens, ^{129}I was the lowest activity nuclide measured and required neutron activation analysis for its detection. Although ^{129}I has a relatively low activity inventory in spent fuel, it is relatively soluble, may possibly be mobile in the vapor phase as I_2 (although the present data do not support this), and has a potential for incorporation into the biosphere.

Iodine-129 analyses were made only on single midcycle and final solution samples from each cycle, plus the Cycle 1 acid strip and Cycle 3 rinse samples. Only bare-fuel test samples were analyzed for ^{129}I during Cycle 3. Activities of ^{129}I measured in unfiltered solution samples are plotted in Figure 3.24. Quantities of ^{129}I measured in the different sample types are tabulated in Table 3.12. Since only one periodic solution sample from each cycle was analyzed for ^{129}I, the result of this analysis was assumed for all periodic samples in calculating the "periodic samples" values in Table 3.12. The greatest ^{129}I releases were observed in the two 85°C bare-fuel tests and Cycle 1 of the slit-defect test. Although the acid strip and rinse sample data are limited, these data indicate that most of the ^{129}I was in solution.

Relatively large fractional releases of ^{129}I of about 0.1%, 0.3%, and 0.4% were measured during Cycle 1 of the TP/BF-85, HBR/BF-85, and HBR/SD-85 tests, respectively. Such large releases probably result from dissolution of a fission product phase formed in the gap. However, the mechanism and phases

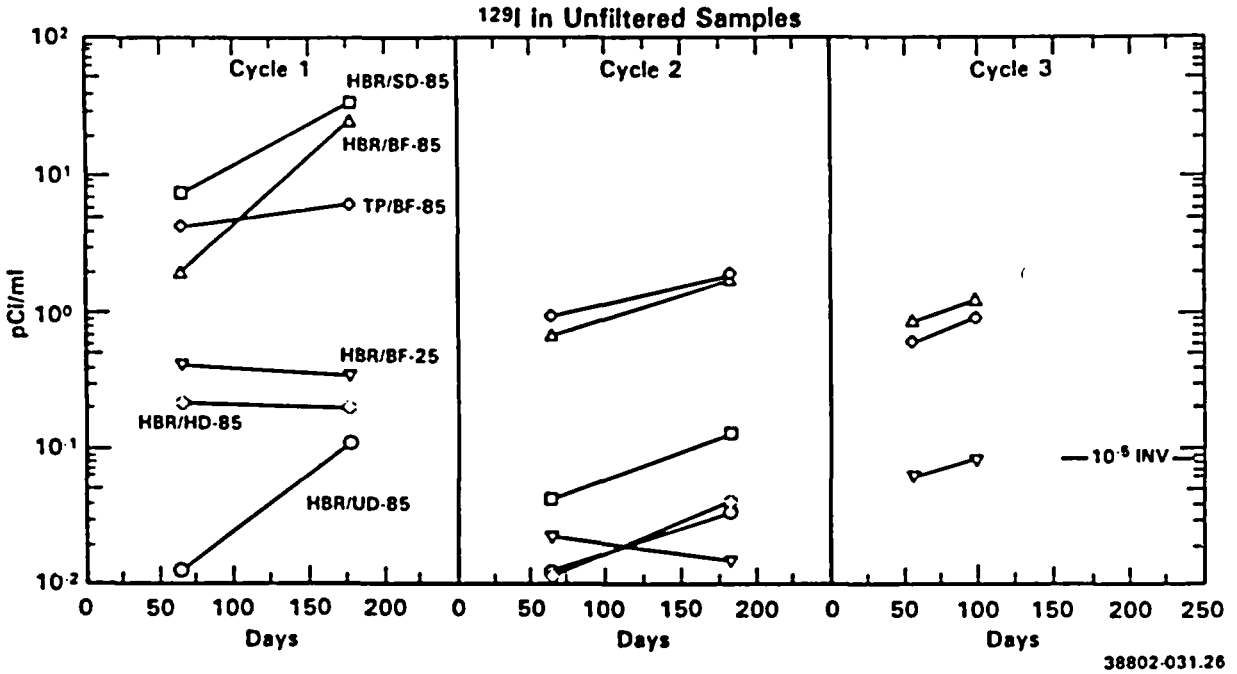

FIGURE 3.24. Activities of ^{129}I Measured by Neutron Activation Analysis in Unfiltered Solution Samples

involved would appear to be different than those involved in the gap release of ^{137}Cs. Cycle 1 fractional releases of ^{137}Cs in these tests were 0.46% in the TP/BF-85 test and about 1.0% in both the HBR/BF-85 and HBR/SD-85 tests. The greatest difference, however, was temperature dependence, with only about 0.076% of the ^{129}I inventory versus 0.75% of the ^{137}Cs inventory being released during Cycle 1 of the HBR/BF-25 test. Also, ^{129}I release appeared to be less rapid than that of ^{137}Cs, particularly in the HBR/BF-85 test where most of the ^{129}I release occurred between the interim 62-d sample and the final 174-d sample. In the HBR/HD-85 test, about 0.8% of the ^{137}Cs inventory was released in Cycle 1, while only about 0.0044% of ^{129}I inventory was released in Cycles 1 and 2 combined. The ^{137}Cs gap inventory appears to be associated with more readily soluble phases that rapidly dissolve at 25°C as well as 85°C, while ^{129}I may be associated with a phase that is only slowly dissolved at the lower temperature. One possibility may be that fission product iodine reacts with and penetrates the cladding inner surface from which it is only slowly dissolved at 25°C.

TABLE 3.12. Quantities of ^{129}I Measured in Samples (pCi)

	HBR/BF-25	TP/BF-85	HBR/BF-85	HBR/SD-85	HBR/HD-85	HBR/UD-85
Cycle 1						
Periodic Samples[a]	62.1	615	290	1058	31.9	1.81
Final Solution	86.7	1522	6200	8375	49.8	27.75
[I (ppb)]	(2.8)	(49)	(200)	(270)	(1.6)	(0.9)
Rinse	--	--	--	--	--	--
Acid Strip	25.8	75	64	4.8	1.2	0.02
Cycle Total	174.6	2212	6554	9438	82.9	29.58
+ 10^{-5} Inv.	7.65	107	306	415	3.9	1.31
% in Solution	85.2	96.6	99.0	99.9	98.6	99.9
Cycle 2						
Periodic Samples[a]	2.9	121	88	5.6	1.5	--
Final Solution	3.7	467	430	32.2	10.0	8.48
[I (ppb)]	(0.12)	(15)	(14)	(1.0)	(0.32	(0.3)
Rinse	--	--	--	--	--	--
Acid Strip	--	--	--	--	--	--
Cycle Total	6.6	589	518	37.8	11.5	8.48
+ 10^{-5} Inv.	0.29	29	24.6	1.66	0.54	0.38
% in Solution	--	--	--	--	--	--
Cycle 3						
Periodic Samples[a]	3.0	30	41			
Final Solution	20.7	229	310			
[I (ppb)]	(0.67)	(7.4)	(10)			
Rinse	8.0	8.9	7.3			
Acid Strip	--	--	--			
Cycle Total	31.7	267	358			
+ 10^{-5} Inv.	1.43	13.2	17.2			
% in Solution	74.6	96.7	98.0			
Sum of Cycles 1, 2 & 3						
Σ Cycle Total	213	3069	7429	9476[b]	94.4[b]	38.1[b]
+ 10^{-5} Inv.	9.4	149	348	417[b]	4.4[b]	1.7[b]

(a) Activity in the single pericdic sample analyzed for ^{129}I times total volume of all periodic samples in the cycle.
(b) Cycles 1 and 2 only.
NOTE: Bare fuel test rinse samples were 0.4-μm filtered. All other values are based on unfiltered data.

During Cycles 2 and 3 of the HBR/BF-85 and TP/BF-85 tests, ^{129}I was continuously released at a rate of about 1.2×10^{-6} of inventory per day, which is somewhat less (35 to 66%) than the continuous fractional release measured for ^{99}Tc in these test cycles and similar to or slightly greater than that measured for ^{137}Cs. However, the ^{129}I continuous release rates were much lower than those of the other soluble fission products during Cycles 2 and 3 of the HBR/BF-25 test. Implications of these continuous release rates are further discussed in the following chapter.

The ^{129}I inventory fractions in solution at cycle termination are compared for the Series 2 and Series 3 tests in Table 3.13. The purpose of this comparison is to indicate if significant portions of the released ^{129}I escaped in the vapor phase from the unsealed Series 2 vessels. If anything, these data show the reverse, with less ^{129}I in solution at 25°C in the HBR/BF-25 test using a sealed stainless steel vessel than in the Series 2 tests using unsealed silica vessels. The data do not provide evidence to support the theory that ^{129}I may be released as I_2 and transported in the vapor phase. These data also again show the temperature dependence of ^{129}I release in the Series 3 tests.

3.12 TIN-126

Tin-126 beta-decays with a 100,000-yr half-life to ^{126}Sb, which decays with a 12.5-d half-life to stable ^{126}Te. The ^{126}Sn inventory at about 0.7 μCi/g of fuel (~770 Ci/1,000 MTHM) is the next lowest activity nuclide after ^{129}I to be analyzed.

TABLE 3.13. ^{129}I Inventory Fractions in Series 2 and Series 3 Final Solution Samples (parts per 100,000)

Test	Cycle 1	2	3	4	5
HBR/BF-2-25	8.2	5.4	5.4	3.2	2.6
TP/BF-2-25	22.4	8.5	5.5	4.7	2.6
HBR/BF-25	3.8	0.17	0.93		
HBR/BF-85	290	20.4	14.9		
TP/BF-85	73.5	22.9	11.3		

The activity of ^{126}Sn in solution samples was not plotted because of the limited number of samples showing detectable activities. Significant ^{126}Sn activities were measured in several solution samples and acid strip samples from the bare-fuel tests. Quantities of ^{126}Sn measured in samples from the bare-fuel tests are tabulated in Table 3.14. Most of the significant ^{126}Sn measured was in the acid strip samples. The total fractional releases measured are slightly less than, but on the order of, those measured for the actinides, suggesting that ^{126}Sn may have been congruently released with the actinides. At less than 10^{-4} g/g fuel concentration in spent fuel, tin may possibly be soluble in the matrix phase and congruently released as the matrix dissolves. However, the current data are somewhat limited for support of such a conclusion.

3.13 CARBON-14

Carbon-14 (5730-yr half-life) is an activation product formed during irradiation by the (n,p) reaction on nitrogen impurities, and from the (n,α) reaction on ^{17}O.[18] ORIGEN calculations for ^{14}C inventories in spent fuel depend on assumed values for initial ^{14}N impurity levels in the fuel and cladding, which are not generally well known and may vary significantly between individual fuel samples. Also, ORIGEN predictions of ^{14}C inventory do not include the possibility of the incorporation of ^{14}C produced by (n,α) reaction on ^{17}O in the cooling water into exterior assembly and cladding surfaces. Carbon-14 was radiochemically measured on two fuel and cladding samples taken from the HBR C5 rod. The average of the two analyses gave 0.49 μCi/g for fuel and 0.53 μCi/g for cladding. This level of ^{14}C corresponds to about 530 Ci/1,000 MTHM. Carbon-14 is of particular concern because it is mobile in the vapor phase [18,19] as CO_2 and in groundwater as HCO_3^- and has a high potential for incorporation into the biosphere.

The ^{14}C activities measured in unfiltered solution samples are plotted in Figure 3.25. The 10^{-5} inventory level shown in Figure 3.25 is based on the ^{14}C results obtained for the HBR C5 rod samples that were analyzed for ^{14}C inventory. Quantities of ^{14}C measured in the different sample types are tabulated in Table 3.15. Fractional release values (+ 10^{-5} Inv.) are not

TABLE 3.14. Quantities of ^{126}Sn Measured in Samples (pCi)

	HBR/BF-25	TP/BF-85	HBR/BF-85	HBR/SD-85	HBR/HD-85	HBR/UD-85
Cycle 1						
Periodic Samples[a]	78.4	<<	57	For these tests ^{126}Sn activity was below the detection limit.		
Final Solution	90.1	<68	<56			
[^{126}Sn (pg/mL)]	(12.7)	(<9.5)	(<7.9)			
Rinse	<135	<135	<135			
Acid Strip	365	2297	1622			
Cycle Total	<668	<2500	<1870			
+ 10^{-5} Inv.	<1.15	<4.78	<3.44			
% in Solution	~30	~3	~5			
Cycle 2						
Periodic Samples[a]	<<	15	<<			
Final Solution	<34	<68	<68			
[^{126}Sn (pg/mL)]	(<4.8)	(<9.5)	(<9.5)			
Rinse	<162	<135	<135			
Acid Strip	162	1297	1270			
Cycle Total	<358	<1515	<1473			
+ 10^{-5} Inv.	<0.63	<2.94	<2.75			
Cycle 3						
Periodic Samples[a]	<<	6.8	<<			
Final Solution	<34	<34	<34			
[^{126}Sn (pg/mL)]	(<4.8)	(<4.8)	(<4.8)			
Rinse	<81	<81	<81			
Acid Strip	230	811	(b)			
Cycle Total	<345	<932	<115?			
+ 10^{-5} Inv.	<0.61	<1.82	<0.22?			
Sum of Cycles 1, 2 & 3						
Σ Cycle Total	<1371	<4947	<3457			
+ 10^{-5} Inv.	<2.4	<9.55	<6.4?			

(a) Periodic sample values are total quantities in unfiltered samples for which detectable levels were reported. << indicates all samples analyzed were reported as "less than" values.
(b) Acid strip sample appeared to be contaminated by fuel particles.

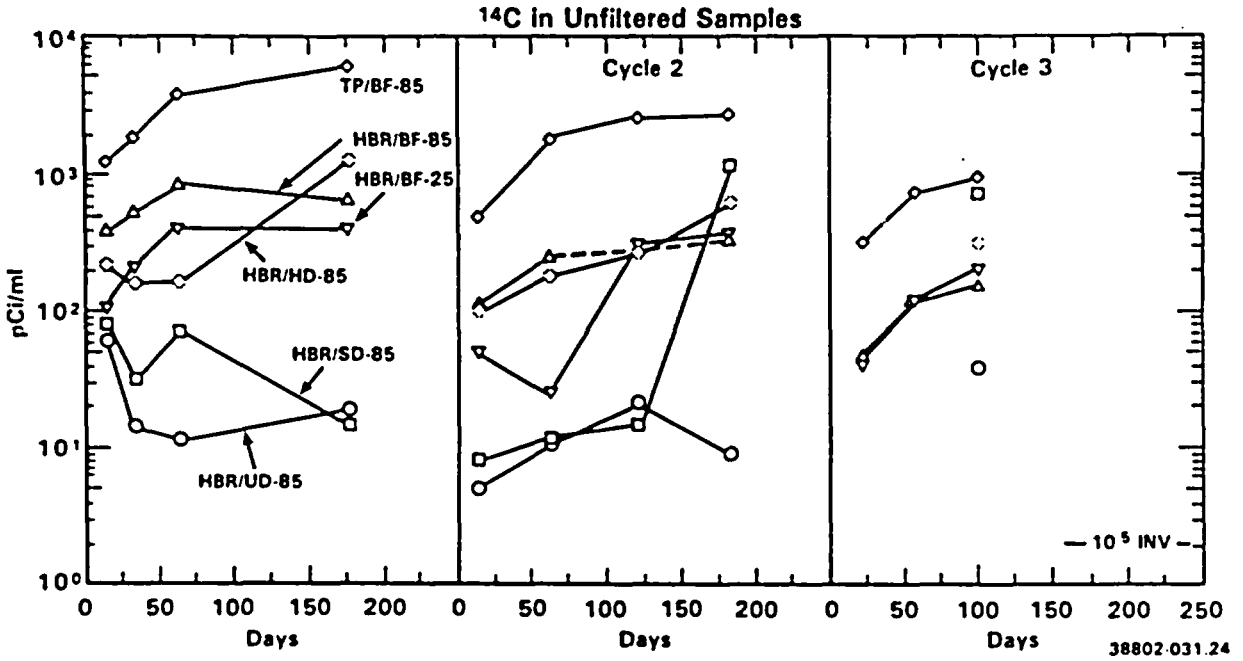

FIGURE 3.25. Activities of ^{14}C Measured in Unfiltered Solution Samples

calculated for the cycle total values in the TP/BF-85 test, since ^{14}C inventory was not determined for the TP fuel. Significantly greater ^{14}C activities measured in the TP/BF-85 test, in comparison to any of the other tests using the HBR fuel, is probably the result of significantly higher ^{14}C inventory for the TP fuel specimen. Comparison of the results from the HBR/BF-25 and HBR/BF-85 tests suggests that the aqueous release of ^{14}C is not strongly dependent on temperature.

Presumably, some of the ^{14}C released to solution in the 85°C tests dropped out of solution along with that portion of HCO_3^- originally in J-13 water that was observed to drop out. It was not possible to determine ^{14}C in the acid strip solution, since it was immediately lost to the atmosphere from any precipitated carbonate phases upon first contact by the 8 M HNO_3. The Cycle 3 rinse solutions from the three bare-fuel tests were analyzed for ^{14}C and were found to contain 4.5 to 6.9% of the total ^{14}C measured in Cycle 3. The "% in solution" values given for Cycle 3 are maximum values and are preceded by a

TABLE 3.15. Quantities of ^{14}C Measured in Samples (nCi)

	HBR/BF-25	IP/BF-85	HBR/BF-85	HBR/SD-85	HBR/HD-85	HBR/UD-85
Cycle 1						
Periodic Samples[a]	20.5	188	49.4	4.8	14.4	2.1
Final Solution	99.0	1486	164	3.7	317.6	4.8
[$^{14}CO_3$ (ppb)]	(0.44)	(6.7)	(0.73)	(0.02)	(1.42)	(0.02)
Rinse	--	--	--	--	--	--
Acid Strip	--	--	--	--	--	--
Cycle Total	119.6	1674	213	8.5	332	6.9
+ 10^{-5} Inv.	235	--	442	16.7	692	13.7
% in Solution	--	--	--	--	--	--
Cycle 2						
Periodic Samples[a]	8.0	99	8.5	0.8	12.0	0.3
Final Solution	89.0	664	84.5	281.5	157.7	<2.3
[$^{14}CO_3$ (ppb)]	(0.40)	(3.0)	(0.38)	(1.26)	(0.71)	(<0.01)
Rinse	--	--	--	--	--	--
Acid Strip	--	--	--	--	--	--
Cycle Total	97.0	763	93.0	282.3	170	<2.6
+ 10^{-5} Inv.	193	--	195	557	353	<5.1
% in Solution	--	--	--	--	--	--
Cycle 3						
Periodic Samples[a]	4.1	26	4.1	--	--	--
Final Solution	51.8	236	39.4	184	78.8	9.7
[$^{14}CO_3$ (ppb)]	(0.23)	(1.1)	(0.18)	(0.82)	(0.35)	(0.04)
Rinse	3.8	12.4	3.2	--	--	--
Acid Strip	--	--	--	--	--	--
Cycle Total	59.7	275	46.7	184	78.8	9.7
+ 10^{-5} Inv.	120	--	99.0	362	164	19.2
% in Solution	<93.7	<95.5	<93.1	--	--	
Sum of Cycles 1, 2 & 3						
Σ Cycle Total	276	2712	353	475	581	<19.2
+ 10^{-5} Inv.	548	--	736	936	1209	<38

(a) Total of quantities in periodic samples for which detectable levels were reported.

NOTE: All values are based on data for unfiltered samples, except for the Cycle 3 rinse samples which were 0.4-μm filtered.

< symbol because some ^{14}C likely precipitated in carbonate phases along with the HCO_3^- originally in the J-13 water and was lost during the acid stripping procedure.

The ~1.2% total measured fractional release (Σ Cycle Totals + 10^{-5} Inv. = 1209) indicated for ^{14}C in the HBR/HD-85 test is the largest fractional release value indicated for any nuclide in the Series 3 tests. The somewhat lower fractional release values for the slit-defect and bare-fuel tests may be due to pretest loss of $^{14}CO_2$ from the more severely defected specimens. The small ^{14}C release values measured in the HBR/UD-85 test indicate that most of the measured release in the other Series 3 tests originated from the fuel or from the gap inventory and not from the cladding exterior. This is a different result than previously reported for the Series 2 tests, where measured ^{14}C releases were not much greater in the defected cladding and bare-fuel tests than in the undefected test.[2] The ^{14}C inventory fractions measured in final solution samples from the Series 2 and Series 3 test cycles using the HBR fuel are compared in Table 3.16. The much higher activities measured in the bare-fuel and defected cladding specimens in the sealed Series 3 vessels indicate that most of the ^{14}C released from the specimens in the Series 2 tests was probably lost to the atmosphere as $^{14}CO_2$. The magnitude of the ^{14}C

TABLE 3.16. ^{14}C Inventory Fraction[a] in Series 2 and Series 3 Final Solution Samples (parts per 100,000)

Test	Cycle 1	2	3	4	5
HBR/BF-2-25	13.0	12.4	13.0	13.9	11.0
HBR/SD-2-25	27.5	33.9			
HBR/HD-2-25	48.1	22.3			
HBR/UD-2-25	10.1	3.7			
HBR/BF-25	194	177	104		
HBR/BF-85	339	178	84		
HBR/SD-85	7.3	555	362		
HBR/HD-85	662	329	164		
HBR/UD-85	9.6	<4.5	19.2		

(a) Based on ^{14}C measured in HBR fuel (0.49 μCi/g) and cladding (0.53 μCi/g).

releases measured in the Series 3 tests suggest that ^{14}C was preferentially released from sources of concentration such as the fuel-cladding gap or grain boundaries.

3.14 COBALT-60

Cobalt-60 is an activation product produced by neutron activation of ^{59}Co and (n,p) reaction on ^{60}Ni. Cobalt-60 is produced in fuel assembly structural components and may also occur in "crud" deposits on the cladding surface where its inventory is variable. With a 5.26-yr half-life, ^{60}Co will decay away during the repository containment period. However, the relatively high-gamma energy (1.3 MeV) associated with its decay requires heavy shielding for attenuation, making ^{60}Co activity a concern during fuel handling and emplacement.

Quantities of ^{60}Co measured in final solution, acid strip, and rinse samples are given in Table 3.17. Cobalt-60 activities were generally less than detectable and were not reported for solution samples from the four 85°C tests using the HBR fuel. Most of the ^{60}Co measured in the 85°C tests was in the acid strip samples. In the 25°C test, most of the ^{60}Co appeared to remain in solution. The TP fuel specimen appeared to release much more ^{60}Co than did the HBR fuel specimens.

TABLE 3.17. Quantities of ^{60}Co Measured in Samples (μCi)

	HBR/BF-25	TP/BF-85	HBR/BF-85	HBR/SD-85	HBR/HD-85	HBR/UD-85
Cycle 1						
Final Solution	5.22	<	<	<	<	<
Rinse	<	1.3	<	<	<	<
Acid Strip	0.68	154	5.46	2.01	0.34	0.34
Cycle 2						
Final Solution	0.52	<	<	<	<	<
Rinse	<	0.14	<	<	<	<
Acid Strip	<	12.9	0.33	0.10	0.12	0.04
Cycle 3						
Final Solution	<	<	0.29			
Rinse	<	0.18	<			
Acid Strip	0.08	3.0	<			

4.0 GENERAL DISCUSSION AND SUMMARY

Nonvolatile radionuclides present in spent nuclear fuel (or vitrified high-level waste) will require dissolution or suspension in water to be transported from a failed waste package in the repository in the absence of a major geological event such as volcanism. The repository horizon under study at Yucca Mountain lies in the unsaturated zone above the water table, and contact of the spent fuel by water that may infiltrate the rock will not occur until the repository has cooled to below the 95°C boiling temperature of water at the repository elevation. This is predicted to be several hundred years after disposal. Results from the Series 3 tests are summarized and discussed in this chapter relative to their implications for spent fuel storage in the repository during the postthermal period. Except as noted, the following discussions focus on results from the three bare-fuel tests. Areas where additional information would be useful are also identified.

The present results indicate that the radionuclides of interest in spent fuel fall into three general categories relative to potential release mechanisms under predicted Yucca Mountain repository conditions. The first category is radionuclides whose release will be limited by low solubility. The actinides, which account for most of the long-term radioactivity of spent nuclear fuel, are the primary radionuclides of interest in this first category. The second category is the more soluble radionuclides for which dissolution rates from the fuel may be an important factor in predicting potential release. Long-lived fission and activation product radionuclides are of primary concern in this category. The third category is radionuclides that may be mobile in the vapor phase and do not require water contact for release. The primary long-lived radionuclide in spent fuel known to be transported in the vapor phase is ^{14}C. There is also a potential for vapor transport of ^{129}I as I_2 that has not been clearly defined.

4.1 THE ACTINIDES

4.1.1 Summary of Actinide Results

Actinide concentrations (uranium, neptunium, plutonium, americium, and curium) measured in solution samples rapidly reached maximum levels during the first test cycle and then generally dropped to lower steady-state levels in Cycles 2 and 3. The approximate steady-state concentrations measured for the actinides in the bare-fuel tests are summarized in Table 4.1. The data for 0.4-μm filtered solutions are considered the most relevant for release estimates, since particles of greater size would likely settle out, and finer colloidal particles that could remain in suspension and be transported with water movement would be retained by the 18-Å filters. The data for 25°C 18-Å filtered solutions given for americium and curium suggest that most of the

TABLE 4.1. Approximate Steady-State Actinide Concentrations[(a)] in the Bare-Fuel Tests

Actinide	25°C		85°C
	0.4 μm	18 Å	(0.4 μm)
Uranium			
μg/mL	0.3	--	0.15
Log M	-5.9	--	-6.2
Neptunium			
^{237}Np (pCi/mL)	0.2	--	0.14
Log M	-8.9	--	-9.1
Plutonium			
$^{239+240}$Pu (pCi/mL)	100	--	1.0
Log M	-8.4	--	-10.4
Americium			
^{241}Am (pCi/mL)	100	3.6	0.1
Log M	-9.8	-11.3	-12.3
Curium			
^{244}Cm (pCi/mL)	100	4.5	0.1
Log M	-11.3	-12.6	-14.3

(a) Estimated, based on plotted Cycles 2 and 3 data for 0.4-μm filtered solutions and the Cycle 2 34-d data for 18-Å filtered solutions.

activity in the 0.4-μm filtered ^{241}Am and ^{244}Cm solution samples was associated with suspended phases in the 25°C test. A portion of the plutonium measured in unfiltered and 0.4-μm filtered solution samples also appears to be associated with suspended phases, but this fraction was much less than measured for americium and curium. No significant filtration effects were noted for uranium or neptunium.

Approximate steady-state uranium concentrations measured during Cycles 2 and 3 of the Series 3 bare-fuel tests (about 0.3 μg/mL at 25°C and 0.15 μg/mL at 85°C) were somewhat lower than the 1 to 2 μg/mL range measured in unsealed silica vessels in the Series 2 tests. Significantly lower uranium concentrations, on the order of 0.01 μg/mL or less, were measured for the slit-defect and holes-defect tests. Calcium-uranium-silicate mineral phases identified as uranophane (confirmed) and haiweeite (likely) were characterized in rinse filter residues from the 85°C bare-fuel tests. Formation of these phases likely controlled or influenced the uranium concentrations in these tests. Phases controlling the concentrations of the other actinide elements were not identified. Detection and characterization of such secondary phases may be difficult because of the extremely small masses of these actinides involved.

The steady-state solution activities measured for nuclides of plutonium, americium, and curium were much lower at 85°C than at 25°C. Kinetic factors involved in the nucleation and growth of secondary phases that limit the concentration of these elements were probably key factors in accounting for the lower concentrations at 85°C. Therefore, lower actinide concentrations may eventually occur at 25°C. Uranium and plutonium concentrations were lower in the slit-defect and holes-defect tests were than in the bare-fuel tests, but americium and curium concentrations during Cycles 2 and 3 were not greatly affected by specimen type. The neptunium data were not greatly affected by temperature.

4.1.2 Comparisons With EQ3/6 Predictions[a]

Spent fuel dissolution in J-13 well water was simulated using the geochemical modeling code EQ3/6[20] to determine whether steady-state actinide concentrations measured in the laboratory dissolution tests could be related to the precipitation of actinide-bearing solids. Version 3245 of the EQ3/6 code and version 3270R13 of the supporting thermodynamic database were used to simulate spent fuel dissolution at 25°C and 90°C assuming atmospheric CO_2 gas fugacity and two different O_2 fugacities, $10^{-0.7}$ (atmospheric) and 10^{-12} bars. The lower 10^{-12} bar oxygen fugacity value was initially chosen because its use resulted in a predicted neptunium concentration at 25°C that matched the experimentally measured neptunium concentration. The simulation process is described in more detail in Reference 14. The computer simulations predict the sequence of solid precipitates that form to sequester elements released via spent fuel dissolution, and the corresponding elemental concentrations in solution. Approximate steady-state actinide concentrations measured at 25°C and 85°C in the Series 3 tests are compared in Table 4.2 to concentrations of actinides in equilibrium with the listed solids as calculated in the EQ3/6 simulations.

The concentrations of uranium in the EQ3/6 simulation vary not only as the precipitates vary, but also during the precipitation of a single mineral, such as soddyite, because of changes in the pH and overall chemical characteristics of the solution. As previously discussed, uranophane, haiweeite, and possibly soddyite were indicated in the 85°C Series 3 tests. Unfortunately, reliable thermodynamic data for uranophane are not available, which complicates comparison of the laboratory test results to the calculated solubility limits. Haiweeite, a calcium-uranium-silicate, as is uranophane, is predicted to precipitate at uranium concentrations that are lower than the measured steady-state values. In the absence of thermodynamic data for

---

(a) The EQ3/6 calculations were performed at LLNL to Quality Assurance Level III under the direction of C. J. Bruton. This section, including Tables 4.2 and 4.3, is excerpted from Reference 17 with editorial changes for adaptation to the present report.

TABLE 4.2. Comparison of Measured and EQ3/6 Predicted Actinide Concentrations (Log M)

Actinide	Measured[a] 25°C	Measured[a] 85°C	EQ3/6[b] 25°C -0.7	EQ3/6[b] 25°C -12.0	EQ3/6[b] 90°C -0.7	EQ3/6[b] 90°C -12.0	Phase
U	-5.9	-6.2	-7.2/7.0[c]	7.1/-6.9	-8.8/-7.6	-8.5/-7.5	H
			-7.0/-6.9	-6.9/-6.8	-7.6	-7.5	H + S
			-6.9/-4.3	-6.8/-4.2	-7.6/-6.0	-7.5/-5.9	S
			-4.3	-4.2	-6.0	-5.9	S + Sch
			-4.2	-4.1	-6.0/-5.8	-5.8/-5.6	Sch
Np	-8.9	-9.1	-6.2	-9.0	-5.2	-8.0	NpO_2
Pu	-8.4	-10.4	-12.4	-13.8	-11.9	-14.6	PuO_2
			-4.3	-5.7	-4.2	-6.9	$Pu(OH)_4$
Am	-9.8	-12.3	-8.3	-8.3	--	--	$Am(OH)CO_3$
			--	--	-8.4	-8.4	$Am(OH)_3$
Cm	-11.3	-14.2	Cm not in thermodynamic database				

(a) Series 3 tests, 0.4-μm filtered.
(b) At oxygen fugacities log f_{O2} = -0.7 (atmospheric) and log f_{O2} = -12.0 with solubility control by precipitated secondary phases as listed. H = haiweeite; S = soddyite; Sch = schoepite. All phases are in crystalline state except $Pu(OH)_4$, which is amorphous.
(c) -7.2/-7.0 refers to a range in concentration from -7.2 to -7.0.

5.0 CONCLUSIONS

The following conclusions and observations are made based on the results of the NNWSI Series 3 Spent Fuel Dissolution Tests.

1. Actinide concentrations (uranium, plutonium, americium, curium, and neptunium) generally appeared to reach steady-state levels in all three test cycles of the bare-fuel tests. Control of actinide concentrations at stable levels in solution was attributed to the achievement of a steady-state between fuel dissolution and secondary-phase formation or other mechanisms such as sorption.

2. Uranium-bearing secondary phases were found in significant amounts in filter residues from the 85°C bare-fuel tests. Formation of the calcium-uranium-silicate phase uranophane was confirmed, and haiweeite was tentatively identified. A possible indication of soddyite formation was also found in one of the filter residues. Secondary phases controlling plutonium, americium, curium, and neptunium concentrations were not identified.

3. Plutonium, americium, and curium activities measured in solution samples from the 85°C bare-fuel tests were from two to three orders of magnitude lower than those measured in unfiltered and 0.4-μm filtered samples from the 25°C test. Slightly lower uranium concentrations were also measured at 85°C in Cycles 2 and 3. Lower actinide concentrations at 85°C are attributed to faster kinetics for formation of solubility-limiting secondary phases at the higher 85°C temperature. Neptunium activities showed no significant dependence on temperature or filtration.

4. Plutonium, americium and curium activities measured in 18-Å filtered samples from the 25°C bare fuel test were significantly less than those measured in unfiltered and 0.4-μm filtered samples suggesting that these elements were present as colloids in this test. The effects of filtration were generally greater for americium and curium than for plutonium. Notable reductions in americium and curium activities also occurred with 0.4 μm filtration in the 85°C bare fuel tests.

5. Steady-state actinide concentrations measured in 0.4-μm filtered samples from the 25°C bare-fuel test were at least three orders of magnitude below those necessary to meet the NRC 10 CFR 60.113 controlled release requirements based on reasonable assumed water flow rates through the repository. This result is of particular significance, since plutonium and americium isotopes account for ~98% of the activity in spent fuel at 1,000 yr, and eventual plutonium and americium concentrations may be lower than those measured in 0.4-μm filtered samples from the 25°C tests.

6. Measured uranium concentrations were consistent with those predicted by the EQ3/6 geochemical modeling code for precipitation of soddyite. Good agreement between measured and predicted concentration was obtained for neptunium based on equilibration with NpO_2 at 25°C when the oxygen fugacity in the simulation was set at 10^{-12} bars. A broad range of concentrations that bracketed the measured values was predicted for plutonium depending upon the assumed oxygen fugacity and concentration-controlling phase. Measured americium concentrations were less than predicted based on data for equilibration with $Am(OH)CO_3$ or $Am(OH)_3$.

7. Actinide fractional releases from the bare-fuel tests were much greater than in the slit-defect or hole-defects tests. Actinide releases from the slit-defect test were somewhat greater than in the hole-defects test, with most of the difference accounted for in the Cycle 1 acid strip samples. Actinide releases in the hole-defects test were not significantly different from those measured in the undefected test.

8. The radionuclides ^{137}Cs, ^{90}Sr, ^{99}Tc, ^{129}I, and ^{14}C were continuously released in the bare-fuel tests at rates exceeding 10^{-5} of inventory per year. Of these radionuclides, only ^{90}Sr showed significant indications that its concentration was limited by solubility. Cesium-137 showed the greatest fractional release during Cycle 1, while ^{14}C showed the greatest fractional release during Cycles 2 and 3.

9. Iodine-129 release was much greater at 85°C than at 25°C. Comparison of the Series 3 test results to those from the Series 2 tests gave no indication that ^{129}I had been lost as I_2 from the unsealed Series 2 vessels. The ^{129}I release in the slit-defect test was equivalent to that in the bare-fuel test, but ^{129}I released in the hole-defects test was not significantly greater than in the undefected test.

10. Comparison of ^{14}C solution activity data measured in the sealed Series 3 tests to that measured in the unsealed Series 2 tests indicated that most of the ^{14}C released in the Series 2 tests was probably lost to the atmosphere as $^{14}CO_2$. The TP fuel appeared to have a much greater ^{14}C inventory (or gap inventory) than did the HBR fuel on which fuel and cladding ^{14}C inventory was radiochemically determined.

11. Long-term release rates for soluble nuclides are uncertain. The relative contributions of fuel matrix phase dissolution, versus preferential release from locations such as grain boundaries where soluble nuclides may be concentrated, was not determined. Preferential release would likely decrease as the inventory of soluble nuclides on exposed grain boundaries is depleted. However, there is reason to suspect that accelerated dissolution of soluble nuclides may eventually occur as a result of degradation of the fuel by oxidation in the repository air atmosphere.

12. A vessel corrosion anomaly occurred during Cycle 1 of the 85°C HBR bare-fuel test. The most significant effects associated with the apparent vessel corrosion were: 1) uranium concentration dropped to about 10 ppb, and 2) ^{99}Tc activity dropped to less than detectable. These effects are attributed to removal of uranium and technetium by coprecipitation with or sorption on iron-bearing precipitates, or to reduction of the soluble UO_2^{+2} and TcO_4^- species as a result of redox coupling with Fe^0 to Fe^{+2}/Fe^{+3} reactions.

13. Calcium, magnesium, silicon, and HCO_3^- precipitated from solution during all 85°C tests cycles, while the chemistry of the starting

J-13 well water remained essentially unchanged during the 25°C test. In addition to the calcium-uranium-silicate phases observed in the two 85°C bare-fuel tests, scale formation was observed at the waterline in all of the 85°C tests. The SEM-EDX examinations suggest that calcite, SiO_2 (possibly as a gel), and possibly dolomite were formed during the 85°C tests. A portion of the released ^{14}C is likely to be incorporated in the carbonate phases. A portion of the released ^{90}Sr is also likely to be incorporated in secondary phases, possibly as a partial substitute for calcium.